OPTIMIZATION AND CHARACTERIZATION OF CONGO RED DYE BIOSORPTION BY *Serratia marcescens* MM06

By

SABO IBRAHIM ALHAJI

Thesis Submitted to the School of Graduate Studies, Universiti Putra Malaysia, in Fulfilment of the Requirement for the Degree of Doctor of Philosophy

June 2023

FBSB 2023 10

DEDICATION

This thesis is dedicated to my late father Alhaji Sabo Yunusa, may Allah (SWT) forgive his shortcomings and grant him Jannatul Firdaus, and to my mother Khadija Mika'il, as well as the TETfund body that sponsored my Ph.D. program.

Abstract of thesis presented to Senate of Universiti Putra Malaysia in fulfilment of the requirements for the Degree of Doctor of Philosophy

OPTIMIZATION AND CHARACTERIZATION OF CONGO RED DYE BIOSORPTION BY *Serratia marcescens* MM06

By

SABO IBRAHIM ALHAJI

June 2023

Chairman : Professor Mohd Yunus bin Abd Shukor, PhD
Faculty : Biotechnology and Biomolecular Sciences

Dyes, toxic and carcinogenic substances, have detrimental effects on the environment and human health when present in wastewater. Biosorption is the most effective and versatile method for removing dye from wastewater since it is highly efficient and cost-effective. The impact of dye pollution has been felt in many countries, including Malaysia. Dye is a frequent pollutant found in water that can come from a variety of places, including manufacturing companies, research centres, and medical centers. Dye pollution has major negative consequences on both the environment and human health. The purpose of the research is to investigate the efficacy of bacterial biomass biosorption of Congo red dye for industrial applications. The objectives of this study are to: (a) screen and optimize the bacterial sorption of Congo red dye using one factor at a time (OFAT) and response surface methodology (RSM); (b) conduct Fourier Transform Infrared (FTIR), scanning electron microscope (SEM), and energy dispersive x-ray (EDX) analysis; (c) determine the kinetics and equilibrium model for Congo red dye biosorption; and (d) study the thermodynamics of Congo red dye biosorption. Numerous bacterial isolates from twelve (12) different species were tested against Congo red. The amount of dye removed from *Serratia marcescens* strain MM06 biomass was found to be greater compared to the other 11 bacterial isolates. The biomass was incubated with a known dye concentration (100 ppm), centrifuged, and the absorbance was measured at 507 nm. The results were investigated under various biosorption conditions, including agitation, dye concentrations, time, temperature, and pH. The optimal conditions for dye removal were determined to be 90 mg/L dye concentration, 125 rpm agitation, 20 minutes contact time, pH 7.0, and 25 °C, resulting in 91.75% Congo red dye removal. The biosorption process was characterized and confirmed using FTIR analysis. Using this approach, the functional groups involved in the biosorption of congo red dye were thoroughly studied, and include alkyl, hydroxyl, amide, and thiol. SEM was used to examine the surface morphology of the biomass before and after adsorption, and it revealed the presence of macro-pores on the surface that were unevenly distributed smoothly and tightly, and that these macro-pores improved the adsorption of Congo red dye molecules onto the surface of *Serratia marcescens* strain MM06. Because of the material's porosity and the electrostatic interaction between the biosorbent and the Congo

red dye, the physical adsorption process was found to predominate based on SEM and FTIR analysis. In the EDX study, various components from biomass were detected by the EDX spectrum before and after biosorption. C, O, P, and S were found, and elemental analysis revealed that C (53.44% and 69.63%) and O (79.96% and 28.17%) had the largest percentages before and after dye treatment, respectively. Nonlinear regression was employed to study biosorption isotherms, kinetics, and finally thermodynamic parameters. Pseudo-second order kinetics and the Langmuir isotherm best describe the biosorption process. In the Isotherms investigations, all eight of the Isotherm models tested on the dye (Henry, Langmuir, Freundlich, BET, Toth, Sips, Fritz-Schlunder IV, and Fritz-Schlunder V), with the exception of the Henry and Toth model, yielded a satisfactory fitting result. The parameters of the fitted isotherms, namely, Langmuir, Freundlich, BET, Sips, Fritz-Schlunder IV, and Fritz-Schlunder V were 4.387657 mg/g, 3.750862 mg/g, 4.387657 mg/g, 2.800659 mg/g, 12.178957 mg/g, 2.557313 mg/g respectively. The parameters of thermodynamics Gibbs free energy (DG°), enthalpy (DH°), and entropy (DS°) changes showed that the biosorption process was exothermic and spontaneous. Based on the findings, Congo red dye can be removed from wastewater effluent using *Serratia marcescens* mm06 as biosorbent.

Keywords: Biosorption, Congo Red, Isotherms, Response Surface Methodology.

SDG: GOAL 3: Good Health and Well-being, GOAL 6: Clean Water and Sanitation

Abstrak tesis yang dikemukakan kepada Senat Universiti Putra Malaysia sebagai memenuhi keperluan untuk ijazah Doktor Falsafah

PENGOPTIMUMAN DAN CIRI-CIRI BIOSORPTION PEWARNA MERAH CONGO OLEH *Serratia marcescens* MM06

Oleh

SABO IBRAHIM ALHAJI

Jun 2023

Pengerusi : Profesor Mohd Yunus bin Abd Shukor, PhD
Fakulti : Bioteknologi dan Sains Biomolekul

Pewarna boleh menyebabkan kesan alam sekitar dan toksik dengan kesan karsinogenik. Rawatan air sisa yang mengandungi pewarna adalah salah satu masalah yang paling sukar untuk diselesaikan. Biosorpsi adalah kaedah yang paling berkesan dan serba boleh untuk menyingkirkan air sisa kerana ia sangat cekap dan menjimatkan kos. Tujuan penyelidikan adalah untuk menguji keberkesanan biosorpsi biojisim bakteria pewarna merah Congo untuk aplikasi industri. Objektifnya adalah untuk menyaring dan mengoptimumkan biosorpsi pewarna merah Congo menggunakan pendekatan satu faktor pada satu masa (OFAT) dan kaedah permukaan tindak balas (RSM), analisis FTIR dan SEM, untuk menentukan model Kinetik dan keseimbangan dan kajian termodinamik tentang biosorpsi pewarna merah Congo. Banyak pengasingan bakteria daripada dua belas (12) spesies berbeza telah diuji terhadap merah Congo. Jumlah pewarna yang dikeluarkan daripada biojisim *Serratia marcescens* strain MM06 didapati lebih besar. Biojisim diinkubasi dengan kepekatan pewarna yang diketahui, disentrifugasi, dan penyerapan pada 507nm diukur. Keputusan telah disiasat di bawah pelbagai keadaan biosorpsi, termasuk pengadukan, kepekatan pewarna, masa, suhu, dan pH. Kepekatan pewarna pengadukan, masa, pH dan suhu optimum selepas RSM ditentukan masing-masing ialah 90 mg/L, 125 rpm, 20 minit, pH 7.0 dan 25 ºC. Pengoptimuman RSM meningkatkan peratusan penyingkiran pewarna merah Congo kepada 91.75% dan menyediakan keadaan yang paling sesuai untuk penyingkiran pewarna. Proses biosorpsi telah dicirikan dan disahkan menggunakan analisis Inframerah Transformasi Fourier (FTIR). Dengan menggunakan pendekatan ini, kumpulan berfungsi yang terlibat dalam biosorpsi pewarna merah kongo telah dikaji dengan teliti. Mikroskop pengimbasan elektron (SEM) digunakan untuk memeriksa morfologi permukaan biojisim sebelum dan selepas penjerapan, dan ia mendedahkan kehadiran liang makro pada permukaan yang tidak sekata diedarkan dengan lancar dan ketat, dan liang makro ini meningkatkan penjerapan molekul pewarna merah Congo ke permukaan Serratia marcescens strain MM06. Oleh kerana keliangan bahan dan interaksi elektrostatik antara biosorben dan pewarna merah Congo, keputusan analisis SEM dan FTIR mencadangkan bahawa proses penjerapan fizikal mendominasi. Dalam kajian EDX, pelbagai komponen daripada biojisim dikesan oleh spektrum EDX sebelum dan selepas biosorpsi. C, O, P, dan S

didapati, dan analisis unsur mendedahkan bahawa C (53.44% dan 69.63%) dan O (79.96% dan 28.17%) masing-masing mempunyai peratusan terbesar sebelum dan selepas rawatan pewarna. Regresi tak linear digunakan untuk mengkaji isoterma dan kinetik biosorpsi dan akhirnya parameter termodinamik. Urutan pseudo-saat ialah kinetik terbaik dan Langmuir ialah isoterma terbaik. dalam penyiasatan isoterma, kesemua lapan model isoterma yang diuji pada pewarna (Henry, Langmuir, Freundlich, BET, Toth, Sips, Fritz-Schlunder IV dan Fritz-Schlunder V), kecuali model Henry dan Toth, membuahkan hasil pemasangan yang memuaskan. Parameter isoterma yang dipasang, iaitu, Langmuir, Freundlich, BET, Sips, Fritz-Schlunder IV, dan Fritz-Schlunder V ialah 4.387657 mg/g, 3.750862 mg/g, 4.387657 mg/g, 2.800657 mg/g, 2.800657 mg/g. /g, masing-masing 2.557313 mg/g. Parameter perubahan termodinamik Gibbs tenaga bebas (DG◦), entalpi (DH◦), dan entropi (DS◦) menunjukkan bahawa proses biosorpsi adalah eksotermik dan spontan. Berdasarkan penemuan, pewarna merah Congo boleh dikeluarkan daripada efluen air sisa menggunakan serratia marcescens mm06 sebagai biosorben.

Kata kunci: Biosorpsi, Merah Congo, Isoterma, Kaedah Permukaan Tindak Balas.

SDG: MATLAMAT 3: Kesihatan dan Kesejahteraan Yang Baik, MATLAMAT 6: Air Bersih dan Sanitasi

ACKNOWLEDGEMENTS

All praise is due to Almighty Allah for providing me with the golden opportunity and strength to complete my thesis work. I owe my deepest gratitude to my main supervisor and guide Professor Dr. Mohd Yunus bin Abd Shukor, who has been an outstanding mentor to me. My research would not have been possible without his enthusiastic guidance, encouragement, and assistance. I also want to thank my Co-supervisors Dr. Nur Adeela binti Yasid and Dr. Ahmad Razi bin Othman for their tireless effort throughout my research.

I must thank all of my lab mates especially Motharasan and research colleagues, as well as my friends in both Malaysia and Nigeria, for their unwavering support and tremendous help before I can sign off. To the success of this work, their contributions have been enormously beneficial.

I would also like to dedicate the thesis to my parents; the late Alhaji Sabo and Khadija Mika'il for their support, prayers, and encouragement. I should not forget to mention my brothers and sisters. Thanks for your love and well wishes.

Lastly, I want to express my gratitude to everyone who contributed to this research in any way, whether directly or indirectly. I sincerely appreciate it. May Allah, the Almighty, richly bless you all. Overall, despite all of our efforts, none of it would have been possible without the supreme blessing and guidance from Almighty Allah. Alhamdulillah!

This thesis was submitted to the Senate of Universiti Putra Malaysia and has been accepted as fulfilment of the requirements for the award of Doctor of Philosophy. The members of the Supervisory Committee were as follows:

Mohd Yunus bin Abd. Shukor, PhD
Professor
Faculty of Biotechnology and Biomolecular Sciences,
Universiti Putra Malaysia
(Chairman)

Nur Adeela binti Yasid, PhD
Senior Lecturer
Faculty Biotechnology and Biomolecular Sciences
Universiti Putra Malaysia
(Member)

Ahmad Razi bin Othman, PhD
Senior Lecturer
Faculty of Engineering and Built Environment
Universiti Kebangsaan Malaysia
(Member)

ZALILAH MOHD SHARIFF, PhD
Professor and Dean
School of Graduate Studies
Universiti Putra Malaysia

Date: 8 May 2025

TABLE OF CONTENTS

LIST OF TABLES

LIST OF FIGURES

LIST OF ABBREVIATIONS

Abs	Absorbance
ANOVA	Analysis of variance
BBE	Biomonitoring, Bioremediation, and Ecotoxicology Laboratory
BOD	Biochemical oxygen demand
C.I	Colour index
$CaCl_2$	Calcium chloride
CCD	Central composite design
CO_3	Carbonate
COD	Chemical oxygen demand
CR	Congo red
DB	Disperse blue
dH_2O	Distilled water
DNA	Deoxyribonucleic acid
DO	Disperse orange
DOE	Department of Environment
DV	Disperse violet
EPA	United States Environmental Protection Agency
Eq	Equation
EQA	Environmental Quality Act
et al	and friends
FT-IR	Fourier transform-Infrared
GDP	Gross domestic product
H_2O_2	Hydrogen Peroxide
J	Joule

K	Kelvin
K	Potassium
N	Normality
nm	Nanometer
OFAT	One factor at a time
ppm	Part per million
RR 120	Reactive red 120
RSM	Response surface methodology
SEM	Scanning electron microscope
SO_3H	Sulfonic acid
SS	Suspended solid
STDEV	Standard deviation
T	Temperature
x g	Gravitational force

LIST OF NOMENCLATURE

A_T	Temkin isotherm equilibrium binding consant
B	Heat of sorption constant
b_B	Baudu constant
b_H	Hill constant
b_K	Khan constant
b_T	Temkin isotherm constant
b_T	Toth equilibrium constant
b_U	Unilin constant
b_{VS}	Vieth-Sladek constant
C_e	Equilibrium adsorbate
C_o	Adsorbate initial concentration
E	mean free energy
k_1	Pseudo-first model constant rate
K_{1H}	Hill – de Boer constant
K_2	energetic constant of the interaction between adsorbed molecules
k_2	Pseudo-second model constant rate
K_{BS}	Brouers-Sotolongo constant
K_D	Dubinin – Radushkevich isotherm constant
K_{DR}	Dubinin-Radushkevich isotherm
K_E	Elovich equilibrium constant
K_F	Freundlich isotherm constant
K_{FH}	Flory-Huggins equilibrium
K_{FS}	Marczewski-Jaroniec isotherm constant
K_H	Henry isotherm constant

K_J	Jovanovic isotherm constant
K_L/b_L	Langmuir isotherm constant
K_{MJ}	Marczewski-Jaroniec constant
K_{RP}	Radke-Prausnitz constant
K_{RP}	Redlich – Peterson model isotherm constant
q_e	adsorption capacity at equilibrium
q_{mB}	Baudu isotherm adsorption capacity at equilibrium
q_{mBET}	BET isotherm adsorption capacity at equilibrium.
q_{mBS}	Brouers-Sotolongo isotherm adsorption capacity
q_{mDR}	theoretical isotherms saturation capacity
q_{mFS}	Fritz-Schlunder-III isotherm adsorption capacity at equilibrium
q_{mFS}	Fritz-Schlunder-IV isotherm adsorption capacity at equilibrium
q_{mFS5}	Fritz-Schlunder-V isotherm adsorption capacity at equilibrium
q_{mK}	Khan isotherm adsorption capacity at equilibrium
q_{mL}	adsorption capacity at equilibrium for Langmuir
q_{mMJ}	Marczewski-Jaroniec isotherm adsorption capacity at equilibrium
q_{mP}	Parker isotherm adsorption capacity at equilibrium
q_{mRP}	Radke-Prausnitz isotherm adsorption capacity at equilibrium
q_{mS}	Sips isotherm adsorption capacity at equilibrium
q_{mT}	Toth isotherm adsorption capacity at equilibrium
q_{mU}	Unilin isotherm adsorption capacity at equilibrium
q_{mVS}	Vieth-Sladek isotherm adsorption capacity at equilibrium
q_t	adsorption capacity at time *t*
R	Universal gas constant
R_L	Equilibrium parameter of Langmuir
ΔG	Gibbs Free energy change

ΔH	Enthalpy change
ΔS	Entropy change
E	Polanyi potential

CHAPTER 1

INTRODUCTION

1.1 Background

Treatment of wastewater streams has long been a challenging and essential research area, and there are a variety of physicochemical and biological processes for removing colour from various industrial effluents which contain high levels of poisonous dyes that are mutagenic and carcinogenic to living organisms (Maurya et al., 2014). Many pharmaceutical products are made to cure diseases caused by pollution, there is a need to remove pollution to minimise the burden on pharmaceutical industries (Ismail et al., 2019). Diseases spread quickly due to dirty water, among other environmental pollutions (Ismail et al., 2019). Dyes are important compounds commonly used in various industries such as textile, paper, printing, leather, and plastic manufacturers (Gb, 2016; Y. Wang et al., 2006). Textile industries use dyes to colour their products and consume substantial volumes of water, as a result, they generate considerable amounts of coloured wastewater (Litefti et al., 2019). Many industries, mainly those of dye manufacturing, textile finishing, food coloring, cosmetics, pulp, and paper use dyes or pigments for the coloration and a great number of these products can induce an environmental impact if they are loosed into wastewater (Kousha et al., 2015). Dyes have been considered hazardous pollutants and the presence of dyes in water even in small concentrations, can have hostile environmental impacts due to their carcinogenic nature (Ihsanullah et al., 2020). A great number of dyes and pigments can induce an environmental impact and are toxic with suspected carcinogenic and mutagenic effects (Kousha et al., 2015; Mall et al., 2005; Suyamboo, 2012). Dye affects photosynthesis, inhibits the growth of aquatic biotics, and interferes with the solubility of gases in bodies of water by interfering with the penetration of sunlight into the aquatic environment (Silva et al., 2019). Because of their resistance to light, heat, chemicals, and water, dyes are difficult to biodegrade in the environment (Ahmad et al., 2008). Various governments have imposed environmental limitations on the quality of coloured wastewater, requiring dye-producing industries to remove dyes from their effluents prior to discharge (Dotto et al., 2013). However, because of the high solubility of these colours in the water, certain traditional wastewater treatment methods cannot provide adequate removal of the pollutants (Vijayaraghavan & Yun, 2008).

Microbes, including bacteria, play a crucial role in the study of azo dyes biosorption and their environmental impact.Certain microbes, particularly bacteria, have the ability to degrade and metabolize azo dyes. This bioremediation potential is essential for developing eco-friendly and sustainable strategies to remove azo dyes from contaminated environments, such as wastewater (P. K. Singh & Singh, 2017). Bacteria can absorb azo dyes through various mechanisms, and the specific process depends on the characteristics of both the bacteria and the dye. Bacterial cells have surfaces with functional groups (such as hydroxyl and amino groups) that can interact with azo dye molecules through physical forces, such as hydrogen bonding and van der Waals interactions. This adsorption is a non-specific physical interaction, and it does not involve a chemical change in the dye molecule. Can also interact through biofilm

formation, intracellular accumulation, enzymatic binding, electrostatic interactions, and bacterial extracellular polymers (EPS) (Gadd, 2009; Singh & Singh, 2017). The choice of Congo red dye and Serratia marcescens in this study is based on the need to explore microbial interactions with azo dyes, understand potential biosorption pathways, and assess the applicability of specific bacteria in environmental remediation efforts.

Worryingly, dye pollution in Malaysia and many other parts of the world is compounded by a lack of remediation (Manogaran et al., 2021; Ramakreshnan et al., 2020). Effluents from dye-using enterprises are typically discharged directly into bodies of water, posing a serious wastewater treatment challenge (Jayasri et al., 2014). Numerous Malaysian textile industry small and medium-sized companies, such as Batik processing industries, are significant contributors of chemical pollution in the environment.

This project is focused on the utilisation of bacterial biomass (*Serratia marcescens* mm06) to address these challenges. To more effectively address the difficulties, this research identifies bacterial biomass (*Serratia marcescens* MM06) that has the potential to absorb Congo red dye. The process was enhanced by applying OFAT and RSM to achieve maximum adsorption capacity, and it was then described using kinetics, isotherm, and thermodynamic models, and also characterized using FTIR, and SEM. The aim of this study is to determine the efficacy and future potential of bacterial biomass (*Serratia marcescens* MM06) in the adsorption of congo red dye.

1.2 Statement of the problems and significance of the study

In Malaysia, numerous cases of dye pollution in local rivers have been documented a number of times. Many small and medium-sized businesses in Malaysia's textile industry, such as Batik processing industries, are critical contributors to dye pollution in the environment. In 2017, Malaysia's 473 rivers were monitored, with 244 (52%) being clean, 186 (39%) being mildly contaminated, and 43 (9%) being polluted. Ammonia, nitrogen, biochemical oxygen demand (BOD), and suspended solids (SS) remained high in these contaminated rivers, with high BOD attributable to insufficient sewage or effluent treatment from the agriculture and dye manufacturing industry. Small-scale manufacturers are responsible for most of these contaminations, with the cost of treating effluents being the main barrier. Textile sludges in Selangor contain dyes such as Azo dye (Congo red) and Reactive Red dyes, which are widely utilized in the Batik industry. As a result, cost-effective remediation is critical to solving this problem. Among the bio- and physicochemical techniques that are currently available. Biosorption is the most effective and versatile method for removing wastewater. Biosorption using microorganisms (bacterial biomass) has some advantages over other agricultural products (Activated Carbon) because there is no maintenance required. After all, biomass can be stored for long periods without losing effectiveness, toxicity issues are avoided, regeneration is more feasible, and it is possible to work on a wider range of environmental variables.

1.3 Research hypothesis

The application of RSM, as stated in the literature, has greatly enhanced adsorption over the traditional OFAT approach, and it is believed that a similar result would be obtained in this research. The kinetics may be pseudo-1st order or pseudo-2nd order, with the best model revealing the underlying sorption process. The isotherms can be calculated using any of the various isothermal models available, including Henry, Langmuir, Freundlich, BET, Toth, Sips, Fritz-Schlunder IV, and Fritz-Schlunder V. The use of nonlinear regressions in all modeling exercises and error function analyses instead of the popular linearized forms often found in the literature in securing the best models are all recommended by statisticians in the sorption field and is expected to result in better reliability in the correct model, parameters obtained, and their interpretations. The rate constant values can be employed in thermodynamics studies to provide parameters such as DG, DH, and DS, which can all provide critical assessments and insights into the sorption mechanism.

1.4 Aim and Objectives

1.4.1 Aim of the Study

Based on the statements above, the present study aims to utilise bacterial biomass as a low-cost biosorbent as a substitute to be utilised for the removal of dye pollution in Batik wastewater industry. With this in mind, the objectives of the study are as follows:

1.4.2 Objectives of the Study

The objectives of this study are to:

i. screen and optimize the bacterial sorption of Congo red dye using one factor at a time (OFAT) and response surface methodology (RSM);

ii. conduct Fourier Transform Infrared (FTIR), scanning electron microscope (SEM), and energy dispersive x-ray (EDX) analysis;

iii. determine the kinetics and equilibrium model for Congo red dye biosorption; and study the thermodynamics of Congo red dye biosorption.

CHAPTER 2

LITERATURE REVIEW

2.1 Dye

Textile industries are the most significant users of dyes. During the colouring process in the textile and paint industries, a significant amount of dye is lost to the waste stream (Ismail et al., 2019)**.** Man has employed dyes throughout his life since 3000 B.C. for a variety of purposes. Egypt, Romania, and India had a thriving dyeing industry. Dyes have a non-biodegradable and stable aromatic structure that consists of a chromophore and polar groups (Tonghao et al., 2012). Colour compounds are one of the major pollutants, as well as a 'discernible pollutant.' In a given year, roughly 10 103 tonnes of varied commercial dyes and pigments are produced, with over 70 104 tonnes being manufactured globally (Garg et al., 2004; Slama et al., 2021). In ancient days, textiles were dyed using natural dyes, but the colour spectrum was limited. Furthermore, due to everyday washing and sunshine exposure, the fabric's colour fastness decreases over time (Kant, 2012). Alternatively, mordant was used to achieve the intricate coloration, which made the dyeing procedure more time-consuming. W. H. Perkins discovered artificial dyes in 1856, which provided a wide range of coloured materials fast and in a wider range of colours and hues. As a result, "dye application" has become a multibillion-dollar business. The harmful and deleterious consequences of synthetic dyes on all forms of life, however, have reignited global interest in natural colours. Dyes can be poisonous and have a significant negative impact on the wastewater value. Natural dye painting necessitates a considerable amount of water. The dye usage is estimated to be almost equivalent to or twice the mass of the fibre to be coloured. About 80% of the colourant stays on the fabric after dying, while the rest is flushed off as effluent (Essawy et al., 2008; Kant, 2012). The textile industry accounts for over 22% of the total volume of industrial wastewater produced in the United States (Tan et al., 2008).

2.1.1 Classification of dye

There are various types of dyes. The following are some classification bases:

- Based on the source of dyes
- Based on the nature of chromophore
- Based on the application of dye

2.1.1.1 Based on the source of dyes

Dyes are categorized as **natural** or **synthetic** based on the source from which they are obtained.

2.1.1.2 Natural dye

These dyes come from natural sources. Most of the natural dyes are derived from plants (extracted from leaves, flowers, roots, berries, roots, bark, etc.). Insects and mineral compounds are also sources of natural dye. Indigo, madder, saffron, osage orange, safflower, madder, and so on. They typically produce wastewater that can be treated by biodegradation and are less toxic and allergenic than synthetic dyes (Benkhaya et al., 2020).

Natural dyes are classified into two types: additive dyes and substantive dyes. To adhere to the textile, additive dyes require a mordant (For example, madder). Substantive dye does not necessitate the application of a mordant (For example, cochineal and safflower).

2.1.1.3 Synthetic dyes

Synthetic dyes are those made from organic or inorganic Materials. An English chemist named William Henry Perkin discovered the first synthetic dye Mauveine, in 1856 which paved the door for the development of a wide range of dyes for varied applications. (Nagendrappa, 2010). Because of their low cost and colorfastness, thousands of different synthetic dyes have been developed and utilised since then. Textile dyes are classified into several classes based on this classification, including direct, vat, sulphur, organic pigments, reactive, disseminated, acidic, azoic, basic, oxidative, developed, mordant, and solvent dyes (Demirbas, 2009).

Certainly, the classification of dyes based on their source—natural or synthetic—has significant implications for both the environment and safety, the environmental and safety aspects of each type, highlighting their benefits and drawbacks are depicted in Table 2.1.

Table 2.1: Benefits and drawbacks of Natural and Synthetics dyes

Type	Benefit	Drawback	Safety	Cost-effective
Natural dye	1. Renewable Resources: Natural dyes are often derived from plants, animals, or minerals, making them renewable and sustainable. 2. Biodegradability: Natural dyes are generally biodegradable, which means they break down naturally without causing long-term environmental harm.	1. Resource Intensity: The production of natural dyes may require significant land, water, and energy resources. 2. Limited Color Range: Natural dyes can offer a more limited color palette compared to synthetic dyes, restricting their use in certain applications.	Non-toxic: Natural dyes are often perceived as safer than synthetic counterparts as they are less likely to contain harmful chemicals.	Low Environmental Impact: The overall environmental impact is usually lower than that of synthetic dyes.
Synthetic dye	1. Wider Color Range: Synthetic dyes offer a vast array of colors, allowing for more versatile applications. 2. Higher Yield: Synthetic dye production can be more efficient, requiring less land and water.	1. Non-Biodegradable: Many synthetic dyes are persistent in the environment, leading to potential long-term pollution. 2. Toxic Byproducts: The production of synthetic dyes may generate harmful byproducts, impacting ecosystems and human health.	Consistent Purity: Synthetic dyes can be produced with consistent purity levels, reducing the risk of impurities.	Lower Cost: Synthetic dyes are often more cost-effective to produce on a large scale.

(Radhakrishnan, 2014; Benkhaya et al., 2020; Hunger, 2002)

2.1.1.4 Based on the nature of chromophore

Textile dyes could be grouped in the colour index based on their chromophore structure, colour, and manner of application. Dyes are categorised into different groups based on their chromophores, such as Anthraquinone eg Alizarin, triphenylmethane eg crystal violet, azo eg Congo red, Nitroso eg Nitroso R salt, Nitro eg Reactive red 120, Indigoid eg synthetic indigo, diphenylmethane eg Malachite green, oxazine eg Nile blue, Phthalein eg Phenolphthalein, Acridine eg Acridine Orange, xanthene eg Fluorescein, and so on. Each colour of textile dye has a specific chemical structure. They can be identified by the chemical structure of their chromophoric group. A chromogenic chromophore is a collection of atoms found in dye compounds that are responsible for colour.

2.1.1.5 Based on the application of dye

Dyes are classified based on their application as shown in Table 2.2

Table 2.2: Classification of Dye based on their application

Class	Main substrates	Method of application	Chemical types	Example
Direct	cotton, rayon, paper, leather, and nylon	Applied from baths containing extra neutral or slightly alkaline electrolytes.	Azo, phthalocyanine, stilbene, and oxanine	Direct orange 39, Direct blue 86, Direct red 10, etc.
Reactive	cotton, wool, silk, and nylon	Under the influence of heat and pH, the reactive site on the dye interacts with the functional group on the fibre to covalently bind the dye.	Azo, anthraquinone, phthalocyanine, formazan, oxanine, and basic	Reactive yellow HE6G, Reactive red, Reactive violet C2R, Reactive golden yellow MR, Reactive yellow MGR, etc.
Disperse	Polyester, polyamide, acetate, acrylic, and plastics	Fine aqueous dispersions are commonly applied using high temperature/pressure or low temperature carrier techniques, and dye can be padded on fibre and baked on or thermofixed. .	Azo, anthraquinone, styryl, nitro, and benzodifuranone	Disperse Violet, Disperse yellow, Disperse red, Disperse blue, Disperse green, etc
Basic	Paper, polyacrylonitrile, modified nylon, polyester, and inks	Applied from acidic dyebaths	Cyanine, hemicyanine, diazahemicyanine, diphenylmethane, triarylmethane, azo, azine, xanthene, acridine, oxanine, and anthraquinone	Crystal violet, methylene blue, safranin, basic fuschin, etc.
Acid	nylon, wool, silk, paper, inks, and leather	Usually from neutral to acidic dyebaths	Azo (including premetallised), antraquinone, triphenylmethane, azine, xanthene, nitro, and nitroso	Acid black, Acid blue S5R, Acid green 20, Acid red 119, etc
Sulphur	cotton and rayon	Aromatic substrate vatted with sodium sulphide and reoxidized on fibre to yield insoluble sulphur-containing compounds.	Indeterminate structures	sulphur black 1, Sulphur red 1, Sulphur orange 1, Sulphur brown 21, Sulphur green 12, etc
Vat	Cotton, rayon, and wool	Water-insoluble colours are dissolved in sodium hydrogen sulphide before being drained and reoxidized on fibre.	Anthraquinone (including polycyclic quinines) and indigoids	Vat blue 1, Vat orange 3, Vat yellow 1, etc.
Solvent	plastics, gasoline, varnishes lacquers, stains, inks, fats, oils, and waxes wool, leather, silk, paper and modified cellulose fibers	Dissolution in the substrate.mostly used on textile fibres with the help of transition metal ions such as Cr3+.	Azo, triphenylmethane, anthraquinone and phthalocyanine	Solvent red 24, Solvent yellow 124, solvent blue 35, Solvent orange 5, Solvent black 3, etc.
Mordant			Azo,Anthraquinone, dichromates and chromium complexes	Chrome blue 2K, Alizarin red S, Celestine blue B, Eriochrome cyanine R, Mordant Blue 13, Mordant Brown 40 etc.

(Benkhaya et al., 2020; Hunger, 2002)

2.2 Toxicity and environmental impacts of dyes

Toxic and dangerous compounds found in dye effluents are carcinogenic, teratogenic, or mutagenic to numerous organisms. Many dye-effluent compounds are extremely poisonous and dangerous because they can destroy genetic material without being expressed right away (Ismail et al., 2019).

Textiles are currently the second polluting industrial sector in the world and are considered to be one of the worst wastewaters to be treated for the high demand for chemical oxygen, as well as for high requirements for biological oxygen, suspended solids, turbidity, and toxic constituents, but also colour, the first eyesight-detectable contamination (Benkhaya et al., 2018; Ramachandra, 2014). There are several environmental devastating and permanent repercussions, such as the demise of the Aral Sea by over-water to cultivate cotton crops (Benkhaya et al., 2020). Dyes may influence photosynthetic activity in aquatic life through lower light penetration. Dyes can also be poisonous for some aquatic species because of the presence of aromatic materials, metals, etc. (Aljeboree et al., 2017; Ramachandra, 2014; Yagub et al., 2014). Because the majority of the dyes are toxic and carcinogenic, they act as a barrier to aquatic life in water bodies. They don't fade in the presence of water or sunlight, and they can't be efficiently treated in traditional wastewater treatment plants due to their complexity in structure (Mahmoud et al., 2012).

In many microbiological and fish species, dyes are carcinogenic, mutagenic, or teratogenic. Moreover, human beings may be severely affected, such as renal dysfunction, reproductive system, liver, brain, central nervous system, mutagenesis and chromosomal fractures, carcinogenesis, and pulmonary toxicity have been documented (Yagub et al., 2014). Many azo dyes induce bladder cancer, hepatocarcinoma, and splenic sarcomas in humans, as well as chromosomal and nuclear abnormalities in mammalian cells and animals (Ismail et al., 2019).

Dyes are also a serious hazard to human health, and they can have a long-term negative impact if they enter human organs through the food chain (Ihsanullah et al., 2020). Due to the frequent use of alkaline dyes textile industry effluents are very colorful and have high salinities and eco-toxicity (Benkhaya et al., 2020). The presence of hazardous amines in the effluent means that dyes are harmful. Likewise, the degradation-resistant anthraquinone-based dyes remain colored in wastewater for a long period. dyes are water-soluble and 5-10% of the colors move to a colorful wastewater bath, producing major environmental problems. Furthermore, chemically stable, low-biodegradability dyes will pass through untreated conventional treatment facilities, it is therefore desired to concentrate on specialized procedures and technology to remove dye from various wastewater and industrial effluent (Yagub et al., 2014).

2.2.1 Dye Pollution on a global scale

It is estimated that Azo dyes make up about 70% of the 9.9 million tons of dye used each year, with a global turnover of $30.42 billion in sales. There is a 3.5 percent annual growth in supply due to the ongoing need for dyes and pigments(Manogaran et al., 2021). The industry participants have been forced to increase and diversify their products in order to keep up with the growing needs of the market as a result of the Malaysian government's authorization of the usage of batik as a national outfit on official occasions. There are around 320 registered batik industries operating in Malaysia at the present time, with the biggest concentrations being centred in the states of Kelantan and Terengganu. The vast majority of these types of businesses in Kelantan are either constructed as Small and Medium Enterprises (SMEs) or as modestly sized family enterprises that make use of technology that is very straightforward. It is important to note that many business owners in the batik sector choose to construct their production units in the backyards of their homes or along the banks of adjacent rivers since these locations provide easy access to water supplies and allow for the disposal of wastewater. In this scenario, wastewater from the batik manufacturing facilities was typically dumped into the surrounding water bodies with either very little or no pretreatment at all (Ramakreshnan et al., 2019). Due to the large amounts of water needed in dyeing processes, the textile sector is one of the largest producers of liquid effluent pollutants. Furthermore, the different effluent properties in terms of pH, dissolved oxygen, organic and inorganic chemical content are determined by the different processing stages and types of synthetic dyes used during this conversion. Every year, 280,000 t of textile dyes are expected to be emitted in such industrial effluents around the world. Azo dyes account for over 70% of all dyestuffs used worldwide by weight, making them the most frequent synthetic dyes discharged into the environment and the largest group of synthetic colourants (Saratale et al., 2011). Dying industries have relied on synthetic dyes ever since and have begun to expand globally, with about 8×10^5 tonnes of synthetic dyes manufactured each year. The textile sector accounts for over ten thousand distinct dyes used for printing and/or colouring various types of fabrics, accounting for approximately 75% of the global dyestuff market. Textile industries are mostly found in developing nations such as India, Bangladesh, Sri Lanka, and Vietnam, where they have helped to increase employment opportunities, strengthen economies, and earn foreign cash (Slama et al., 2021). However, dye production has dropped in the United States and Europe over the last 20 years, the dye industry has increased significantly in Asia, particularly in China, South Korea, and India. The transformation in synthetic dye industries and markets began about 1995 because of price competitiveness and globalisation of international trade. China has surpassed all other countries as the world's leading textile producer, while also accounting for half of global synthetic dye usage. China and India are at the same time the world's largest exporters of pigments, raw intermediate materials, chemicals, and synthetic colours to the rest of the world, notably western countries. Nowadays, there are more than 90,000 different varieties of synthetic dyes that are used in a variety of industries, including textile manufacturing (Moradihamedani, 2022).

Government legislation is becoming increasingly stringent, especially in developed countries, regarding the removal of dyes from industrial effluents. In the United Kingdom, such matters are regulated by the Environment Agency (EA) for England and Wales and the Scottish Environment Protection Agency (SEPTA). Since September 1997, UK environmental policy has stipulated that no synthetic chemicals should be

introduced into the maritime environment. The law's enforcement will ensure that textile companies treat their dye-containing wastewater to the required standard. Regulations in the European Community (EC) are also growing increasingly strict.

2.3 Congo red dye

Congo Red (sodium salt of benzidinediazobis-1-naphthyl-amine-4-sulfonic acid) is a benzidine-based Azo dye that is recognised for its complicated chemical structure, water solubility, and endurance once discharged into the natural environment. It is converted to benzidine, which is a recognised human carcinogen and can trigger allergic reactions in some people (Dandge et al., 2016). Congo red (CR) is one of the most widely used azo dyes in the world. CR is an anionic dye based on diazo benzidine with a double azo (-N=N-) linkage. In many organisms, CR is very poisonous and carcinogenic, and it is well metabolized by the known human carcinogen benzidine. CR dye has been banned in some countries because of health concerns, although it is still commonly used in others. CR dyes are difficult to biodegrade due to their complex aromatic molecular structures, which give them optical, thermal, and physicochemical stability. As a result, even at low concentrations, the presence of CR dye in water is highly unwanted (Ismail et al., 2019). The structure of congo red dye is shown in figure 2.1.

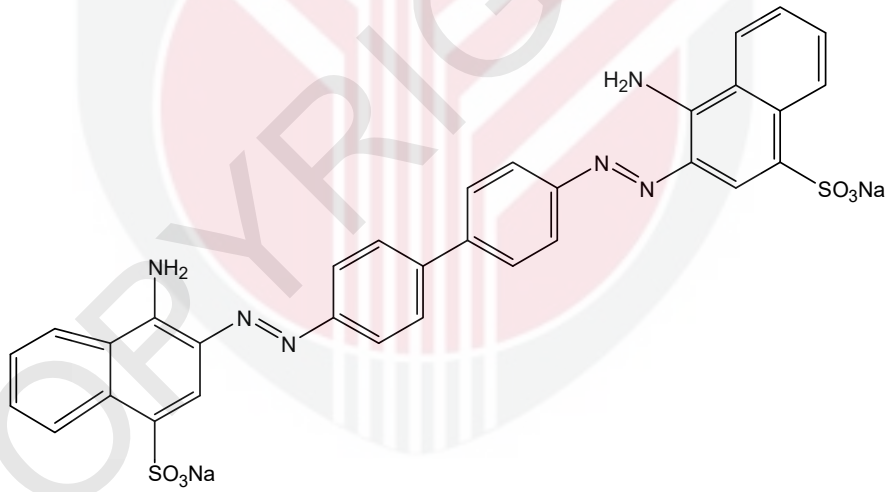

Figure 2.1: Structure of congored dye

2.4 Dye removal techniques

There have been several reported methods for removing contaminants from effluents have been published. A potential environmental threat may be present in wastewater effluents, which contain synthetic dye. In order to remove colours from aqueous solutions without harming the environment or human health, a variety of separation

techniques have been developed (Dawood & Sen, 2014). Biological, chemical, and physical are the three types of technologies that can be classified. All of them have their own set of pros and disadvantages. Because of the high cost and disposal issues associated with many of these conventional technologies for treating dye effluent, they have not been widely implemented on a significant scale in the textile industry (Crini, 2006; Kant, 2012; Demirbas, 2009; Dawood & Sen, 2014). There is currently no single procedure that can provide effective treatment for effluents, primarily as a result of the complexity of the effluents(Demirbas, 2009).

2.4.1 Physical method of dye removal

Physical dye removal methods are often uncomplicated procedures that are achieved through the mass transfer mechanism. Adsorption, coagulation or flocculation, ion exchange, irradiation, membrane filtration, nanofiltration or ultra-filtration, and reverse osmosis are all physical dye removal procedures that are commonly used (Katheresan et al., 2018).

2.4.1.1 Adsorption

This procedure involves the transfer and adhesion of the adsorbate's ions, atoms, or molecules to the surface of the adsorbent's material, which results in a thin film being formed between them. The adsorbate can exist in a variety of phases, including gas, liquid, and dissolved solute. Physical and chemical adsorption are the two types of adsorption techniques. Physisorption is another term for the physical adsorption process, and it is governed by physical forces such as Van der Waals forces, hydrophobicity, hydrogen bonding, polarity, static interaction, dipole–dipole interaction, and ∏ - ∏ interaction, amongst other factors. However, physical adsorption occurs when pollutants adhere to the adsorbent's surface as a result of the interactions described above, whereas chemical adsorption (also known as chemisorption or Langmuir adsorption) occurs when the adsorbate becomes chemically bound to the adsorbent's surface as a result of the exchange of electrons between the two substances (Dawood & Sen, 2014). Adsorbents typically have porous structures to increase the overall exposed surface area and facilitate fluid passage more quickly. To remove dye from water and wastewater, an easy and affordable method is adsorption. Adsorbents can be regenerated for numerous re-uses and, in general, have high treatment efficiency. The performance of the majority of the adsorption process is typically governed by the initial dye concentration, solution pH, temperature, contact time, and adsorbent dosage. Bacterial biomass, activated carbon, nanoparticle, low-cost adsorbents, and other types of adsorbents are commonly used in the adsorption process to remove dyes from water and wastewater (Ahmad et al, 2015).

The extent of adsorption is determined by the nature of the adsorbate, including its molecular weight, molecular structure, molecular size, polarity, and solution concentration. It is also determined by the surface properties of the adsorbent, including particle size, surface area, surface charge, and so on. When it comes to wastewater treatment, the adsorption process is a highly effective separation technique that is considered superior to other available techniques due to its low initial cost, simplicity of

design, ease of operation, and insensitivity to toxic substances when compared to other techniques. The physical and chemical properties of adsorbents and adsorbates are important factors in the efficacy of an adsorption process (Dawood & Sen, 2014).

2.4.1.2 Ion-Exchange

The term "ion-exchange adsorbent" refers to a substance that binds contaminants with opposite charges (Hassan & Carr, 2018). One of the most popular methods is the ion exchange procedure, which efficiently removes colours from aqueous solutions through the interaction of charged dyes with functional groups on ion exchange resins. To effectively separate the solutes from the resins by the exchange of ions, strong bonds between the two are formed. For the purpose of separating solutes with various surface charges, the resins are offered as cation exchangers or anion exchangers (Ahmad et al, 2015).

Adsorbents that are capable of binding harmful anions or cations of the opposite charge are introduced into wastewater in either solid or liquid form, and they are used to release an equivalent number of non-hazardous hydrogen ions as a result. Previous research investigated the use of the ion exchange method to remove reactive dyes from a solution. During the ion exchange procedure, cationic dyes were also removed from the water, resulting in a cleaner water source. Previous research has combined ion exchange with chemical or electrochemical techniques to remove dye from textile effluents. Although this method is extremely effective at removing dangerous and soluble contaminants from effluent water, its implementation has been limited due to the high expense associated with it (Slama et al., 2021).

2.4.1.3 Microfiltration

In order to effectively eliminate dyes from wastewater, the application of MF for the removal of colours from wastewater is restricted due to the small pore size range of the material, which is around 0.1 to 10 μm. This range of pore size even has an impact on the feed pressure during filtration, which must be less than 2 bar in order to be effective. As a result, the use of MF for the removal of colours from wastewater is limited. Its use in dye removal is confined to the elimination of suspended particles in dye and the removal of colloid dye from the dye bath, which are the only two applications for MF. All other organic contaminants and chemicals dissolved in dyes will be carried away by the permeate as it passes through the MF membrane. Since dye elimination from wastewater has become increasingly difficult, MF is only rarely used as the primary treatment technology. Instead, it is typically used as a pre-treatment unit in a combination system, followed by the primary treatment technique, which targets dyes and other organic contaminants present in wastewater (Moradihamedani, 2022).

2.4.1.4 Nanofiltration

Nanofiltration (NF) is a relatively recent membrane technology used for wastewater treatment and purification. Nanofiltration membrane pores range in size from 1 to 10 angstrom. Nanofiltration technology has demonstrated qualities that are intermediate between ultrafiltration (UF) and reverse osmosis (RO) (RO). Furthermore, NF outperforms UF and RO in terms of smaller osmotic pressure difference, higher permeate flux, higher retention of multivalent salts, minimal investment, and low operation and maintenance expenses (Ahmad et al, 2015). In recent years, nanofiltration (NF) has gained popularity as a potential method for the treatment and recycling of industrial dye effluent. Under reasonable operating pressure, NF is the most practicable approach for effectively eliminating organic molecules with low molecular weights in the range of 200–1000 g/mol such as reactive dyes from wastewater. However, during the filtration phase, the NF method has been confronted with a significant setback due to flow reduction caused by concentration polarisation and membrane fouling. It is the collection of solute molecules close to the membrane surface layer that is referred to as concentration polarisation. This accumulation of solute molecules may cause pores to get blocked, resulting in flux reduction in the operating NF membrane. As a result, because of the high concentration of pollutants in unprocessed industrial dye effluent, NF cannot treat it directly. To avoid membrane fouling and degradation, it is critical to adopt a comprehensive pre-treatment approach as soon as possible. The pre-treatment process can be carried out either on the dye effluents or on the membrane, as demonstrated in the previous study, which used electrocoagulation as the pre-treatment unit followed by NF for the purification of industrial dye wastewater (Moradihamedani, 2022).

2.4.1.5 Ultrafiltration

The use of ultrafiltration (UF) is yet another membrane separation technology that is useful for the removal of particles and macromolecules from solutions. Currently, it is being used as a wastewater treatment technology by sectors such as pharmaceutical, chemical, and food production companies on a daily basis (Moradihamedani, 2022). In comparison to reverse osmosis and nanofiltration, ultrafiltration requires less pressure, making it more cost-effective. Large pores might only produce low rejection, though. Pore sizes in ultrafiltration membranes range from 0.1 to 0.001 microns (Ahmad et al, 2015). Also being considered is the treatment of dye wastewater discharged by textile manufacturing industries. However, because the molecular weight of the dyes is smaller than the molecular weight cutoff (MWCO) of the UF membrane, the application of UF for dye removal from wastewater is constrained. The dye removal percentage of the UF approach is not greater than 90 percent, while some evidence suggests that the dye removal performance of UF membranes can be improved to greater than 90 percent removal by incorporating hydrophobic membranes (Moradihamedani, 2022).

2.4.1.6 Reverse osmosis

Using reverse osmosis (RO) technology, ions, and macromolecules can be efficiently removed from wastewater effluent. The permeate water recovered through RO is typically colourless and low in salinity. In contrast, the use of a dense polymeric membrane in conjunction with a high osmotic pressure caused by a high salt concentration result in a significant reduction in permeate flux, as well as the development of critical membrane fouling, both of which have a negative impact on the membrane performance. Because of this, in order to achieve an adequate, permeate flux and reduce membrane fouling in RO applications, the transmembrane pressure must be greater than 20 bar, resulting in substantial operation and maintenance expenses. When the salt concentration is very high in wastewater treatment studies and Nanofiltration penetrates water quality is not satisfactory to be reclaimed in the system, the application of RO membranes is generally favoured. Because of these restrictions, there aren't many investigations on the removal of dyes from wastewater by reverse osmosis membranes (Moradihamedani, 2022).

2.4.2 Chemical method

Chemical dye removal procedures are those that employ chemistry or chemical-related theories to achieve dye removal (Katheresan et al., 2018). The use of a coagulating/flocculating agent in the chemical treatment of dye wastewater is one of the most reliable methods of colour removal. The procedure requires adding agents to the dye effluent, such as aluminium (Al^{3+}), calcium (Ca^{2+}), or ferric (Fe^{3+}) ions, in order to promote flocculation. In addition to these agents, other agents have also been employed in the procedure. Sometimes a mixture of two or more of these may also be used to improve the process (Gupta, V.K., 2009). The advanced oxidation process, electrochemical destruction, Fenton reaction dye removal, oxidation, ozonation, photochemical, and ultraviolet irradiation are all examples of conventional chemical dye removal processes (Katheresan et al., 2018). Coagulation, flocculation, and ozonation are the most popular chemical treatment methods for pollutant removal, particularly those discharged in textile effluent (Slama et al., 2021). The chemical techniques are frequently prohibitively expensive, and while the colours are removed, the accumulation of concentrated sludge causes a disposal challenge. There is also the chance that a secondary pollution problem will occur as a result of the excessive usage of chemicals (Demirbas, 2009).

2.4.2.1 Coagulation/Flocculation

The simplest chemical procedures for the processing of textile dye effluent are coagulation and flocculation. Adding charged chemical colloids (Aluminium sulphate ($Al_2(SO_4)_3$), Iron (III) chloride ($FeCl_3$), Iron (II) sulphate ($FeSO_4$), alum, lime, etc.) to polluted water causes coagulation and settling with oppositely charged particles, allowing insoluble elements to be removed (Slama et al., 2021). The idea is to destabilise dispersed solid particles in water by lowering their surface charge and clumping them together into bigger particles. Flash mixing, coagulation, and flocculation are the three

processes of operation. Coagulants are first added and mixed vigorously. The coagulants then work to lower or neutralise the surface charge of finely dispersed particles. The fine particles are then brought closer together and formed into larger particles using flocculants and gentle mixing. After that, sedimentation is used to get rid of the bigger particles (Ahmad *et al*, 2015). The key limitations of this approach are the generated residues and the need for additional treatments to assure the removal of any remaining soluble pollutants (Slama *et al*., 2021).

2.4.2.2 Ozonation

This method employs ozone as a powerful oxidant, and its cleaning qualities enable it to remove harmful textile effluent chemicals such as azo dyes (Slama *et al*., 2021). Because of the powerful oxidative activity of ozone, it is one of the most appealing and successful procedures for removing colours from water (Ahmad *et al*, 2015).

The main drawbacks of this method are that it is highly subject to a variety of conditions (pH, salts, temperature, and so on), that it can release dangerous substances, and that it is expensive (Slama *et al*., 2021).

2.4.2.3 Oxidation

The use of oxidising chemicals in wastewater treatment is known as oxidation. Chemical oxidation and UV-assisted oxidation employing chlorine, hydrogen peroxide, Fenton's reagent, ozone, or potassium permanganate for the treatment of industrial and wastewater effluents are the most commonly described methods. pH and catalysts are crucial in the oxidation process (Ahmad et al, 2015).

2.4.3 Biological method

Because they are environmentally friendly, use few chemicals, and require little energy, biological treatment processes for the removal of contaminants from wastewater are thought to be very effective. The basic idea behind biological treatment methods is the biological breakdown of waste materials into simpler and harmless species through the action of numerous microorganisms (Ahmad et al, 2015). Pollutant removal is a natural process that takes place in the presence of a wide variety of suitable microorganisms such as bacteria, fungi, algae, and yeast in wastewater and/or polluted environments (Slama *et al*., 2021). The various treatment methods can be divided into aerobic and anaerobic processes. Both procedures are typically used to treat wastewater. It's possible to utilise bacteria, fungi, algae, or plants as organisms. Additionally employed in biological treatment is the enzyme system. Carbon dioxide, water, and biomass are the end results of aerobic treatment while carbon dioxide, methane, and biomass are the end products of anaerobic treatment. With minimal expense and investment, this method can handle dye solutions in an environmentally acceptable manner (Ahmad et al, 2015; Rai et al., 2005).

Bacteria and fungi are the most commonly utilised microorganisms in the aerobic decolorization of dyes. Bacteria can grow and multiply faster than fungi because they can metabolise chlorinated and other organic pollutants and use them as a carbon or energy source (Dawood & Sen, 2014).

This process might potentially be generated in the laboratory by isolating and screening suitable bacteria, followed by a scale-up to enable textile effluent treatment and decolorization. The relevant microorganisms such as bacteria, fungi, and algae convert toxic wastewater molecules into non-damaging or even useful products using a variety of strategies such as adsorption, biosorption, bioaccumulation, alleviation, elimination, or mineralization. This approach attracted a lot of attention because it was eco-friendly, safe, clean, and cost-effective because it could be integrated with other technologies and leads to further development (Slama et al., 2021; Yaashikaa et al., 2021). Environmental pollutants are being removed from the environment through the use of biochar, microbial biomass, industrial waste, and the modification of organic substances, which has been proven to be an effective technique for improving the fertility and quality of soil (Yaashikaa et al., 2021). Bioremediation techniques use recombinant and natural bacteria to decompose harmful chemicals such as dyes under aerobic or anaerobic conditions into harmless substances such as carbon dioxide and water. The versatility of these biological techniques may be recognised by the fact that they can be executed in situ or ex-situ and conciliated by a mixed consortium of microorganisms and/or pure strains of microbes, as well as plants (i.e., phytoremediation) (Vikrant et al., 2018). The exploitation of microbial biomass for pollution removal from soil and water is a new technology that is being developed. Biosorption is a biological technique that employs a variety of biological materials, including bacteria, fungi, yeast, algae, and other organisms, to remove environmental pollutants that have been shown to be effective. a sorbent (biosorbent) and an adsorbent are used in this procedure. Biosorption is a potential approach for removing or recovering contaminants from aqueous solutions that are relatively modest in cost. The uptake of pollutants occurs as a result of physicochemical interactions between the pollutant and the adsorbent material. This concept has gained popularity in recent years, and a variety of materials, as well as biological materials, have been employed as adsorbents to effectively remove environmental toxins from the environment (Yaashikaa et al., 2021).

Table 2.3: Pros and cons of dye removal techniques

Technique	Pros	Cons
Adsorption	- Effective for a wide range of dyes.	- Adsorbents may need regeneration or disposal.
	- Can be applied to both small and large-scale operations.	- Initial cost of adsorbents can be high.
	- Relatively simple operation.	
Biological Treatment	- Environmentally friendly.	- May require longer treatment times.
	- Can handle complex dye structures.	- Temperature and pH sensitivity.
	- Low operating and maintenance costs.	- Biomass production and disposal challenges.
Chemical Precipitation	- Effective for metal-complex dyes.	- Generates sludge, requiring proper disposal.
	- Fast removal of dyes.	- pH adjustments may be needed.
	- Applicable to a variety of dye types.	
Membrane Filtration	- High removal efficiency.	- Membrane fouling requires regular maintenance.
	- Selective removal based on molecular size.	- Energy-intensive in some cases.
	- Compact and modular design possible.	

(Mohan et al., 2004; Sangeeta Sharma & Kaur, 2018; Yagub et al., 2014)

Despite advancements in dye removal techniques, several challenges persist:

- **Treatment of Complex Dye Mixtures**: Efficient removal of mixtures of dyes with diverse structures remains a challenge.
- **Energy Consumption**: Some techniques, especially those involving membrane filtration, can be energy-intensive.
- **Scale-Up Issues:** Scaling up laboratory-proven techniques to industrial levels without compromising efficiency and cost-effectiveness.
- **Byproduct Management:** Proper handling and disposal of byproducts, such as sludge generated in chemical precipitation.
- **Cost-Efficiency for Small-Scale Operations:** Developing affordable and efficient methods suitable for smaller facilities or decentralized systems.
- **Regeneration of Adsorbents:** Sustainable methods for regenerating adsorbents in adsorption processes.

Addressing these challenges requires interdisciplinary research and innovative solutions to make dye removal processes more sustainable, economically viable, and adaptable to various scenarios.

2.5 Biosorption

Biosorption is the passive absorption of contaminants from aqueous solutions using non-growing or dead microbial biomass, allowing the pollutants to be recovered and/or disposed of in an environmentally responsible manner (Dotto et al., 2013). Biosorption is a form of sorption in which the sorbent is a biologically derived material. The majority of chemical and physical methods for determining absorbent effectiveness are straightforward in design, but their high cost is a drawback (Ahmad et al., 2008). Biosorption is now widely regarded as a simple, cost-effective, and environmentally friendly process that can be used as a viable alternative to existing pollution removal methods. It is a type of bioremediation that is used to reduce environmental pollution in the context of improper textile waste disposal (Fomina & Gadd, 2014; Torres, 2020). It is a process in which ions from an aqueous solution bind to functional groups on the surface of biomass in a fast and reversible manner. It is the removal or binding of soluble or insoluble compounds from an aqueous solution by biological components. This method is effective, selective, and unaffected by cellular metabolism (Gadd, 2009).

Nature provides a wide range of biomaterials that have been used as biosorbents to achieve the desired pollution removal results. In a variety of methods and relations with a range of substances, all forms of microbial, plant, and animal biomass, as well as their derivative products, have piqued the interest of researchers. However, microbial biomass is employed as biosorbents for their potential application as biosorbents (Hu & Reeves,

1997), and has been studied in the biosorption of dyes (Aksu, 2005; Gadd, 2009), including mixed organism/biomass systems. These include archaea, bacteria e.g., *Azotobacter, Ahthrobacter spp., Bacillus megaterium, Bacillus subtillis, Staphylococcus spp., Pseudomonas marginalis* (Cai Y et al., 2018; Gadd, 2009), algae (including macroalgae, i.e., seaweeds, *C. vulgaris, Sargassum nayans, Sargassum wightii* (Cai Y et al., 2018; Gadd, 2009; Kucuker et al., 2017) and fungi which include the filamentous forms e.g., *Aspergillus niger, Rhizopus arrhizus, Basidomycetes,* and *Mucor Penicillium spp* (Cai Y et al., 2018) as well as unicellular yeasts e.g., *Saccharomyces cerevisae*, fruiting bodies (mushrooms, brackets, etc.) and lichens (Gadd, 2009).

Biosorption processes are critical in both environmental and conventional biotreatment operations. Biological materials, such as living or dead microbes and their components, marine algae, plants, agricultural wastes, and naturally produced inhabitants, are designed to remove or reclaim organic and inorganic debris from solution (Tripathi, 2012). Biological oxidation and chemical precipitation, for example, are very expensive, take a lot of energy, and can produce hazardous by-products. The adsorption method offers a potential alternative for dye decontamination from wastewater in terms of cost, energy needs, flexibility, and ease of design and application (Edokpayi & Makete, 2021). Biosorption is a long-promised and surprisingly cost-effective biotechnology. Despite substantial progress in understanding the complex phenomenon and the number of publications in this field, biosorption technology marketing remains a developing global business (Fomina & Gadd, 2014). AlgasorbTM, AMT-BIOCLAIMTM(MRA), and Bio-fix were commercialised biosorbents in the early 1990s (Volesky & Naja, 2007). The biosorption technique has been shown to be significant due to its ability to attach to contamination on various biological materials. Because sorbents have different biological resources, biosorption mechanisms vary. Understanding the mechanism aids in controlling the removal of contaminants, increasing the sorbent's efficiency, and allowing for in-situ bio-rehabilitation. Because numerous factors work together on biosorbents, a general process is implausible. Numerous metals binding mechanisms, including coordination/chelation, complexation, ion exchange, and physio-adsorption, have also been proposed.

Due to their chemical properties, dyes are resistant to fading when exposed to water, light, and many chemicals, while many are difficult to decolorize due to their complex structure and synthetic origin (Edokpayi & Makete, 2021). Because synthetic dyes are difficult to remove from wastewater using existing methods, dye adsorption on a low-cost, high-efficiency adsorbent material is seen as a simple and cost-effective solution. The power to remove synthetic colours has been tested and evaluated for a wide range of inorganic and organic supports. Weak interactions between the adsorbate and the adsorbent, such as van der Waals interaction, hydrogen bonding, and dipole-dipole interactions, cause physical adsorption to occur reversibly. Chemical adsorption is irreversible when strong interactions between an adsorbate and an adsorbent take place, such as the formation of covalent and ionic bonds (Aljeboree et al., 2017). In this respect, it would be interesting to see if *Serratia marcescens* MM06 biomass is suitable for use as a biosorbent to remove congo red dye. To better depict the utilisation of bacterial biomass in dye biosorption, a Scopus keyword search on "Adsorption," "Dyes," and "Bacteria" yielded 19 journal papers published since 2012. **Figure 2.2** shows the keyword co-occurrence of the 19 papers created with the VOS Viewer software.

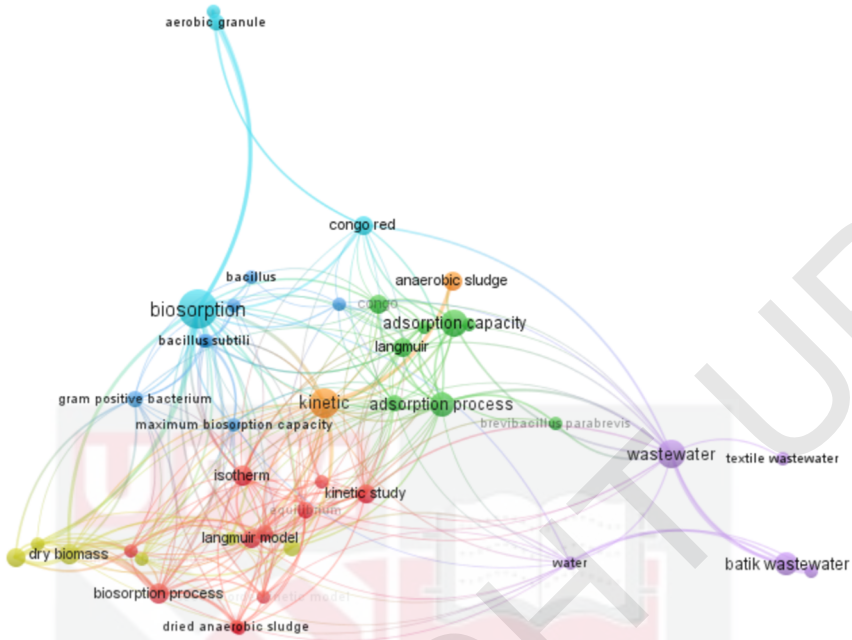

Figure 2.2: Keyword mapping for SCOPUS from 2012 to 2021 based on the co-occurrence of author keywords in SCOPUS papers
(Keywords: adsorption, dyes, and bacteria)

2.5.1 BIOSORBENTS

Biosorption employing dead microbial cells offers substantial advantages for water purification because to their tolerance to hazardous wastes, independence from a constant supply of nutrients, and regenerative and recyclable nature. If dead cells are stored at room temperature for an extended period of time, no putrefaction will occur. They require little maintenance and recover rapidly from harm. Furthermore, research has revealed that dead cells can acquire contaminants like dyes at the same rate as active or dormant cells (Aksu, 2005).Utilizing microorganisms for the treatment of dye wastes is one of the most advantageous methods compared to other applications due to its practicability, productivity, simplicity, and low cost (Manogaran et al., 2021). Biological adsorbents are derived from living organisms. These biosorbents have a strong affinity for a variety of contaminants that can be found in soil and bodies of water (Yaashikaa et al., 2021). Microbial biomass is employed as biosorbents for their potential application as biosorbents (Hu & Reeves, 1997), and has been studied in the biosorption of dyes (Aksu, 2005; Gadd, 2009), including mixed organism/biomass systems. These include archaea, bacteria e.g., *Azotobacter, Ahthrobacter spp., Bacillus megaterium, Bacillus subtillis, Staphylococcus spp., Pseudomonas marginalis* (Cai Y et al., 2018; Gadd, 2009), algae (including macroalgae, i.e., seaweeds, *C. vulgaris, Sargassum nayans, Sargassum wightii* (Cai Y et al., 2018; Gadd, 2009; Kucuker et al., 2017) and fungi which include the filamentous forms e.g., *Aspergillus niger, Rhizopus arrhizus, Basidomycetes,* and *Mucor Penicillium spp* (Cai Y et al., 2018) as well as unicellular yeasts e.g.,

Saccharomyces cerevisae, fruiting bodies (mushrooms, brackets, etc.) and lichens (Gadd, 2009).

2.5.2 Benefits of using bacterial biomass for biosorption

i. It is highly efficient and cost-effective as there is no maintenance needed, the biomass can be stored for extended periods of time without losing effectiveness and regeneration is more feasible.

ii. Low operational Cost, the process is straightforward in design, quick, and effective.

iii. Environment–friendly, as it is possible to focus on a wider variety of environmental factors

iv. Living cells are not constrained, and aseptic conditions might not be required.

v. Biosorption can be done with the help of leftover bacterial biomass, which can be obtained from fermentation industries.

vi. Does not result in the formation of harmful substances. The amount of chemical reagent it uses is extremely small, and it doesn't produce toxic byproducts or metabolites. Thus toxicity related problems are avoided

vii. Minimization of chemical or biological sludge

2.5.3 Drawbacks of using bacterial biomass for biosorption

i. Since biosorption involves the transfer of sorbate from one medium to another, the final disposal of the bacterial biomass has been a major concern

ii. There is a restriction on potential improvements to biological processes, such as when cells are genetically altered. That is to say, since biomass consists of nonliving cells, there is no biological control over the biosorbent.

iii. The specificity of ions or functional groups is a concern because ion exchange and biosorption are the two processes most frequently compared.

The use of bacteria for the adsorption of synthetic and natural dyes is an intriguing area of study with potential applications in wastewater treatment and environmental remediation. Bacteria possess various mechanisms for adsorbing dyes, and understanding these processes is crucial for optimizing their use in dye removal (Roy et al., 2018).

2.5.4 Role of Bacteria in Dye Adsorption

i. Metabolic Activities: Bacteria can use dyes as a carbon and energy source through metabolic activities. Some bacteria produce enzymes that can degrade or transform dyes into less harmful compounds (Roy et al., 2018; Kumar et al., 2015).

ii. Adsorption on Cell Surfaces: The cell surfaces of bacteria often have functional groups such as hydroxyl, amino, and carboxyl groups that can interact with dye molecules through electrostatic forces, hydrogen bonding, and Van der Waals forces (Roy et al., 2018).

iii. Bioaccumulation: Some bacteria have the ability to accumulate dyes within their cellular structures, leading to the removal of dyes from the surrounding environment (Aksu, 2005; Gadd, 2009).

2.5.5 Mechanism of Action

i. Physical Adsorption: Bacteria can physically adsorb dye molecules onto their cell surfaces. The electrostatic interactions between charged functional groups on the bacterial cell surface and the dye molecules play a crucial role in this adsorption process (Singh & Singh, 2017; Sharma & Kaur, 2018) .

ii. Chemical Adsorption: Chemical adsorption involves covalent bonding between the dye molecules and functional groups on the bacterial cell surface. Enzymatic activities of bacteria may be involved in the chemical transformation of dye molecules (P. K. Singh & Singh, 2017).

iii. Intracellular Uptake: Bacteria may take up dye molecules into their cells through active transport or passive diffusion. This intracellular uptake can contribute to the removal of dyes from the aqueous environment (P. K. Singh & Singh, 2017).

2.5.6 Analysis of Bacteria-Mediated Dye Adsorption

i. Spectrophotometric Analysis: Spectrophotometry can be used to analyze the concentration of dyes in solution before and after bacterial treatment. A decrease in the absorbance of the dye at its characteristic wavelength indicates adsorption (Khan et al., 2018; Yenikaya et al., 2010).

ii. FTIR (Fourier Transform Infrared) Spectroscopy: FTIR spectroscopy can be employed to study the functional groups present on bacterial cell surfaces and how they interact with dye molecules (Öztürk et al., 2020).

iii. SEM (Scanning Electron Microscopy) and TEM (Transmission Electron Microscopy): Microscopic techniques like SEM and TEM can provide visual evidence of the adsorption process by showing the attachment of dye molecules on bacterial cell surfaces (Dandge et al., 2016).

iv. Biosorption Isotherm Models: Mathematical models such as Langmuir and Freundlich isotherms can be applied to understand the equilibrium relationship between dye concentrations and their adsorption onto bacterial surfaces (Öztürk et al., 2020; Roy et al., 2018).

Studying the role and mechanism of action of bacteria in dye adsorption is crucial for developing efficient and sustainable methods for dye removal from industrial effluents and wastewater. Researchers continue to explore new bacterial strains and optimize conditions for maximizing dye adsorption efficiency.

2.6 Mechanism of dye removal

Biosorbents are made from a variety of raw biomass, including plants, fungi, yeast, algae, and bacteria (Torres, 2020; Roy et al., 2018; Vijayaraghavan & Yun, 2008). Because different biomass has complex properties that vary, different mechanisms exist for these biosorbents to remove dyes (biosorbates) (Cid et al., 2015; Du et al., 2012; O'Mahony et al., 2002; Mona et al., 2011). However, a few of these mechanisms are still poorly understood. The structure and characteristics of the extracellular polymeric component of the biosorbents are generally considered to be responsible for the dye's biosorption mechanism (Du et al., 2012; McKay et al., 1999). Different functional groups either draw or shield the dye pollutants depending on the biosorbent being used (Hastuti et al., 2020; Pereira & Alves, 2012; Sassi Mohamed, Bestani Benaouda, 2014). The biomass contains functional groups such as carboxyl, sulfonate, amide, carbonyl, imine, sulfhydryl, phenolic, imidazole, phosphodiester, and phosphate groups (Fawzy et al., 2019; Karthik et al., 2016). The significance of these groups for the biosorption of dye pollutants by a given biomass depends on a number of distinct factors. These specific components include the number of the biosorbent's reactive sites, their number, and the strength or affinity of the binding between a given dye and the site (site availability, site functional chemical condition, and reactive site availability) (Asgher, 2012; Won et al., 2008). Because of this, the presence of some of these functional groups does not ensure efficient dye biosorption in the presence of conformational, steric, or other obstructions (Nath & Ray, 2015; Pereira & Alves, 2012). Adsorption complexation, surface adsorption, chemisorption, and diffusion are the main mechanisms by which dye biosorption is mediated (Fomina & Gadd, 2014; Venkata Mohan et al., 2002). pore diffusion, film diffusion, and chemical processes like complexation and ion exchange are most crucial (Tran et al., 2016; Iftekhar et al., 2018). Intermolecular interactions are most likely in the biomass-dye system, with the amine site being the most reactive group and followed by the hydroxyl group (Iftekhar et al., 2018).

2.6.1 Complexation

A complexation or coordinate complex is made up of a number of bound molecules or ions known as ligands (Abdi & Kazemi, 2015; Mahmood et al., 2016). A central ion or atom, which is typically metallic, makes up the substance. Numerous metal-containing compounds contain these complexes (Iddou et al., 2011). It might be covalent or electrostatic. It can be confusing because there are so many different ways to represent the mechanisms and reactions of coordination complexes (Fawzy et al., 2019). The atom bonded to the primary metal atom or ion is known as the donor atom (atom in the ligand) (Abdi & Kazemi, 2015). Several donor atoms, which may or may not be the same, are bound to a metal ion in a specific complex. Any ion or molecule that has multiple atoms that bond to the central atom is referred to as a multiple-bonded ligand (Karakagh et al., 2012). The words "complexation," "chelation," and "coordination" are used to describe these complexes (Abdi & Kazemi, 2015).

2.6.2 Chelation

This process involves the bonding of molecules and ions to metal ions (Abdi & Kazemi, 2015; Asgher, 2012). Two or more distinct coordinate bonds are created between the single central atom and the multiple-bonded (polydentate) ligand. Forming complexes with multidentate ligands is another name for chelation (Fomina & Gadd, 2014). The biosorption process can be independent of or combined with electrostatic interaction, ion exchange, precipitation, chelation, and complexation processes, as has been realized and described in numerous studies. In order for the technique to work, dye molecules are partially dissolved in textile wastewater before the hazardous residues are left in the effluents (Buthelezi et al., 2012).

2.6.3 Precipitation

In this procedure, a chemical substance that is soluble is changed into a solid. Precipitation can produce extremely high absorption capacities but can also prevent desorption, with bound metal/radionuclide species acting as loci for eventual deposition (Fawzy et al., 2019; Kiran et al., 2006). Precipitation or cation exchange processes were the main causes of cadmium adsorption onto feedstock-derived biochar. The adsorption processes of Cadmium onto magnetic graphene oxide were also reported by Huang et al. (2018) as metal hydroxide precipitation, isomorphic exchange, and complexation with functional groups. The adsorption processes are, however, currently the subject of a thorough investigation.

2.7 Factors affecting the adsorption of dye

The biosorption process is mostly influenced by environmental factors. A previous study has shown that temperature, biosorbent dosage/adsorbent size, pH, initial dye concentration, time, and agitation are the parameters that have an impact on the

effectiveness and capacity of the biosorption process (Kucuker et al., 2017). The binding properties are also found to be impacted by physical processes like drying, boiling, mechanical disruption, and autoclaving. Other factors include biomass concentration, surface area to volume ratio, and pollutant solubility (Gadd, 2009; (Mahmood et al., 2016). The solution pH is said to play a significant role in biosorption in numerous pieces of literature. It has an impact on the solution chemistry as well as the functional groups of the biosorbents' activity (Iftekhar et al., 2018; Pereira & Alves, 2012). Additionally, in various biosorbent systems, including bacteria, dye biosorption is influenced by the pH of the solution. The most important biosorption factor is probably pH out of all the other factors (Liu Chen et al., 2011).

2.7.1 pH

In adsorption capacity, the pH of the dye solution has a vital effect where both the ionization of the dye and the surface connection points of this adsorbing product are affected (Suyamboo, 2012). Dye-containing wastewater treatment is pH-dependent (Mall et al., 2005). The pH of the dye solution might have a significant impact on the adsorption of a molecule because pH variations might encourage adsorbent and adsorbed load changes (Alnajrani & Alsager, 2020). Because pH modifies the ionization state of the binding groups of both adsorbate and adsorbent, it affects the adsorption behavior of the systems studied, increasing or decreasing adsorption capacity, therefore is necessary to optimize the pH for better absorption (Litefti et al., 2019), Lower pH results in high concentrations of protons, which neutralize the negative charge on both R. arrhizus and humic acid. Because pH is the most critical parameter influencing not only biosorption capacity but also the color of the dye solution and the solubility of dyes, several studies have explored the influence of pH on dye removal (Aksu, 2005).

2.7.2 Adsorbent size

The amount of biosorption is significantly influenced by the biosorbent dosage. In many cases, higher uptakes are achieved with lower biosorbent dosages (Roy et al., 2018; Velkova et al., 2018). But as the surface area increases, the number of binding sites for the biomass also rises, increasing the amount of dye absorbed (Vijayaraghavan & Yun, 2008). The kinetics of biosorption is linked to the biosorbent surface area such that particle size is also a major component that influences Biosorption capacity (Aksu, 2005). The amount of biosorbent employed is an important parameter for the sorption process since it is responsible for the number of surface groups capable of connecting biomass under certain process conditions (Witek-Krowiak, 2013). The previous research showed that the adsorption percentage increases when adsorbent doses are raised, and the amount of adsorbed dye decreases with the increase in dosage per unit weight of the adsorbent. The former statement can be because the active sites can be efficiently used and exploited when the dosage is low while the latter may be ascribed to the addition of adsorbent particles at large doses, thereby reducing the adsorbent's total surface, and increasing the diffusion path length (Suyamboo, 2012).

2.7.3 Initial dye concentration

A crucial driving factor to overcome any mass transfer impedance between the acoustic and solid phases of the dye is the initial concentration of the dye. Thus, a larger initial concentration of dye would improve biosorption (Aksu, 2005; Hubbe et al., 2012; Y. Wang et al., 2006). At larger concentrations of dye, the biosorption capacity rose dramatically, this indicates some form of cooperativity to interactions between the dye and the biomass (Aksu, 2005).

2.7.4 Temperature

Temperature is one of the most important parameters influencing the biosorption process (Rosca et al., 2018; Witek-Krowiak, 2013). As the sorption processes tend to be exothermic the sorption performance varies with the temperature, which has already been proven. Although biosorption is not a significantly exothermic process like other physical adsorption processes, temperature fluctuation can increase its efficacy (Rosca et al., 2018). Temperature is also an essential design element that would impact the capacity for biosorption in the actual application of biomass biosorption (Aksu, 2005). Along with temperature, thermodynamic parameters were utilized to identify the nature of the adsorption process, such as exothermic or endothermic, spontaneity and unpredictability, and whether or not the temperature is suitable for the process. The main thermodynamic parameters are $\Delta G°$, $\Delta H°$, and $\Delta S°$, which indicate changes in Gibbs free energy, enthalpy, and entropy, respectively. The negative values of $\Delta G°$ indicate that the adsorption process is spontaneous. Similarly, positive $\Delta H°$ values suggest that the process is endothermic. Also, the amount of $\Delta H°$ appears to be connected to the kind of sorption, namely physisorption ($\Delta H°$ 50 kJ/mol) and chemisorption ($\Delta H° > 50$ kJ/mol) [30].

2.7.5 Effect of contact time

The contact time has a considerable impact on the adsorption process. Contact time can also affect the process's economic efficiency as well as the adsorption kinetics. As a result, contact time is another performance-determining factor in the adsorption process (Iftekhar et al., 2018). Kinetic experiments were conducted to establish the contact time needed for the biosorbent to achieve equilibrium with the adsorbed adsorbate (Witek-Krowiak, 2013). Previous research has explained that an optimal time of contact can be achieved if an optimal pH, biomass dose, and temperature of the mixed solution has been standardized to shake a number of centrifuge tubes in an electrically thermostatic reciprocal shaker for different intervals, and then centrifuged to obtain the result (Cai Y et al., 2018). Most biosorption experiments have indicated a quick initial adsorption rate before the process is slowed and an equilibrium concentration is reached (Fathollahi et al., 2021).

2.7.6 Agitation

Agitation speed is an essential parameter in sorption processes, as it has a significant impact on the distribution of the solute in the bulk solution and the creation of the external boundary layer**.** The biosorption process reacts to the speed at which the rotary shaker agitates. The recording of biosorption at various rates thus indicated the optimal speed. Initial dye concentration, adsorbent size, temperature, contact time, and pH are maintained continuously. With an increase in agitation speed from 50 rpm to 130 rpm, the percentage of dye adsorbed increased from 88 to 93 percent, confirming that the influence of external diffusion on the sorption kinetic control plays a significant role in increasing the agitation speed, Because of increased turbulence and a decrease in the thickness of the liquid boundary layer, the rate of diffusion of dye molecules from the bulk liquid to the liquid boundary layer around the particle increases (Suyamboo, 2012).

2.8 Fourier transform infrared spectroscopy (FTIR) Study

The technique of FTIR spectroscopy detects the different groups with biosorbent which may bind the dye ion to bio-sorbent surfaces. (El messaoudi et al., 2016). It delivers essential information on the nature of the bonds and permits the identification of a cell wall structure of several functional groups. The magnitude of band shift by natural (pure) and dye-loaded (treated) biomass shows the level of interactions between functional groups and dye cations. The FTIR of the dye, bacterial biomass, and the absorbed dye are studied at different temperatures, and earlier research has shown that the microbial biomass absorbs the dye molecule more efficiently at low temperatures. The majority of the dye's functional groups are absorbed by the microbial biomass significantly more than at higher temperatures. (Öztürk et al., 2020)**.** In FTIR analysis, the biomass is mixed with dye, and an incubation routine is followed. The mixture is centrifuged to generate a pellet, which is then dried before analysis. The pellet is used to record the spectra within the region of 400-4,000 cm^{-1} of the FTIR spectrophotometer. The study is conducted before and after the biosorption process to determine the particular bond or functional group, for example, aliphatic sulfoxides, aliphatic ethers, and primary aliphatic alcohols that occur on the surface of the adsorbents with a substantial amplitude (A. Gupta & Balomajumder, 2015).

2.8.1 Scanning electron microscopy (SEM)

Scanning electron microscopy (SEM) images are routinely used to study the morphological features and surface characteristics of adsorbent materials. It shows the surface texture and porosity of the adsorbent. It's also useful for calculating how much surface area of adsorbents is available for dye adsorption (Dandge et al., 2016).

2.9 Adsorption Kinetic

The dye uptake rate is described by adsorption kinetics, which regulates the adsorption residence time. It also aids in the evaluation of sorbent efficacy for usage in the adsorption process (Karthik et al., 2019). Adsorption kinetic was utilized to determine the adsorption mechanism, such as physisorption induced by van der Waals force and chemisorption induced by chemical interaction between adsorbate and adsorbent. The goal of the adsorption kinetic investigations was to estimate the effectiveness of dye biosorption on biomass (Caner et al., 2011). Kinetic modeling explains how the adsorption capacity changed over time and how it may be used for the adsorption of adsorbate onto the surface of an adsorbent. (A. Gupta & Balomajumder, 2015). According to earlier research and literature, pseudo-first-order and pseudo-second-order models generally describe the kinetics of microbial biosorption (Gadd, 2009; Suyamboo, 2012) as well as Elovich's kinetic model (Tan & Hameed, 2017) and are used to test the experimental data in order to explore the governing mechanisms of adsorption processes such as mass transfer and chemical reactions (H. Chen & Zhao, 2009). as shown in **equation 2.1** and **2.2** respectively (Yasid et al., 2020). Therefore Pseudo-first-order, Pseudo-second-order, and Elovich models are examples of widely used biosorption kinetic models **(Table 2.4).**

$$q_t = q_e(1 - e^{-k_1 t}) \tag{2.1}$$

Where,
$k_1^{(h-1)}$ = the pseudo-first-order model constant rate,
qe and qt (mg/g) are the adsorption capacity at equilibrium and at time t (h), respectively

$$q_t = \frac{k_t q e^2 t}{1 + k_2 q_e t} (\tag{2.2}$$

Where k_2 (g $mg^{-1}h^{-1}$) is the second-order kinetic constant.

$$\frac{dq}{dt} = a \exp(-bq_t) \tag{2.3}$$

where α is the initial sorption rate (mg/g min), and β is the extent of surface coverage and activation energy for chemisorption (g/ mg).

Table 2.4: Commonly used kinetic models

Model	Equation	Reference
Pseudo-1st order	$q_t = q_e(1 - e^{-K_1 t})$	(Lagergren, 1898)
Pseudo-2nd order	$q_t = \frac{K_2 q_e^2 t}{(1 + K_2 q_e t)}$	(Ho and McKay, 1999)
Elovich	$q_t = \frac{1}{\beta ln \alpha \beta} + \frac{1}{\beta ln t}$	(Zeldovich, 1934)

2.10 Biosorption equilibrium Isotherms

Adsorption isotherms reveal the sorbent-sorbate interaction mechanism and reflect the adsorbent's performance. They can also be used to define the ratio between the amount of adsorbate adsorbed on an adsorbent and the adsorbate's equilibrium concentration in an aqueous solution (Edokpayi & Makete, 2021). The term "biosorption isotherm" refers to the connection or relationship between the concentrations of adsorbate in solution (liquid phase) and adsorbent (solid phase) at a constant temperature under a given condition, such as pH and ionic strength, fixed mass, and particle size of adsorbent (Tran et al., 2016; Zhou et al., 2019)**.** When the biosorption process achieves an equilibrium state, biosorption isotherms describe how dye molecules are distributed between the liquid and solid phases at a constant temperature. (Aryal, 2020; Gb, 2016; Nayak & Pal, 2020). The biosorption equilibrium has been described by several isothermal equations. Equilibrium adsorption isotherms give important information on the likely process for biosorption, capacity, surface characteristics, and biosorbent affinity (Gb, 2016; Nayak & Pal, 2020; Tafakori et al., 2017)**.** Equilibrium biosorption studies give essential insight into how the reaction pathways or interaction between biosorbent and biosorbate occur, the mechanism of the reaction, and other fundamental information is gained by creating an appropriate model that matches the biosorption data effectively (Gadd, 2009; Tafakori et al., 2017; Zhou et al., 2019). The Langmuir and Freundlich theoretical models are the most common Isotherms and were used in their linear forms. (Alnajrani & Alsager, 2020; Tafakori et al., 2017; Vijayalaks et al., 2019; Y. Wang et al., 2006) **,** and are determined from equations 1 and 2 (Wu et al., 2020; Yahuza et al., 2020). Others include Temkin, Redlich- Peterson, Dubinin−Radushkevich (D− R) (Witek-Krowiak, 2013; Wu et al., 2020), Hill–de Boer, Jovanovic, Hill, Toth, Fritz–Schlunder, Sips, Khan, Radke–Prausnitz, Baudu, and BET, etc. These biosorption isotherms represent the optimal biosorption system as well as the biosorbent's efficacy. As a result, it's critical to look into real-world (practical) data to come up with the best isotherm model for dye biosorption (Karthik et al., 2019). The Isotherm models for different dyes using microbial biomass are shown in **Table 2.5**. The equilibrium of the biosorption process is described by mathematical models in **Table 2.6**.

Table 2.5: Commonly used isotherm models for describing the equilibrium of the adsorption studies

Isotherms model	Parameter	Application	Formula	References
Henry's law	1	Not appropriate for processing data absorption in equilibrium.	$q_e = HC_e$	(Ridha & Webley, 2009)
Langmuir isotherm	2	Describe quantifiable monolayer adsorption in detail.	$q_e = \frac{q_{mL} b_L C_e}{1 + b_L C_e}$	(Langmuir , 1918)
Freundlich isotherm	2	Detailing multilayer adsorption. Refers to the uniform distribution systems used for adsorption on heterogeneous surfaces. referred also as reversible adsorption.	$q_e = K_F C_e^{\frac{1}{n_F}}$	(Adamson, 1993)
Temkin isotherm	2	The majority of applications included predicting gas phase equilibria. Due to molecule orientation, the model does not adequately describe the equilibrium data of liquid adsorption.	$q_e = \frac{RT}{b_T}\{ln(a_T C_e)\}$	(Temkin and Pyzhev, 1940)
Dubinin-Radushkevich	2	Use to figure out the parameters of adsorption and apparent free energy employing temperature-dependent adsorption data.	$q_e = q_{mDR} exp\left\{-K_{DR}\left[RTln\left(1 + \frac{1}{C_e}\right)\right]^2\right\}$	(Dubinin, 1965; Radushkevich, 1949)
Sip	3	has a finite limit once the concentration employed is significant enough to run into the issue of continuous adsorption rise with concentration.	$q_e = \frac{K_s q_{mS} C_e^{\frac{1}{n_S}}}{1 + K_s C_e^{\frac{1}{n_S}}}$	(Sips, 1948)
Toth	3	The equation is far more matched to multilayer adsorption. The relationship probably applies for liquid-solid adsorption.	$q_e = \frac{q_{mT} C_e}{\left(K_T + C_e^{n_T}\right)^{n_T}}$	(Toth, 1971)
BET	3	Designed to facilitate multilayer sorption.	$q_e = \frac{q_{mBET}\alpha_{BET} C_e}{(1 - \beta_{BET} C_e)(1 - \beta_{BET} C_e + \alpha_{BET} C_e)}$	(Brunauer S, Emmett PH, 1938)
Baudu	4	The constant is calculated by taking into account the parallel measurements at the various equilibrium concentrations, which demonstrates that they are not standards throughout a wide concentration range.	$q_e = \frac{q_{mB} b_B C_e^{(1+x+y)}}{1 + b_B C_e^{(1+x)}}$	(Baudu, 1990)
Parker isotherm	4		$q_e = q_{mP}\left\|-a_P\left(RTln\frac{C_s}{C_e}\right)^{b_P}\right\|$	(Parker, 1995)
Fritz-Schlunder-IV	4		$q_e = \frac{A_{FS} C_e^{a_{FS}}}{1 + B_{FS} C_e^{b_{FS}}}$	(Fritz & Schluender, 1974)
Weber-van Vliet	4		$C_e = P_1 q_e^{\left(P_2 q_e^{P_3} + P_4\right)}$	(Vliet et al., 1980)
Fritz-Schlunder-V	5	Use an empirical formula with five parameters to represent a wide range of equilibrium data.	$q_e = \frac{q_{mFS5} K_1 C_e^{\alpha_{FS}}}{1 + K_2 C_e^{\beta_{FS}}}$	(Fritz & Schluender, 1974)

Table 2.6: Kinetic and isothermal models of various bacterial sorption using different dyes

Absorbents	Absorbates	Isotherm model	absorption capacity	Kinetic model	Regression	Ref.
Acidithiobacillus Thiooxidans	sulfur dye	Langmuir	87.5%	PSO	-	(Nguyen et al., 2016).
Nostoc linckia HA 46	reactive red 198	-	93.5 mg/g	PSO	Linear	(Mona et al., 2011)
Bacillus cereus $M^{1}{}_{16}$ (MTCC 5521)	Malachite green	Langmuir	485 mg/g	PSO	Linear	(Nath & Ray, 2015)
Rhodopseudomonas palustris **51ATA**	Fast Black K salt	Langmuir, Freundlich, and Temkin.	-	-	Linear	(Öztürk et al., 2020).
Bacillus catenulatus JB- 022 strain	cationic basic blue 3	Langmuir	139.74 mg/g	PSO	Nonlinear	(Kim et al., 2015).
C. glutamicum	Reactive black 5	Langmuir	352, 282 and 291 mg/g for free, alginate and polysulfone immobilized respectively.	-	Non-linear	(Vijayaraghavan et al., 2007).
Anaerobic sludge	Rhodamine B	Langmuir and Freundlich	-	PSO	-	(Y. Wang et al., 2006).
Pseudomonas sp. strain DY1	Acid Black 172	-	-	PSO	-	(Du et al., 2012).
Bacillus megaterium	Reactive blue 5	Langmuir	-	PFO and PSO	Linear	(Liu Chen et al., 2011).
Bacillus cereus $M^{1}{}_{16}$	Acridine orange	Redlich Peterson	210.46 mg/g	PSO	Linear	(Bag et al., 2021).
Bacillus rigiliprofundi	Remazol Brilliant Blue R (RBBR)	Langmuir	-	PFO	-	(Biswas and Basak, 2021).
Bacillus subtilis	Safranin O	Langmuir	-	PSO	Linear	(Serap et al., 2023).
Cereus sp	Congo red	Langmuir	-	PSO	-	(Jeyavishnu & Alagesan, 2020)
Lysinibacillus sp. SS1	Malachite green	Langmuir	178.57 mg/g	PFO	Linear	(Kamath Miyar et al., 2021)
Streptomyces rimosus	Methylene blue	Langmuir and Freundlich	30.48 mg g−1	PSO	Linear	(Nacèra & Aicha, 2006)
Bacillus amyloliquefaciens	Acid Blue 225 and Acid Blue 062	Langmuir	111.15 and 112.19 mg/g, respectively	PSO	Linear	(Yenikaya et al., 2010)
Agrobacterium fabrum strain SLAJ731	Methylene blue	Freundlich	91 mg g−1	PSO	Linear	(Swati Sharma et al., 2018)
dried anaerobic sludge	Burazol Blue ED (BB)	Langmuir	127.5 mg/g	PSO	Linear	(Caner et al., 2009)
Corynebacterium glutamicum	Reactive Red 4	Langmuir	104.6 ± 8.7 mg/g	-	Nonlinear	(Sung et al., 2005)
Paenibacillus macerans	Acid Blue 225 and Acid Blue 062	Langmuir	94.98 and 95.08 mg g−1	PSO	Linear	(Çolak et al., 2009)

Table 2.6: Continued

Corynebacterium glutamicum	Reactive Black 5	Langmuir	419 mg/g	PSO	Nonlinear	(Vijayaraghavan & Yun, 2007)
Bacillus licheniformis	Congo red	Langmuir	-	PSO	Nonlinear	(Jinwon et al., 2021)
Bacillus subtilis KK01	Congo red	Freundlich	-	PSO	Nonlinear	(Sarim et al., 2019)
Bacillus macerans	Basic blue 41	Langmuir	89.2 mg/g	PSO	Linear	(Atar et al., 2008)
Bacillus subtilis	Methylene Blue	Freundlich	59 ±0.6 mg g–1	PSO	Linear	(Tural et al., 2017)
Planococcus sp VITP21	Black TSB (BT)	Freundlich	9.6 mg/gm	-	Linear	(Choudhary et al., 2015)
Bacillus cereus M^{1}_{16} (MTCC 5521)	Malachite green	Redlich Peterson	91 %	PSO	Linear	(Nath et al., 2015)
Flavobacterium mizutaii	Napthol blue black	Langmuir	-	PSO	Linear	(Das et al., 2012)
Rhodococcus erythropolis AW3	Crystal violet (CV)	Langmuir	289.8 mg g−1	PSO	-	(Canizo et al., 2019)
Pseudomonas pseudoalcaligenes	acid blue 25 (AB 25)	Langmuir,and Freundlich,	98 and 113.4 mg/g for AB 25 and Biofilm respectively	PSO	Linear	(Mawad et al., 2014)
Dried activated sludge	Reactive dye	Langmuir	74 mg/g	PSO	Linear	(Gulnaz et al., 2006)

Key: PFO =Pseudo first order, PSO =Pseudo second order

Kinetic Models Focus on time and emphasize the dynamic aspect of adsorption. They are concerned with how the concentration of adsorbate changes with time and provide insights into the rate at which adsorption occurs and the mechanisms involved. On the other hand isotherm Models Focus on equilibrium, emphasize the equilibrium state, and provide insights into the distribution of adsorbate at a particular point in time. They are concerned with the relationship between adsorbate concentrations in the liquid and solid phases at equilibrium (Mudhoo & Pittman, 2023).

Both kinetic and isotherm models are complementary tools, offering different perspectives on the adsorption process. While kinetic models reveal the temporal evolution of adsorption, isotherm models provide equilibrium information, helping to design and optimize adsorption systems.

2.11 Thermodynamic study

The thermodynamic behaviour for the adsorption of dye using bacterial biomass should be studied and investigated. It should be estimated and computed using Van't Hoff equation to establish thermodynamic parameters such as Gibb's Free Energy ($\Delta G°$), entropy ($\Delta S°$), and enthalpy ($\Delta H°$) change (Litefti et al., 2019; Olayinka et al., 2020) as shown in **Eq. (2.4)** and **(2.5).** The negative value of $\Delta G°$ indicated the feasibility and spontaneity of the biosorption reaction [3], and the positive value of $\Delta G°$ indicated the process is not spontaneous and requires external energy for the reaction to occur (Netzahuatl-Muñoz et al., 2015). The negative and positive values of $\Delta H°$ indicated the exothermic and endothermic nature of the reaction, respectively. The biosorption process is stated to be an exothermic ($-\Delta H$) reaction, where the heat in the form of energy is released into the environment. Several studies have shown that a rise in temperature causes a decrease in the biosorption process. When the energy in the form of heat ($+\Delta H$) is acquired from the environment, the reaction is considered to be endothermic (Velkova et al., 2018). The total energy generated in bond breaking is less than the total energy absorbed in bond formation between the sorbate and the adsorbent in the endothermic process (Tran et al., 2016). The negative value of $\Delta S°$ suggested a decrease in randomness at the solid/liquid interface, which also indicates surface stability and that no significant changes occur in the internal structure of the dye during the biosorption process (Litefti et al., 2019; Netzahuatl-Muñoz et al., 2015)**,** the positive values of ΔS indicate the increased disorder and randomness at the solid-solution interface of dyes with the adsorbent/biomass (Suyamboo, 2012). The thermodynamic equilibrium constant (KC; dimensionless) has a direct effect on ΔG, ΔH, and ΔS calculations. In adsorption thermodynamics, the equilibrium constant KC can be computed using the constants of numerous adsorption isotherms (Tran et al., 2016). The thermodynamic parameters of different dyes using different using bacterial biomass are shown in **table 3**.

$$\Delta G^o = \Delta H^0 - T\Delta S^0 \tag{2.4}$$

$$ln\left(\frac{q_e}{c_e}\right) = \frac{\Delta S}{R} - \frac{\Delta H}{R}\left(\frac{1}{T}\right) \tag{2.5}$$

It is the lowest amount of energy needed to initiate a chemical reaction between molecules and atoms (Shukor et al., 2020; Tran et al., 2016). The activation energy (E_a) of the adsorption process can be calculated using the Arrhenius equation (Litefti et al., 2019; Y. Wang et al., 2006), which explained a linear relationship between the rate constant and temperature as shown in **equation 2.6** (Litefti et al., 2019; Netzahuatl-Muñoz et al., 2015).

$$\text{Lnk}_2 = \text{InA} - \frac{E_a}{RT} \tag{2.6}$$

where A is the Arrhenius factor, R is the ideal gas constant and T is the temperature (K).

Table 2.7: Thermodynamic parameters of different dyes using different Microbial biomass

Adsorbent	Adsorbate	Temp.(K)	$\Delta G°$ Kjmol^{-1}	$\Delta H°$ Kjmol^{-1}	$\Delta S°$ Kjmol^{-1}	Chemisorption/physisorption	Ref
Rhodococcus erythropolis AW3	crystal violet	298	-26.13	-13.08	0.04	physisorption	(Canizo et al., 2019)
		308	-26.98				
		318	-27.25				
		328	-27.50				
Bacillus macerans	Basic blue 41	298	-4.72	-22.90	-0.061	Chemisorption	(Atar et al., 2008)
		308	-3.91				
		318	-3.25				
		328	-2.09				
C. glutamicum	Reactive Black 5	298	-26.1	7.4	0.11	physisorption	(Vijayaraghavan & Yun, 2007)
		303	-26.7				
		308	-27.2				
		313	-27.8				
Paenibacillus macerans	Acid Blue 225	298	-25.62	-107.72	-273.62	Chemisorption	(Çolak et al., 2009)
	Acid Blue 062	308	-24.81	-50.07	-81.50		
		318	-21.65				
		328	-12.79				
		298	-25.87				
		308	-25.43				
		318	-23.50				
		328	-21.87				
Bacillus megaterium	Reactive blue 5	303	-4.45	43.88	0.16	Chemisorption	(Liu Chen et al., 2011)
		308	-5.08				
		313	-6.44				
		318	-6.93				
		323	-7.48				
Dried anaerobic sludge	Burazol Blue ED	298	-0.36	-	-	-	(Caner et al., 2009)
		313	-0.52				
		323	-0.52				
anaerobic sludge	Rhodamine B	293	-26.64	-1.21	0.09	physisorption	(Y. Wang et al., 2006)
		311	-28.21				
		333	-30.11				
Agrobacterium fabrum strain SLAJ731	Methylene blue	298	-15.11	-3.82	37.92	Chemisorption	(Swati Sharma et al., 2018)
		303	-15.31				
		310	-15.59				
		325	-15.86				

Table 2.7: Continued

Bacillus amyloliquefaciens	Acid Blue 225	298	-22.09	-13.52	+28	Chemisorption	(Yenikaya et al., 2010)
		308	-22.15				
		318	-22.16				
		328	-22.63				
	Acid Blue 062	298	-21.21	-13.61	+24		
		308	-20.95				
		318	-21.26				
		328	-21.57				
Aspergillus carbonarius	Congo red	293	-3.05	48.42	0.154	Chemisorption	(Bouras et al., 2017)
		298	-2.61				
Penicillium glabrum		303	-1.50				
	Congo red	293	-2.99	74.13	0.243		
		298	-1.31				
		303	-0.57				
Red marine algae	Lac dye	303	4.32	-30.64	-115.38	physisorption	(Chairat & Bremner, 2016)
		313	5.47				
		323	6.63				
		333	7.78				
S. fradiae	Congo red	298	-2320.17	-17.47	-50.94	Physisorption	(Velkova et al., 2018)
		303	-1996.15				
		313	-1996.15				
	Methylene blue	298	-5354.24	-35.04	-100.07	physisorption	
		303	-4637.15				
		313	-3723.05				
Mycelial pellets	Congo red	298	-2.326	251.667	0.956	Chemisorption	(Wu et al., 2020)
		303	-2.510				
		308	-3.042				
		313	-3.302				
T. harzianum	Reactive black	298	-2.750	-42.53	0.151	physisorption	(Karthik et al., 2019)
		303	-3.478				
		308	-4.499				
		313	-5.551				
S. cerevisiae	Brilliant red	278	-28.4841	11.368	143.2	physisorption	(Suteu et al., 2013)
		293	-30.5333				
		308	-32.7812				

CHAPTER 3

METHODOLOGY

3.1 Experimental design

The overall research plan for the equilibrium, kinetics, and thermodynamic studies of the biosorption of congo red dye by the biomass of *Serratia marcescens* mm06 is shown in **Figure 3.1.**

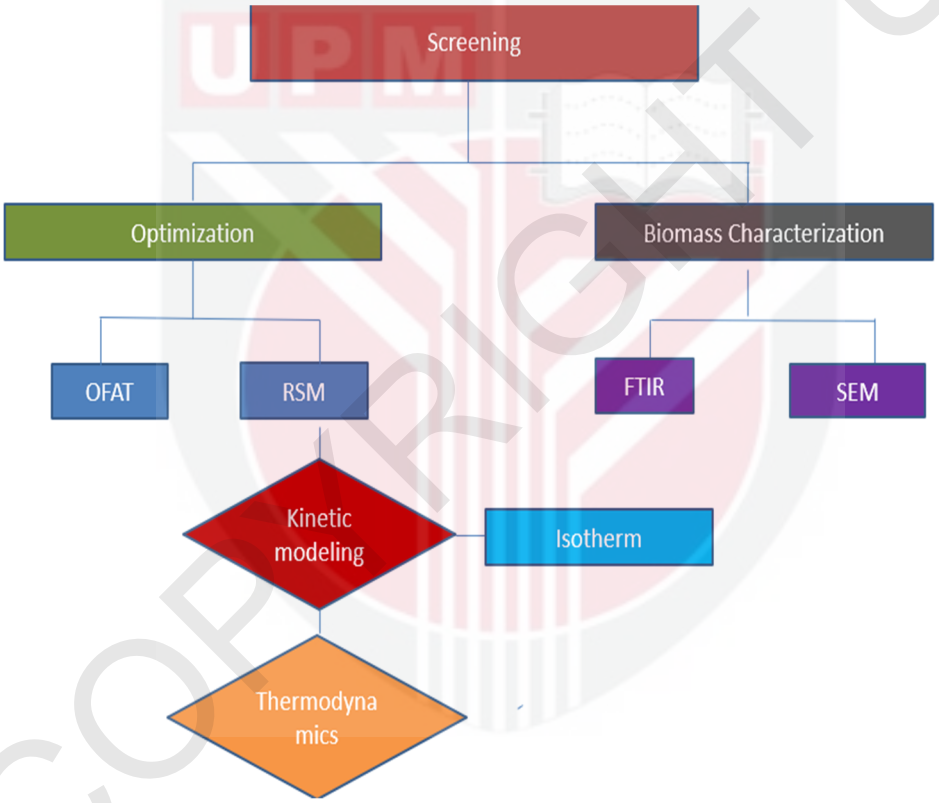

Figure 3.1: Research Plan for the adsorption of Congo red dye using Bacterial Biomass

3.2 Equipment, chemicals, and reagents

The reagents employed were all of the highest analytical quality. The Congo red dye used in this study was bought from Sigma Aldrich Co. in the United States. The

Appendix contains a list of all the substances, reagents, and equipment used in this study and in the preparation of each of the solutions, deionized and distilled water was used. In the laboratory, synthetic wastewater was created by combining Congo red dye with deionized water to achieve a targeted concentration. To generate a stock solution, 100 mg of the dye salt was dissolved in 100 mL of deionized water, resulting in the formation of the wastewater.

3.3 Preparation of dye solution

1000 ppm Congo red dye stock solution was made by diluting 1000 mg of the dye salt in 100 mL deionized water. Dye solutions of the desired concentration were prepared by diluting the stock solution (1000 ppm) using distilled water and used for the batch experiments. Using a pH meter, the pH of the solution was changed with either 0.5 N HCl or 0.1 mol NaOH.

(The greatest peak of absorption spectra was used to normalise dye absorbance using a spectrophotometer (scanned from 400 to 800 nm, visible range). Between A450 and A507 nm, the best absorbance peak was observed) (S. K. Das et al., 2012).

3.4 Preparation of the media for bacterial growth

3.4.1 Media preparation

Nutrient broth (NB) (Oxoid, Thermo Fisher (Heysham), Ireland) was made by dissolving 18 grams of media in one litre of distilled water (dH_2O), then autoclaving it for twenty minutes at 121 °C, and finally storing it in a chiller at four degrees Celsius. The NB has the following general composition in grams per litre: 3.0 beef extract, 10.0 peptone, and 5.0 sodium chloride (Nordin et al., 2013).

3.4.2 Preparation of Glycerol Stock [Glycerol Stock]

A single colony of the bacterial strain was used to inoculate 10 mL of nutrient broth, which was then placed in an incubator at a temperature of 10 °C with a rotational speed of 150 rpm. The bacterial glycerol stock was made in 20 percent (v/v) glycerol by transferring 600 µL of overnight culture into a sterile 1.5 mL Eppendorf tube that contained 400 µL of 20 % sterile glycerol. This was done in order to maintain the sterility of the preparation. After that, the stock was stored for later use at a temperature of -80 degrees Celsius. Therefore, sterile glycerol was utilised for the long-term preservation of bacteria (Gorman & Adley, 2004).

3.5 Bacterial Source

Twelve (12) different pure bacterial cultures (Isolate 34XR, Isolate 34XW, Isolate 52, Isolate 2, Isolate 1, Isolate 29, Isolate 7, Isolate 8, Isolate 4, Isolate 5.2, Isolate 30, and Isolate 5.1) were obtained from the internal culture collection of the Bioremediation, Biomonitoring & Ecotoxicology Laboratory (BBE), Faculty of Biotechnology and Biomolecular Sciences, Universiti Putra Malaysia. These bacteria were originally identified from the sample collected from Juru riversides in Pulau Pinang, Malaysia (Manogaran et al., 2021). The river and the area have been reported to have high levels of pollution from local textile and pigment companies (Izuan et al., 2015). As a result, regular sub-culturing was performed under aseptic laboratory settings utilising Nutrient Broth (NB) as a growth medium to maintain the purity of each isolate.

3.6 Bacterial Biomass Harvesting

The biomass of each of the twelve (12) isolates was harvested and screened to see whether or not they had the ability to adsorb Congo red dyes. A culture of the isolates that was one day old and had an absorbance of about 1 OD600 was centrifuged at a speed of 10,000 rpm for ten minutes (Canizo et al., 2019). The supernatant that was collected from each individual isolate was discarded, and the pellets were washed twice with Tris Buffer with a pH of 7.0. After that, the cells on the pellets were rendered nonviable by heating them to 60 degrees Celsius in a water bath for one hour (Busi et al., 2015; Huang, 2013; Liu et al., 2011). Studies (research) on the adsorption of Congo red were then carried out using pellets.

3.6.1 Bacterial biomass screening

A volume of 10 mL Congo red dye was mixed with 0.94 g of each of the 12 inactivated bacterial biomass in a 50 mL flask. The flasks were labelled appropriately and incubated at 25 °C and 150 rpm. To monitor each bacterial biomass adsorption potential, a two (2) mL aliquot was obtained at regular intervals of 5 minutes, centrifuged at 10,000 rpm for 10 minutes, and measured using an OD507 nm spectrophotometer (Cheng et al., 2020). This procedure was repeated until the absorbance peak for each flask set became uniform. All experiments were carried out in triplicate. The formula below was used to compute the % adsorption.

$$Dye\ adsorption\ percentage\ (\%) = \frac{Y-Z}{Y}\ \chi\ 100 \qquad (3.1)$$

Where Y is the initial absorbance before incubation and Z is the final absorbance after incubation.

For further analysis, the isolate with the highest Congo red dye absorption % was chosen.

3.7 Batch adsorption experiment

A dye batch adsorption study was conducted to explore the influence of different factors on dye removal by bacterial biomass. In a 50 ml flask with 94 g bacterial biomass and 10 ml dye solution, a biosorption experiment was set up. The flask was sealed and stored at room temperature on a rotary shaker. The dye solution was stirred using a rotary shaker at a constant speed (rpm). The adsorbate was removed from the adsorbent after the specified time intervals by centrifuging the flask contents. On a UV-VIS spectrophotometer, the absorbance of the dye solution was measured before and after the batch experiment at the corresponding λ max. The amount of dye adsorbed onto the adsorbent was determined by subtracting the dye concentration in the solution before and after the biosorption process. A standard graph was used to calculate the initial and ultimate dye concentrations.

The amount of Congo red dye adsorbed at equilibrium and the removal percentage were calculated as shown in **equations (3.2)** and **(3.3**) respectively.

$$q_e = \frac{(C_0 - C_e)}{m} V \tag{3.2}$$

$$\frac{(C_0 - C_e)}{C_0} x\ 100\% \tag{3.3}$$

where qe (mg/g) is the amount of dye adsorbed by the adsorbent (bacterial biomass), Co (mg/L) is the initial concentration of the adsorbate, Ce (mg/L) is the concentration of the adsorbate solution at equilibrium, m is the amount of adsorbent (g) and V is the volume of solution (L).

Following the batch experiment, the disposal of dye-contaminated bacterial bioabsorbent should be done in a manner that is environmentally responsible and compliant with local regulations. Before disposal, it is advisable to deactivate the bacterial bioabsorbent to ensure that the bacteria are no longer viable. This can be achieved through autoclaving or other appropriate sterilization methods.

3.8 Optimization of Congo red dye adsorption using the one-factor-at-a-time (OFAT)

According to the screening results, Isolate 34XR (*Serratia marcescens* mm06) exhibits the highest adsorption percentage on Congo red dye. Serratia marcescens mm06 was previously identified and characterised by (Manogaran et al., 2020). The adsorption of dye is affected by a wide variety of parameters. Hence, the OFAT method was employed to optimise the conditions for congo red dye adsorption using the isolate Serratia marcescens mm06. The development of a dye removal treatment procedure on an industrial scale will be significantly aided by the optimization of conditions such as the effect of initial dye concentration, contact time, pH, agitation speed, temperature, and adsorbent size (Yagub et al., 2014). While maintaining the previously optimised

parameters constant, each parameter was checked one after the other. All experiments were done in triplicate.

3.8.1 Initial dye Concentration

To examine and understand the influence of dye concentration on biosorption by bacterial biomass (*Serratia sp*), initial dye concentrations were varied (10, 15, 20, 30, 40, 50, 90, and 100 ppm). Other parameters remained constant. The absorbance was measured, the adsorption percentage was calculated, and the standard growth curve was drawn to select the best concentration (Liu et al., 2012).

3.8.2 Contact time

The effect of time on the biosorption of Congo red using *Serratia marcescens* MM06 was investigated by running a batch adsorption experiment at varied time intervals (5, 10, 15, 20, 40, 60, 80, and 100 min) while keeping all other parameters constant. The reaction mixture in an Eppendorf tube was centrifuged at 10000 rpm for 10 minutes at each time interval. The supernatant was then analysed with a spectrophotometer set at 507 nm. The percentage of adsorption and graph were calculated and plotted respectively (Rizzi et al., 2014).

3.8.3 pH

The experiment was set up at varied pH values (5, 5.5, 6, 6.5, 7, 7.5, 8, 8.5) while keeping all other parameters constant to assess the effect and influence of pH on the biosorption of congo red dye. By adding either 0.1M HCl or 0.1M NaOH, the pH of the dye solution was changed to the appropriate value. Optimum pH has a maximum percentage of dye removal (Velkova et al., 2018).

3.8.4 Agitation speed

In this study, the influence of agitation speed on the biosorption of congo red dye utilising bacterial biomass was investigated by recording biosorption at various agitation speeds (50, 75, 100, 125, 150, 175, 200, and 250 rpm). The optimum agitation speed was obtained by recording the biosorption with a high percentage of removal while keeping all other parameters constant (Hamzeh et al., 2012).

3.8.5 Temperature

The study of temperature in this research was determined by conducting a batch experiment at different temperatures (25, 30, 35, 40, 45, 50, 55, and 60 ^{o}C) while keeping

Initial dye concentration, contact time, pH, agitation speed, and absorbent size constant (Abdullah et al., 2021).

3.8.6 Biosorbent dosage

The effect of biosorbent dose (biomass) on the biosorption of Congo red dye was recorded by varying the amount (0.5, 0.75, 1.0, 1.25, and 1.5 g) in a batch biosorption experiment, where the initial dye concentration, contact time, PH, agitation speed, and temperature were all kept constant (Rizzi et al., 2014).

RSM involves performing a full factorial search by simultaneously and methodically analysing all of the effective variations of significant components.

3.9 Optimization of Congo red dye adsorption using response surface methodology (RSM)

The traditional approach to process optimization, which focuses on optimizing one factor at a time, is arduous, time-consuming, and insufficient (A. Das & Mishra, 2017). Response surface methodology (RSM) is a collection of statistical techniques that are used in the design of experiments, the construction of models, the analysis of the effect of factors, and the seeking of optimal conditions. It is an experimental protocol that has been constructed using statistical analysis, and it involves the simultaneous variation and manipulation of several factors (A. Tripathi, 2012; Manogaran et al., 2021). RSM is used to optimize and analyse relationships between numerous bioprocess parameters utilising a small number of experiments. It then predicts a model to determine the possible effects of interactions and higher-order effects, as well as the operational conditions that will produce the greatest amount of the response that is desired (A. Das & Mishra, 2017). Placket–Burman design and 3-level full factorial were utilised in design expert 6.0.8 software to determine the factors having a significant effect on the adsorption of Congo red dye (Aly-Eldeen et al., 2018; A. Das & Mishra, 2017).

3.9.1 Optimization using PBD

The Placket–Burman design was utilised to identify process parameters that had a substantial impact on Congo red dye biosorption using bacterial biomass. Each variable was given a high level, which was represented by the symbol (+1), and a low level, which was represented by the symbol (-1). The levels of the parameters that were ultimately chosen were determined by the preliminary experiments as well as the information that was found in the relevant literature (Manogaran et al., 2021; Tripathi, 2012). Following the software's recommendations, 12 individual experiments were conducted to screen Six independent parameters that affect Congo red dye adsorption and were predicted using OFAT parameters. The PBD experimental range and level design for Congo red dye adsorption are shown in Table 3.2. The software was used to do an analysis of variance (ANOVA), and the parameters with $p<0.05$ were found to be statistically

significant. As a result, these parameters were further optimized using the 3-Level full factorial (Aly-Eldeen et al., 2018; Farooq et al., 2017; Manogaran et al., 2021).

Table 3.1: Experimental range and level of independent variables tested using the PBD

Factors	Variable	Unit	-1(Low Level)	+1(High Level)
A	Dye concentration	ppm	50	100
B	Contact time	min	5	20
C	pH		4	8
D	Agitation speed	rpm	100	150
E	Temperature	°C	25	35
F	Adsorbent size	g	0.5	1.5

3.9.2 Optimization using 3 Level full factorial

Following the PBD optimization, the significant parameters were then subjected to a 3-level full factorial for further optimization. pH and adsorbent size were shown to be the most significant parameters determined from the PBD. pH between 4.0 and 8.0 and adsorbent size between 0.5 and 1.5 g were the ranges for which the significant parameters had their high and low levels, respectively. The significant parameters from the PBD, as well as the interactions between the variables, were analysed with the use of the three-level full factorial (Aly-Eldeen et al., 2018; A. Das & Mishra, 2017). A total of 13 sets of experimental runs were performed. All the experiments were done in triplicate. Each experimental run's adsorption % was computed and recorded as a response variable. The software's final projected RSM response was validated experimentally (Lim et al., 2013). The correlation between the independent variables and the response was described using a second-order model (Aly-Eldeen et al., 2018; Das & Mishra, 2017).

3.9.3 Validation of the experimental model

The response surface model was validated in triplicate under the predicted conditions. Based on the findings of statistical RSM analysis (3-level full factorial). Experiments were conducted by selecting an experimental design from the RSM model in order to validate the established three-level full factorial model (Lim et al., 2013). The values of the most significant parameters were used to validate the experimental findings. Therefore, the actual value of the percentage adsorption of Congo red dye using the biomass of *Serratia Marcescens* MM06 was obtained and compared with the predicted value obtained from the three-level full factorial analysis (Das & Mishra, 2017).

3.10 Characterization of biosorbent (biomass)

Biosorbent features such as physical and biochemical properties must be investigated in order to discover the natural characteristics of the bacterial biomass adsorbent surface. Fourier Transform Infrared Spectrometry (FTIR) and Scanning electron microscope

(SEM) were used to analyze the functional groups as well as the surface behaviour of biosorbent.

3.10.1 Fourier Transform Infrared Spectrometer (FTIR)

It is a technique used to draw an infrared spectrum of a liquid, solid, or gas's absorption or emission. At one time, this spectrometer gathers data over a broad spectral range and then estimates data with high spectral resolution. This kind of spectrum is a graph where the Y axis represents percent transmittance and the X axis represents wavelength or frequency (Gedam et al., 2019; V. K. Gupta et al., 2020; Li et al., 2016; Mansour et al., 2020).

In order to characterise the structure of the bacterial biosorbent, a Fourier transforms infrared (FTIR) study was carried out using the biomass of *Serratia marcescens* MM06. Both treated and untreated bacterial biomass with Congo red dye was harvested, washed with buffer, and then oven-dried at a temperature of 60°C for 48 hrs. The biomass was reduced to a powder, which was then sieved to a finer size before being submitted for FTIR scanning (Abbas & Trari, 2015; Gedam et al., 2019; Li et al., 2016). The measurement was performed between 400 and 4000 cm^{-1} in order to determine the functional groups and forms of bonds that are already present in the dyes. The FTIR spectroscopy investigations with attenuated total reflectance (ATR) were carried out with the help of the VERTEX 80v equipment that was supplied by Bruker Optics Korea Co., Ltd. (ATR). The rotational and vibrational displacement of molecular groups and a molecule's chemical bond are responsible for the occurrence of adsorption in the infrared (IR) region of the electromagnetic spectrum. After being compressed, the dry mixture was homogenously crushed using potassium bromide (KBr) to generate a thin and fine pellet. This particle was then scanned using absorbance spectra ranging from 400 to 4000 cm^{-1}.

3.10.2 Scanning electron microscopy (SEM)

The powerful technology known as scanning electron microscopy (SEM), is widely used to analyse the surface morphology, texture, and porosity of an adsorbent both before and after the process of dye biosorption (Dandge et al., 2016). For the surface morphology analysis, a field emission scanning electron microscope (FESEM, LEO1455) with operating data of 20.0 kV and 13.0 mm working distance and accelerating capacity was used. Before being placed on the plating stub, the FE-SEM samples were prepared by following the procedure and being sliced into very small pieces. Before the samples could be scanned, an SEM Coating System Machine was used to first attach them to the sample container and then coat them in gold. Several different SEM micrographs were taken at magnifications ranging from 500 – 5000x, and their sizes ranged from 10 – 50 µm, respectively. An electron beam from a scanning electron microscope first scans the surface of a solid before projecting images onto a computer screen. Different signals are generated when the atoms on the sample's surface are bombarded by the electron beam. The electron detector can identify those signals. The information in those signals reveals

the sample's surface composition and surface structure. Since they must be taken in a chamber designed only for samples of a certain size, samples of the proper size are used.

3.11 Adsorption kinetics modeling

Adsorption kinetic modeling is a crucial aspect of studying the rate at which molecules adhere to a surface, known as adsorption, and understanding the mechanisms governing this process. Several models have been proposed to describe adsorption kinetics, and these models help researchers interpret experimental data and gain insights into the nature of the adsorption process.

One commonly used adsorption kinetic model is the pseudo-first-order model. This model assumes that the rate of adsorption is directly proportional to the number of unoccupied sites on the adsorbent surface (Lagergren, 1898) . The mathematical representation of the pseudo-first-order model is given by the **equation 3.4.**

Another widely used model is the pseudo-second-order model, which suggests that the rate-limiting step in the adsorption process involves the interaction between the adsorbate and adsorbent (Ho and McKay, 1999). The mathematical representation is given by the **equation 3.5.**

These models are applied to experimental adsorption data, and the parameters *(k1, k2)* are determined by fitting the model equations to the experimental results. However, it's important to note that these models are empirical and may not always accurately represent the actual adsorption mechanism. Researchers often use them as initial approximations and, in some cases, more complex models or mechanisms may be required for a more accurate description.

The kinetic study is important to the adsorption process because it describes the adsorbate uptake rate and regulates the residual time during the entire adsorption process (Abbas & Trari, 2015). A batch kinetics experiment was performed at various dye concentrations based on the results obtained from OFAT and RSM. The concentrations were 10, 20, 30, 40, 50, 70, and 90 ppm. Following the incubation period, the supernatant was then analysed using a spectrophotometer at a fixed wavelength of 507 nm at various time intervals. The absorbances were measured, recorded, and plotted using a graph. For dye adsorption kinetics modeling, some previously tested adsorption kinetics models were used to select the best (Edokpayi & Makete, 2021). These models include the pseudo-first-order and pseudo-second-order kinetics as shown in **Equations 3.4 and 3.5** (Yasid et al., 2020; Aljeboree et al., 2017; Das & Mishra, 2017).

$$q_t = q_e(1 - e^{-K_1 t}) \tag{3.4}$$

$$q_t = \frac{K_2 {q_e}^2 t}{(1+K_2 q_e t)} \tag{3.5}$$

where q_e and q_t represent the amount of dye adsorbed (*mg/g*) at equilibrium and time *t* (min), respectively. K_1 and K_2 are the rate constants of pseudo-first-order (min^{-1}) and pseudo-second-order sorption (*g mg/min*), respectively.

3.12 Adsorption isotherm model

Adsorption isotherm analysis was carried out by fitting the equilibrium data to various isotherm models. The adsorption isotherm is the most often used representation of the adsorbate concentration and quantity of the pollutant adsorbed. The equilibrium adsorption isotherm is critical for designing an adsorption system equilibrium of dye adsorption because it describes the relationship between the amount of dye adsorbed and the dye concentration remaining in a solution at a constant temperature under specified conditions (Mansour et al., 2020; L. E. Liu et al., 2012). Following a batch experiment with different dye concentrations of 10, 20, 30, 40, 50, 70, and 90 ppm, isotherm models such as Langmuir, Freundlich, and Bet were used to find the best and most fitted isotherm model for Congo red dye adsorption (Gedam et al., 2019; Silva et al., 2019; Velkova et al., 2018; Tran et al., 2016). The model equations utilized in this research are shown below:

The Langmuir isotherm theory is based on the assumption that adsorption takes place on a homogeneous surface, which means that the surface consists of identical sites that are equally available for adsorption and have equal energies of adsorption and that the adsorbent is saturated after one layer of adsorbate molecules forms onto the surface. This theory was developed by Langmuir in the 1920s (Ahmad et al., 2008).

The Langmuir equation

$$q_e = \frac{q_{mL} b_L C_e}{1 + b_L C_e} \tag{3.6}$$

where
q_e equilibrium dye the adsorbent (*mg/g*),
q_{mL} monolayer capacity of the adsorbent (*mg/g*)
C_e equilibrium dye the sorbate (*mg/L*)
b_L Langmuir constant.

Freundlich isotherm model explains the uptake of the dye takes place on a heterogeneous surface through the process of multilayer adsorption, and the amount of adsorbate adsorbed expands indefinitely with an increase in concentration. It is used in the process of determining the adsorption capacity of the adsorbent in relation to the adsorbate. The binding sites with the highest strength are the ones that are occupied first, and the strength of the bonds weakens as the number of occupied sites increases (Mahmoud et al., 2012; Tran et al., 2016; Edokpayi & Makete, 2021).
The Freundlich eqution is;

$$q_e = K_F C_e^{\frac{1}{n_F}} \tag{3.7}$$

q_e equilibrium dye the adsorbent (*mg/g*)
C_e equilibrium dye the sorbate (*mg/L*)
K_F Freundlich constant

The BET model assumes that a Langmuir equation may be applied to each layer of an adsorbent and represents isotherms with multilayer adsorption at the surface of the adsorbent. Another assumption is that a certain layer does not necessarily have to be completely completed before the formation of the subsequent layer (Gadd, 2009).

The BET equation:

$$q_e = \frac{q_{mBET}\alpha_{BET}C_e}{(1-\beta_{BET}C_e)(1-\beta_{BET}C_e+\alpha_{BET}C_e)} \quad (3.8)$$

In this study, the Langmuir, Freundlich, and BET isotherm models were employed to assess the experimental results. The correlation coefficient was calculated using curve - Expert software to evaluate the best-fitting model.

Table 3.2: List of adsorption isotherm models

	Model	Parameter model	Formula	References
1	Henry's law	1	$q_e = HC_e$	(Ridha & Webley, 2009)
2	Langmuir	2	$q_e = \frac{q_{mL}b_LC_e}{1+b_LC_e}$	(Langmuir I, 1918)
3	Freundlich	2	$q_e = K_F C_e^{\frac{1}{n_F}}$	(Adamson, 1993)
4	Dubinin-Radushkevich	2	$q_e = q_{mDR}exp\left\{-K_{DR}\left[RTln\left(1+\frac{1}{C_e}\right)\right]^2\right\}$	(Dubinin, 1965)
5	Temkin isotherm	2	$q_e = \frac{RT}{b_T}\{ln(a_TC_e)\}$	(Temkin and Pyzhev, 1940)
6	Smith isotherm	2	$q_e = W_{s1} - W_{s2}ln(1-C_e)$	(Smith & Smith, 1944)
7	Jovanovic isotherm	2	$\left(q_e = q_{mJ}(1-e^{-K_jC_e})\right)$	(Jovanović, 1969)
8	BET	3	$q_e = \frac{q_{mBET}\alpha_{BET}C_e}{(1-\beta_{BET}C_e)(1-\beta_{BET}C_e+\alpha_{I}}$	(Brunauer S, Emmett PH, 1938)
9	Sips	3	$q_e = \frac{K_sq_{mS}C_e^{\frac{1}{n_S}}}{1+K_sC_e^{\frac{1}{n_S}}}$	(Sips, 1948)
10	Toth	3	$q_e = \frac{q_{mT}C_e}{\left(K_T+C_e^{n_T}\right)^{n_T}}$	(Toth, 1971)

Table 3.2: Continued

11	Redlich-Peterson isotherm	3	$q_e = \frac{K_{RP1} C_e}{1 + K_{RP2} C_e^{\beta_{RP}}}$	(Redlich & Peterson, 1958)
12	Hill isotherm	3	$q_e = \frac{q_{mH} C_e^{n_H}}{K_H + C_e^{n_H}}$	(Hill, 1910)
13	Khan isotherm	3	$q_e = \frac{q_{mK} b_K C_e}{(1 + b_K C_e)^{a_K}}$	(Khan et al., 1997)
14	Vieth-Sladek isotherm	3	$q_e = \frac{q_{mVS} b_{VS} C_e}{(1 + b_{VS} C_e)^{n_{VS}}}$	(Vieth & Sladek, 1965)
15	Radke-Prausnitz isotherm	3	$q_e = \frac{q_{mRP} K_{RP} C_e}{(1 + q_{mRP} C_e)^{n_{RP}}}$	(Sivarajasekar & Baskar, 2019)
16	Brouers-Sotolongo isotherm	3	$q_e = q_{mBS}\left(-K_{BS} C_e^{n_{BS}}\right)$	(Haul, 1969)
17	Fritz-Schlunder-III isotherm	3	$q_e = \frac{q_{mFS} K_{FS} C_e}{1 + q_{mFS} C_e^{n_{FS}}}$	(Fritz & Schluender, 1974)
18	Unilin isotherm	3	$q_e = \frac{q_{mU}}{2b_U} ln\left(\frac{a_U + C_e e^{b_U}}{a_U + C_e e^{-b_U}}\right)$	(Valenzuela , 1989)
19	Baudu	4	$q_e = \frac{q_{mB} b_B C_e^{(1+x+y)}}{1 + b_B C_e^{(1+x)}}$	(Baudu, 1990)
20	Fritz-Schlunder-IV	4	$q_e = \frac{A_{FS} C_e^{a_{FS}}}{1 + B_{FS} C_e^{b_{FS}}}$	(Fritz & Schluender, 1974)
21	Weber-van Vliet	4	$C_e = P_1 q_e^{\left(P_2 q_e^{P_3} + P_4\right)}$	(Vliet et al., 1980)
22	Marczewski-Jaroniec	4	$q_e = q_{mMJ}\left(\frac{\left(K_{MJ} C_e\right)^{n_{MJ}}}{1 + \left(K_{MJ} C_e\right)^{n_{MJ}}}\right)^{\frac{m_{MJ}}{n_{MJ}}}$	(Parker, 1995)
23	Parker isotherm	4	$q_e = q_{mP}\left[-a_P\left(RTln\frac{C_s}{C_e}\right)^{b_P}\right]$	(Parker, 1995)
24	Fritz-Schlunder-V	5	$q_e = \frac{q_{mFS5} K_1 C_e^{\alpha_{FS}}}{1 + K_2 C_e^{\beta_{FS}}}$	(Fritz & Schluender, 1974)

3.13 Statistical and error function analysis

3.13.1 Fitting of the data

Nonlinear regression was used to fit the adsorption kinetics and isotherms nonlinear data using the Marquardt algorithm in CurveExpert Professional software, Version 2.6.5.

3.13.2 Statistical and error function analysis

To assure accuracy, all assays were run in triplicate. The experimental errors were displayed in the form of standard deviations in an error bar format, indicating three separate determinations. A one-way ANOVA (with a 95 percent confidence interval) was performed to analyse the difference between variables, with a p-value <0.05 considered statistically significant.

Several statistically discriminatory methods, such as the Bayesian Information Criterion (BIC), the Akaike Information Criterion (AICc), Hannan and Quinn's Criterion (HQ), the Bias Factor (BF), the Root Mean-Square Error (RMSE), the Accuracy Factor (AF), and the Adjusted Determination Coefficient (R^2) were used to determine the kinetic and isotherms models.

The root mean square error (RMSE) was determined using **Equation 3.9** (Motulsky & Ransnas, 1987), and it is expected that a lesser number of parameters will result in lower RMSE values. *n* denotes the number of experimental data points. The experimental and predicted data are represented by Ob_i and Pd_i, respectively, whereas *p* denotes the number of parameters.

$$RMSE = \sqrt{\frac{\sum_{i=1}^{n}(Pd_i - Ob_i)^2}{n-p}} \tag{3.9}$$

The coefficient of determination, also known as R^2, does not take into consideration the number of parameters in models. As a result, the modified R^2 is applied in order to avoid this issue. RMS stands for Residual Mean Square and is used to express the overall variation of the y-variable which is denoted by the symbol S_y^2 as shown in **equations 3.10 and 3.11**.

$$Adjusted\ (R^2) = 1 - \frac{RMS}{S_Y^2} \tag{3.10}$$

$$Adjusted\ (R^2) = 1 - \frac{(1-R^2)(n-1)}{(n-p-1)} \tag{3.11}$$

The Akaike Information Criterion (AIC) is a model evaluation method that is founded on information theory and addresses the trade-off between model complexity and goodness of fit (Akaike, 1974). The Akaike Information Criterion (AIC) with correction, often known as AICc, is a corrected version of the original AIC that is used for processing data with either fewer values or a greater number of parameters (Burnham, and Anderson, 2002). The AICc can be computed using **equation 3.12** as follows:

$$AICc = 2p + n\ln\left(\frac{RSS}{n}\right) + 2(p+1) + \frac{2(p+1)(p+2)}{n-p-2} \quad (3.12)$$

Where p represents the number of parameters, and n represents the number of data points that are being considered. The model with the lowest AICc score is the one that is most likely to be accurate (Burnham, and Anderson, 2002). Accuracy Factor (AF) and Bias Factor (BF) are statistical evaluations of models that originate from the work of Ross (Baranyi, J., Pin, 1999). They were computed from (**Equations 3.13 and 3.14**) as follows to test for the goodness-of-fit of the models:

$$\text{Bias factor} = 10^{\left(\sum_{i=1}^{n}\log\frac{(Pd_i/Ob_i)}{n}\right)} \quad (3.13)$$

$$\text{Accuracy factor} = 10^{\left(\sum_{i=1}^{n}log\frac{|(Pd_i/Ob_i)|}{n}\right)} \quad (3.14)$$

3.14 Thermodynamics study for the biosorption of Congo red dye

The variation in dye removal efficiency with temperature was explained with the help of thermodynamic parameters (Gedam et al., 2019). In this study, batch adsorption experiments were conducted at different temperatures of 25, 30, 35, 40, and 45 °C to evaluate the influence of temperature on Congo red dye adsorption. In the thermodynamic batch adsorption investigations that were conducted, various dye concentrations of 10, 20, 30, 40,50, 70, and 90 mg/L were used. In accordance with earlier research, the data were processed by figuring out the thermodynamics parameters (Gedam et al., 2019; Tran et al., 2016). The thermodynamics parameters such as Gibbs free energy Change (*ΔG*), Enthalpy change (*ΔH*), and Entropy change (*ΔS*) were computed to evaluate the thermodynamic feasibility of the adsorption process as well as the spontaneous nature of the reaction using the following equations (Gedam et al., 2019; Gupta et al., 2020).

$$\Delta G° = -RT\ln KL \quad (3.15)$$

$$\Delta G° = \Delta H - T\Delta S° \quad (3.16)$$

$$K_C \approx \frac{K_L\left(\frac{L}{mol}\right)\times C^{\circ}\left(\frac{mol}{L}\right)}{\gamma} \quad (3.17)$$

$$lnK_C = \frac{-\Delta H°}{R} \times \frac{1}{T} + \frac{\Delta S°}{R} \quad (3.18)$$

R is the universal gas constant, 0.00831 kJ/mol×K.

The adsorption thermodynamic parameters *(ΔG°, ΔH°, and ΔS°)* were calculated by using the van't Hoff equation and applying the principles of thermodynamics. When

equilibrium has been reached in adsorption, the free energy undergoes an almost undetectable change. Several individuals have relied on equation (3.17), which is translated into equation (3.18), which is known as the standard Gibbs energy change, in order to arrive at $\Delta G°$.

The Langmuir equation (Equation 3.17) was first derived from a kinetic study, and then, later on, it was derived from a thermodynamic study. The precise analysis of the equilibrium constant between two phases, known as K_C, is directly related to the accuracy of the thermodynamic parameter estimates that are produced.

$$q_e = \frac{q_{mL} K_L C_e}{1 + K_L C_e} \tag{3.19}$$

Kc derived from Langmuir was transformed to dimensionless form using (**Equation 3.17**) and employed in **Equation 3.20** as follows.

$$K_C = 10104 \times 55.5 \times 1000 \times K_L \tag{3.21}$$

where 55.5 is the number of moles of pure water per litre and the term (molecular weight of the dye) x 55.5 x1000 x KL is dimensionless.

CHAPTER 4

RESULT AND DISCUSSION

Wastewater effluent is a complex mixture containing organic and inorganic compounds, suspended solids, nutrients, heavy metals, and potential pollutants. Indicators like BOD and COD reveal organic pollution, while varying pH levels impact environmental and treatment processes. Azo dyes contribute to effluent color, affecting aquatic ecosystems, and temperature influences biological and chemical processes, potentially altering pollutant reactivity (Dey & Islam, 2015).

Azo dye concentrations in wastewater effluent vary widely depending on industry, dye types, and processes, ranging from trace amounts to several hundred ppm. The range of 10-100 ppm is commonly used in experimental studies as it represents a moderate concentration level. It allows researchers to observe significant adsorption or degradation effects without dealing with extremely high or low concentrations (Nath et al., 2015; Choudhary et al., 2015).

4.1 Bacterial biomass screening

Bacterial isolates were sourced from the banks of the Juru River in Pulau Penang, Malaysia (Manogaran et al., 2021). The results of the screening of the twelve (12) distinct bacterial isolates against the Congo red dye are shown in **Figure 4.1.** Isolate 34XR absorbed 82% of the Congo red dye, while Isolate 34XW absorbed 64%, Isolate 52 absorbed 51%, Isolate 2 absorbed 71%, Isolate 1 absorbed 61%, Isolate 29 absorbed 50%, Isolate 7 absorbed 69%, Isolate 8 absorbed 19%, Isolate 4 absorbed 46%, Isolate 5.2 absorbed 68%, Isolate 30 absorbed 49% and, Isolate 5.1 absorbed 81%. In comparison to the other eleven (11) different isolates, it was discovered that Isolate 34XR had the highest adsorption percentage, which was up to 82%. However, each of the isolates demonstrated that they have the capability of adsorbing the Congo red dye out of the solution. According to the findings of Manogaran et al. (Manogaran et al., 2021), the majority of these isolates can either decolorize or multiply when placed in an environment containing Reactive Red 120 dye. **Figure 4.1C** depict the dye's colour change before and after adsorption.

In addition to this, several studies that were conducted in the past showed the potential of bacterial biomass in the adsorption of a variety of dyes (Velkova et al., 2018; Sarkar et al., 2021; Ning et al., 2014).

Isolate 34XR was recently identified and characterised as *Serratia marcescens* strain MM06 by (Manogaran et al., 2021). *Serratia marcescens* is a Gram-negative bacterium in the Yersiniaceae family. It is a facultative anaerobe and an opportunistic pathogen. It was discovered in 1819 by Bartolomeo Bizio in Padua, Italy. All Serratia strains have been shown to grow most effectively at pH 9 and temperatures between 20 and 37 °C.

The isolate, *Serratia marcescens* strain MM06 16S ribosomal RNA gene, the partial sequence has 1,442 bp linear DNA and Accession number MW031902.1 GI: 1908125079 (Manogaran et al. 2020). *Serratia marcescens* typically appear as rod-shaped cells under a microscope. The cells are motile, and they move using peritrichous flagella. One distinctive feature of Serratia marcescens is its ability to produce a red pigment called prodigiosin. This pigment is often observed in cultures, giving them a characteristic red or pink color (Chemaly et al., 2011; Chojniak et al., 2015; Rascoe et al., 2003). Bacteria are ubiquitous organisms that can be incorporated into the ecosystem to serve as abundant and low-cost sources of biosorbents. According to Cristani et al. (Cristani et al., 2012), *Serratia marcescens* MM06 was applied to wastewater in order to eliminate contaminants.

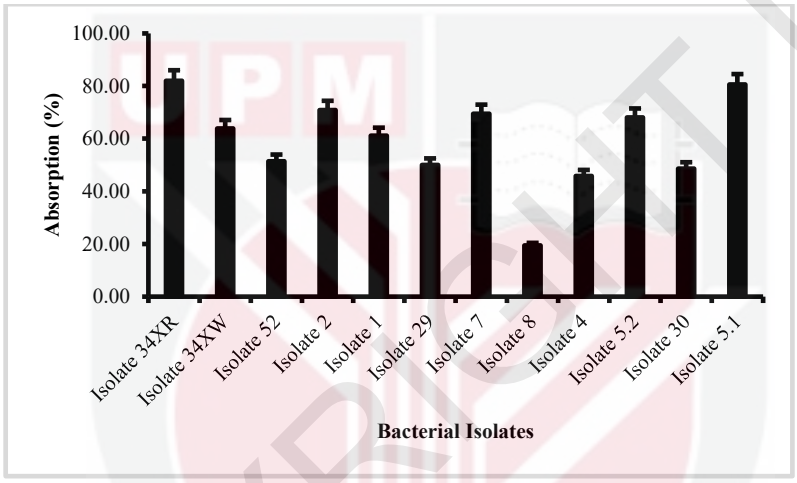

Figure 4.1: displays the results of a screening that compared twelve different bacterial isolates to Congo red dye and showed which had the highest percentage of adsorption. error bars represent mean +/- std deviation (n=3)

4.2 Optimization of congo red dye adsorption using the one-factor-at-a-time (OFAT) method

The OFAT technique was applied to investigate the impact that a variety of environmental conditions had on the adsorption of Congo red dye.

4.2.1 Effect of Initial Dye Concentration

The amount of dye that is adsorbed increases with an increasing solution at a constant adsorbent dosage, even though the percentage of adsorption decreases. That is to say, the number of adsorption sites reduces with increasing concentrations, and dye removal becomes more dependent on the concentration of the dye at the beginning of the process (Grégorio Crini & Badot, 2008). The ability of *Serratia marcescens* strain MM06 to

withstand greater dye concentrations was studied by conducting a batch experiment at varying dye concentrations ranging from 10 to 100 ppm. The results of this experiment are shown in **Figure 4.1A**. When the concentration of the dye is increased, the proportion of adsorption that occurs drops. The Congo red dye was calibrated at many different concentrations, including 10 PPM, 20 PPM, 30 PPM, 40 PPM, 50 PPM, 90 PPM, and 100 PPM, which allowed for the identification of distinct absorbances. Preliminary analysis of the data has indicated that the key trends and behaviors were observable within the chosen concentration range. On the other hand, when the standard curve that was based on the control was plotted as shown in **Figures 4.1A and 4.1B**, it was found that the graph was linear up to the absorbance of 2.96 nm. The coefficient value of the Standard/calibration curve was 0.9961 Congo red dye. The calibrated data were used to determine the dye removal capabilities of the adsorbents. This occurred as a direct result of the powerful driving force behind the mass transfer. Because of an increase in the surface saturation of the binding site on the biosorbent caused by an increase in the initial dye concentration, the adsorption potential decreased as the initial dye concentration increased. This was because the adsorption ability of the biosorbent increased as the initial dye concentration increased (Velkova et al., 2018; Li et al., 2016; C. Liu et al., 2011). According to a study that was conducted by Verma and Madamwar (Verma & Madamwar, 2003), *Serratia marcescens* was able to decolorize Ranocid Fast Blue (RFB) and Procion Brilliant Blue-H-GR (PBB-HGR), which are both members of the azo group and the anthraquinone group, respectively. On day 8 and day 5, respectively, at a temperature of 26 °C under static circumstances and a pH of 7.0, with an individual concentration of 100 mg/l, decolorization of more than 90% was achieved using PBB-HGR and RFB. it was noted that decolorization was dependent on the initial dye concentration, pH, and temperature. This was the case even though the final individual concentration was 100 mg/l. The bacterium was resistant to dyes at a concentration of 100 mg/L. On the other hand, the amount of time necessary for decolorization increases along with the dye concentration.

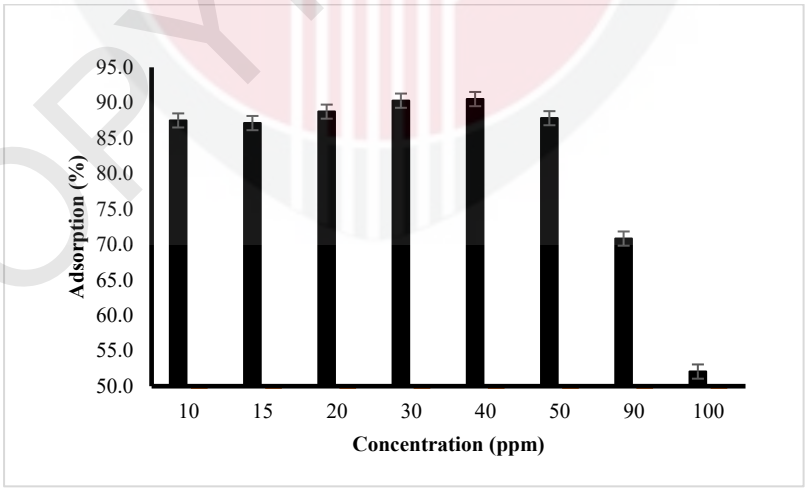

Figure 4.2A: Effect of initial concentration on the adsorption of Congo red dye by the biomass of *Serratia marcescens* strain MM06. error bars represent mean +/- std deviation (n=3)

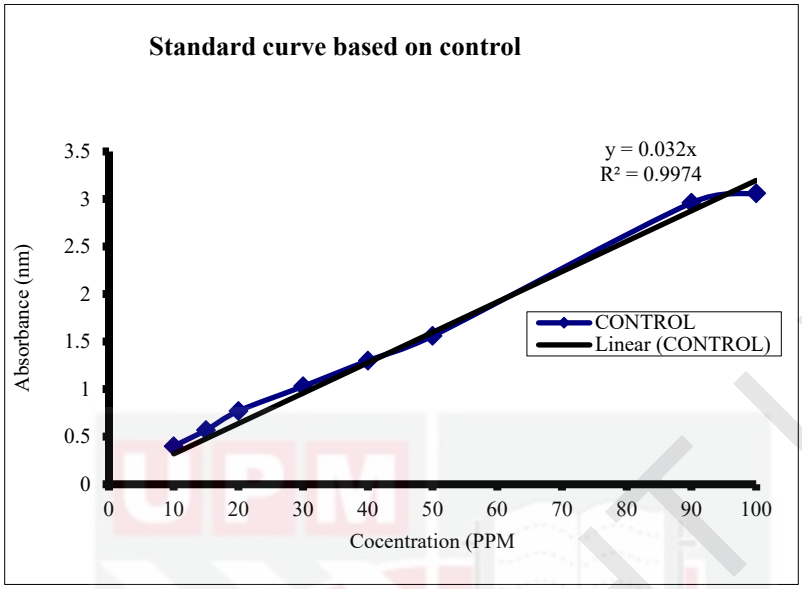

Figure 4.2B: Showing the standard curve of different dye concentrations

Figure 4.2C: depict the dye's colour change before and after adsorption

4.2.2 Effect of Contact Time

As shown in **Fig. 4.2,** the time significantly impacts the adsorption of Congo red dye. percentage dye adsorption was computed at different time intervals ranging from 5 to 100 minutes. Percentage adsorption was less than optimal between 5 and 15 minutes. However, the highest adsorption capacity (70%) was obtained at 20 minutes and

thereafter dropped from 40 to 100 minutes. There was no noticeable change in adsorbed dye after 20 minutes of contact time. Based on this finding, the equilibrium time in batch adsorption experiments was set at 20 minutes (Mohammadi et al., 2011). Adsorption capacity generally increases with increasing time until it reaches an equilibrium where no more dye can be adsorbed from the solution. The amount of the dye adsorbed represents the maximum dye adsorption capacity of the adsorbent (bacterial biomass) and equilibrium time is when the adsorption process reaches a steady state, and additional contact time does not bring significant changes in adsorption (Grégorio Crini & Badot, 2008; Chatterjee et al., 2010).

This could be explained by the presence of enough binding sites on the adsorbent (bacterial biomass) during the first phase. Binding sites, on the other hand, have become more limited. The mechanism for dye removal by adsorption can be attributed to dye migration from the bulk of the solution to the surface of the adsorbent, dye diffusion through the boundary layer to the surface of the adsorbent, and dye diffusion into the internal pores of the adsorbent particle. The boundary layer resistance is regulated by adsorption rate and contact time, which reduces resistance and increases dye mobility during adsorption (Dandge et al., 2016).

Velkova et al. (Velkova et al., 2018) evaluated the influence of contact time on Congo Red and Methylene Blue biosorption by pretreated waste *Streptomyces fradiae* biomass in another investigation. The contact time range investigated was 5 to 180 minutes. They discovered that dye uptake was fast for the first 40 minutes, then slowed until equilibrium was established at 80 minutes for MB and 70 minutes for CR, respectively. Similar results have been observed in the removal of CR dye using roots of *Eichhornia crassipes* roots (Wanyonyi et al., 2014). It is clear that the rate of dye removal was rapid at the beginning of the experiment, but during the investigation, this rate steadily slowed down until it reached equilibrium. The observation can be explained by the fact that the number of vacant sites on the adsorbent reduced over time, reaching a point where they were all occupied when equilibrium was reached.

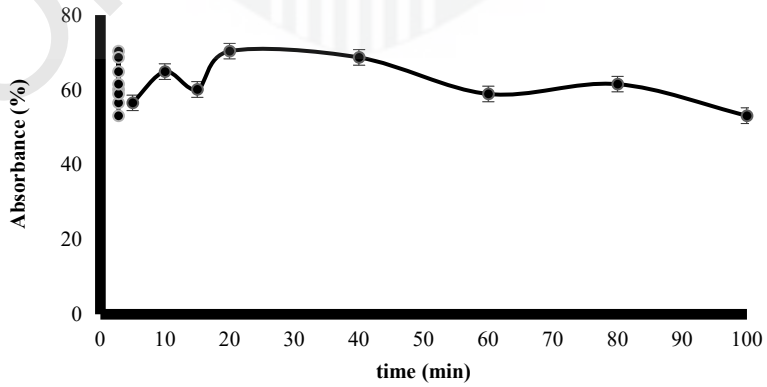

Figure 4.3: Displays the influence of contact time on Congo red dye adsorption.

4.2.3 Effect of pH

The pH of the dye solution and the activity of the functional groups present on the surface of the biosorbents are two of the most critical process parameters influencing biosorption removal. In general, increasing the pH of the solution improves the removal of basic dyes while decreasing the removal of acidic dyes (Velkova et al., 2018). The adsorbate functional groups' surface binding and ionisation degree had a substantial impact on adsorption capacity. Furthermore, it has a significant impact on the charge of adsorbent surface characteristics and the detection of adsorbate species in solution. The structures of the dyes and the adsorbent influence the adsorbate-adsorbent interaction in dye removal. In addition, two important types of dye may be classified, and these are basic (cationic) and acidic (anionic) dyes. The importance of pH measurement in dye adsorption research is because these two types of dye are the most common. When the surface charge of the adsorbent is determined by variations in the pH of the solution, the nature of the adsorbent charge is initially amphoteric (D. Nguyen et al., 2020). The electrostatic charge of the ionised coloured chemical can be affected by the pH of the solution that has adsorbed the compound.

As can be seen in **Figure 4.3**, the highest rate of Congo red dye removal by bacterial biomass was achieved at a pH of 7 (61%), and a lower adsorption capacity was observed at pH 5 (50%). The dye removal percentage increases from 50 to 61% when the pH of the solution increases from 5.0 to 7. However, as the pH of the solution rises to 8.5, the percentage of dye removal drops. However, when the pH of the solution rises, the surface of the biosorbent becomes negatively charged, and electrostatic interactions can occur between the oppositely charged sorbate and sorbent. In general, the surface of the biosorbent is positively charged at low pH values, and it resists the biosorption of cationic species (Velkova et al., 2018; Abbas & Trari, 2015). The dye concentration is calibrated at a specific pH using a pH meter before bacterial inoculation for adsorption. Spectrophotometry is then employed to analyze the dye concentration in the solution both before and after bacterial treatment. A reduction in dye absorbance at its characteristic wavelength indicates successful adsorption (Khan et al., 2018; Yenikaya et al., 2010; Cheng et al., 2020).

Changes in pH can significantly influence various chemical and biological processes, potentially impacting the adsorption behavior of dyes by altering their molecular structure or the properties of the adsorbent. In this study, the change in pH could be significant as it might affect the ionization state of the dye molecules, their solubility, or the surface charge of the bacterial biomass, all of which can influence adsorption behavior. The interaction of dye with bacteria can contribute to changes in pH. Microbial metabolic activities, such as the production of acids or bases during adsorption processes, can influence the surrounding environment (Ribas et al., 2020; H. Wang et al., 2009; Velkova et al., 2018).

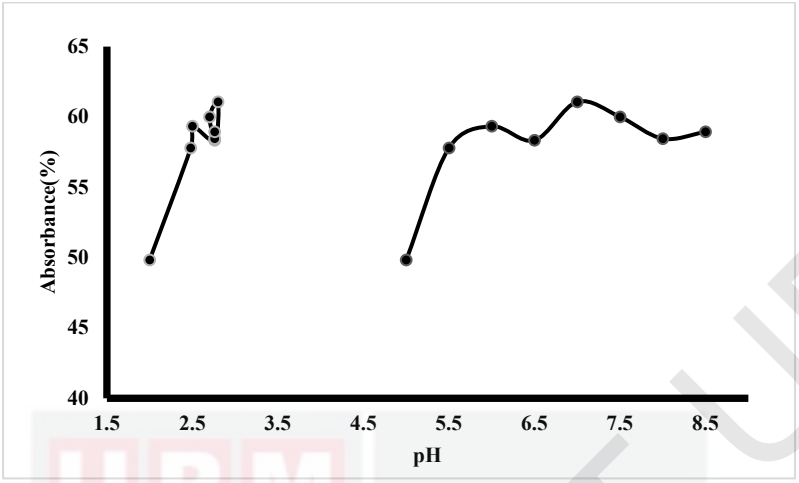

Figure 4.4: Effect of pH on the adsorption of Congo red dye by *Serratia marcescens* strain MM06

4.2.4 Effect of agitation rate

agitation is a significant factor in this experiment as it influences mass transfer, diffusion limitations, kinetics, biomass distribution, experimental reproducibility, and the relevance of the study to real-world conditions. Proper agitation ensures a more accurate representation of the adsorption process and contributes to the robustness and reliability of the experimental results. Agitation is often crucial in adsorption experiments as it enhances mass transfer, ensuring efficient contact between the adsorbent (bacterial biomass) and the adsorbate (dye) by preventing boundary layer saturation. Agitation promotes the movement of the dye molecules toward the bacterial surface, facilitating increased interactions and enhancing the adsorption process. Without agitation, the rate of mass transfer could be limited, affecting the overall adsorption efficiency (Grégorio Crini & Badot, 2008; Bharathi & Ramesh, 2013).

The impact of varying agitation rates on the adsorption of Congo red dye by *Serratia marcescens* strain MM06 was examined across a range of 50 to 250 rpm, as illustrated in **Figure 4.4.** The results reveal that the adsorption capacity is maximized at 125 rpm and diminishes at 200 rpm **(Figure 4.4)**. Consequently, the adsorption capacity exhibits an increase from 50 to 125 rpm and a subsequent decline as the speed goes beyond this threshold.

According to a study, employing raw adsorbent with a delicate and unaltered structure might cause damage to the adsorbent structure, as was seen in lead biosorption by Bacillus cereus, where a high shear rate at a high agitation speed (200 rpm) damages the biosorbent (bacterial) biomass (Jayan, N. and Bhatlu, 2021).

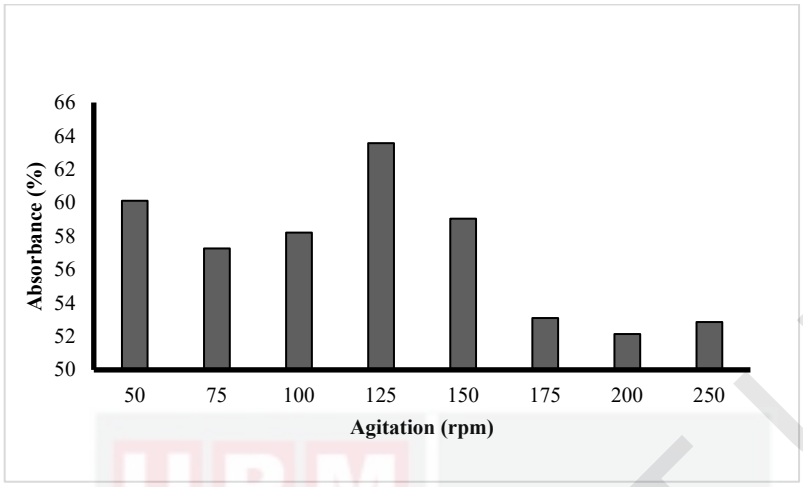

Figure 4.5: Effect of agitation speed on the adsorption of Congo red dye by *Serratia marcescens* strain MM06. error bars represent mean +/- std deviation (n=3)

4.2.5 Effect of temperature

The temperature dependence of the adsorption reaction is a major study that provides information regarding the changes in enthalpy and entropy that occur throughout the adsorption process. It primarily affects the adsorbent's expanding nature, the adsorbent particle's mobility in the dye solution, and the interface between the solid and the liquid (Saha & Chowdhury, 2011). In another study by Caner *et al*. (2009), it was reported that the sorption processes are primarily impacted by temperature in two ways. Firstly, it is well known that when the temperature rises, the viscosity of the solution decreases, speeding up the diffusion of the adsorbate molecules into the pores. Secondly, it will alter the adsorbent's capacity for equilibrium with a specific adsorbate. In this research, the adsorption of Congo red dye was studied at a variety of temperatures, including 25, 30, 35, 40, 45, 50, 55, and 60 °C, and the results are presented in **Figure 4.5**. Based on the findings, it was determined that a temperature of 25°C (61%) was optimal for the adsorption of Congo red dye. The fact that adsorption reduced as temperature increased demonstrates that the adsorption process can be completed with less total energy. Nacèra & Aicha, (2006) shows that biomass has a lower capacity for biosorption as the temperature rises. The amount of methylene blue removed reduces from 86 to 54% when the temperature increases from 20 to 50 ºC. In another study by Mahmoud *et al.* (2012) it was discovered that when the temperature was elevated from 30 to 50 °C, the adsorption capacity increased from 18.18 to 22.73 mg/g, indicating that the adsorption was endothermic. On the other hand, absorption increases with a decrease in temperature as discovered in research by Çolak et al. (2009). The finding shows that a decrease in temperature promotes biosorption, which is also a characteristic of physical adsorption. Therefore, absorption may increase or decrease with increasing or decreasing in temperature depending on the type of sorption such as physisorption or chemisorption.

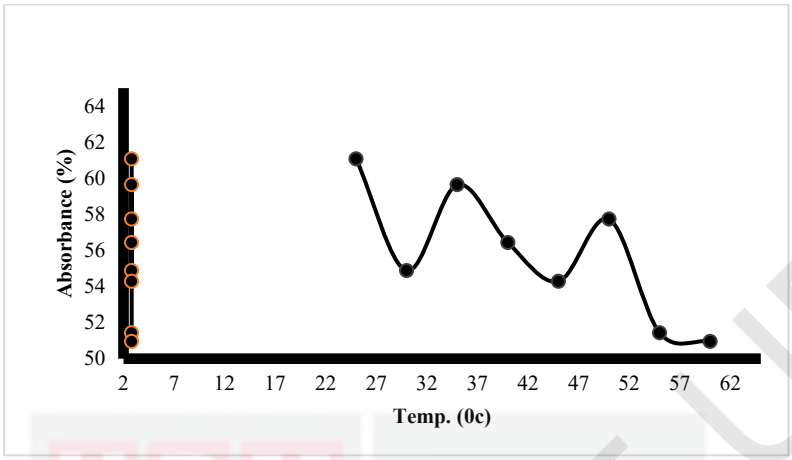

Figure 4.6: Effect of temperature on the adsorption of Congo red dye by *Serratia marcescens* strain MM06

4.2.6 Effect of adsorbent dosage

The number of adsorption sites that are available for the adsorbate to fill can also be used to represent the amount of biosorbent that should be used. Therefore, an increase in the total amount of adsorbent will often increase the amount of dye that is absorbed by the adsorbent. There is a presumption that an increase in the availability of adsorption sites will lead to a corresponding increase in sorption capacity (Chikri et al., 2020). **Figure 4.6** displayed the influence of adsorbent dosage on Congo red removal by *Serratia marcescens* strain MM06. The results show that increasing the amount of bacterial biomass, i.e., increasing the adsorbent dose from 0.5 to 1.5g, improves Congo red dye removal. Dye uptake increases from a minimum of 55% to a maximum of 74%, which may be attributable to increased adsorbent surface area and the availability of more adsorption sites. This is in accordance with the findings of Gupta et al. (Gupta et al., 2020), which show that the adsorption capacity declines as the dosage of the adsorbent increases, however, the percentage of adsorption increases significantly. According to the research conducted by Mane et al. (Mane et al., 2008), the greater the surface area, the greater the number of adsorption sites that are readily available. Similar research by Hamzeh et al. (Hamzeh et al., 2012) on the removal of Acid Orange and Remazol Black dyes from aqueous solutions employing a new biosorbent clearly showed that increasing the biosorbent mass, enhanced the percentage of dye removal from 41 to 51 and from 41 to 95 % for AO7 and RB5, respectively.

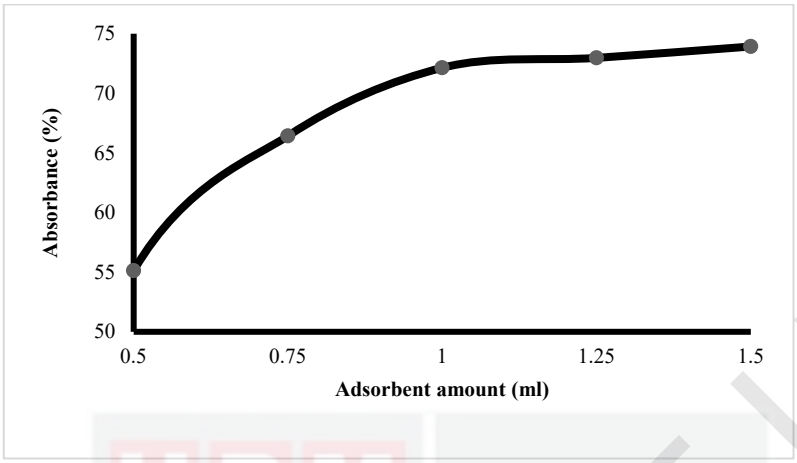

Figure 4.7: Displays the effect of adsorbent dosage on Congo red dye adsorption

4.2.7 Summary of OFAT results

The optimal conditions for Congo red dye adsorption utilising *Serratia marcescens* strain MM06 biomass optimization are listed in **Table 4.1**. Each parameter was optimized using one factor at a time (OFAT). The parameters that were optimised were the initial dye concentration, contact time, pH, agitation speed, temperature, and adsorbent dosage. The Congo red dye was effectively absorbed under the following conditions: dye concentration 90 ppm, contact period 20 min, pH 7, agitation speed 125 rpm, temperature 25 °C, and adsorbent amount 0.94 g. Different optimization condition ranges for dye adsorption parameters were published in numerous pieces of literature (Lim et al., 2013; Manogaran et al., 2021). Lim et al. (Lim et al., 2013) investigated the impact of several parameters on dye removal using a one-factor at a time approach and discovered that the type of nutrients and the amount of the inoculum employed have a significant impact on how effectively azo dyes decolorize. Malachite green was successfully removed from aqueous solutions employing dry *Bacillus cereus* M116 cells as a biosorbent, according to Nath et al. (Nath & Ray, 2015). Environmental factors were discovered to have a substantial impact on the process. The best conditions were pH 5.0, 0.5 g/L biomass concentration, 400 mg/L initial dye, and a contact time of 360 minutes. A maximum dye absorption capacity of 485 mg/g was also determined. In a similar study, Pillai et al. (Pillai, 2017) discovered that the best conditions for the breakdown of Azo blue dye by the bacterium, Streptomyces DJ15, were temperature of 40 °C, pH 7.0, inoculum size 3% (v/v), initial dye concentration of 50 mg/L, and agitation speed 0 rpm. In bacterial studies, the inoculum is the introduction of microorganisms into a system, and its size is a critical parameter, determining the initial population and influencing bacterial kinetics, growth, and metabolic activities (Pillai, 2017). This current study, like many others, found that optimising environmental parameters considerably improves the adsorption process.

Table 4.1: Optimum conditions for the adsorption of Congo red dye using *Serratia marcescens* strain MM06

Parameters	Optimum
Initial Dye concentration	90 ppm
Contact Time	20 min.
pH	7
Agitation speed	125 rpm
Temperature	25 °C
Adsorbent amount	0.94 g

4.3 Optimization of Congo red dye adsorption using Response Surface Methodology (RSM)

After determining the best condition for each factor by the application of OFAT, the optimization process continued with a multivariate statistical method utilising the Respond Surface Methodology (RSM). Response surface methodology is a set of mathematical and statistical techniques for modeling and analysing the response of a process that is influenced by a variety of factors. Design, formulation, development, and optimization all rely heavily on response surface methodology. RSM has been widely used for optimization in a variety of industrial applications such as chemical processes, sheet metal processes, metal joining, cutting, and so on. The response surface plot, a graphical representation of RSM's viewpoint, can be understood. A contour plot is a useful graphical representation technique for understanding the relationship between two input variables and response. The contour is plotted for the same response value for a variety of factors. Contours in the first-order response model will be parallel lines, while in the second-order model, they will be circular (Mishra & Jalan, 2021). RSM is a tool that can be utilised to detect and show the complex nonlinear interactions between independent variables and the system's responses. A response surface design needs to be able to provide an adequate distribution of information over the experimental zone. This is a required property. The design of a response surface enables us to estimate an interaction and even quadratic effects, which provides us with an indicator of the form of the response surface that is being investigated (on a local level).

The ideal (optimal) conditions for the adsorption of Congo red dye were further found with the assistance of statistical methods, the Plackett-Burman, and a 3-level full factorial design.

4.3.1 Screening using Plackett-Burman design (PBD)

The adsorption of Congo red dye was analysed using the Plackett-Burman Design, which involved screening and selecting the important variables that influence the adsorption of the dye. By screening six independent parameters with 12 different combinations of experiments, it was concluded that there was a substantial element in this analysis. Each parameter had two levels: low level (-1) and high level (+1), which matched the minimum and maximum values measured during the OFAT phase. In order to map the response surface and optimise key variables, a regression analysis of the experimental data was performed using Design Expert software version 6.0.8. The six variables that

affect the percentage of dye removal have the following ranges: Initial dye concentration ranges from 50 and 100 mg/L, contact time is between 5 and 20 min., pH from 4 to 8, agitation speed is between 100 and 150 rpm, the temperature is between 25 and 35°C, and the adsorbent dose is between 0.5 and 9.2 g/L **(Table 4.2).** With the settings shown in **Table 4.2**, a total of 12 Plackett-Burman tests were performed, and they were all successful. The lowest dye adsorption was discovered in run 5 (7.96 %), while the maximum adsorption was obtained in run 12. (85.08 %). The result for dye removal percentage was chosen as the response for statistical analysis, and the significant variables that were found were subjected to further optimization using the 3 Level full factorial design.

Table 4.2: Shows the experimental design and percentage dye adsorption of Congo red dye in 12 Plackett-Burman design (PBD) experimental runs

Run	A: Dye Conc. (PPM)	B: Contact Time. (min)	C: pH	D: Agitation (rpm)	E: Temp. (O_C)	F: Adsorbent Size (ml)	Removal %
1	50	20	8	100	35	0.5	55.24
2	100	5	4	100	35	1.5	39.80
3	50	5	4	150	35	1.5	22.39
4	100	5	8	150	25	1.5	65.35
5	100	20	4	150	25	0.5	7.96
6	100	20	4	150	35	0.5	12.94
7	100	20	8	100	35	1.5	79.26
8	100	5	8	100	25	0.5	48.68
9	50	20	4	100	25	1.5	69.65
10	50	5	8	150	35	0.5	55.01
11	50	5	4	100	25	0.5	13.93
12	50	20	8	150	25	1.5	85.08

Table 4.3 displays the first-order model's analysis of variance (ANOVA) and regression analysis. The models were poorly significant and linear, with a minor curvature. The dye concentration, contact time, agitation speed, and temperature were all insignificant. As a result, pH and adsorbent amounts are used in the designing of a three-level full factorial design. The model F value was revealed to be 10.52, indicating that the models were significantly different based on ANOVA analysis (**Table 4.3).** There was only a 1.03% chance that a "model F-value" this large might arise owing to noise. A p-value of 0.05 shows that the model terms are significant. According to the ANOVA, the coefficient of determination (R^2) was 0.9266, indicating that the regression line was not well-fitted. The adjusted and predicted R^2 values were found to be 0.8385 and 0.5771 respectively for dye adsorption. Hence, the adjusted and the predicted R^2 values were not in agreement. The adequate precision value for measuring signal to noise was determined to be 9.379. As a result, an appropriate sound signal is presented. **Figure 4.7** displays the similarity plot between predicted and actual values acquired by the PBD. The final Equation in terms of actual factors is shown in **Equation 4.1**:

$$Y = 2.74036 - 0.15775A + 0.72189B + 9.2482C - 0.1928D - 0.43359E + 27.96056F \quad (4.1)$$

Table 4.3: Analysis of Variance (ANOVA) for dye adsorption from PBD

Source	Sum of Squares	*df*	Mean Square	*F*-Value	Prob > F	
Model	7324.38	6	1220.73	10.52	0.0103	Significant
A	186.65	1	186.65	1.61	0.2606	
B	351.76	1	351.76	3.03	0.1422	
C	4105.4	1	4105.4	35.37	0.0019	
D	278.8	1	278.8	2.4	0.1819	
E	56.4	1	56.4	0.49	0.5168	
F	2345.38	1	2345.38	20.2	0.0064	
Residual	580.4	5	116.08			
Cor Total	7904.79	11				
Std. Dev.	10.77		R^2	0.9266		
Mean	46.27		Adj R^2	0.8385		
C.V.	23.28		Pred R^2	0.5771		
PRESS	3343.11		Adeq Precision	9.379		

4.3.2 Adsorption optimization of dye using three-level full factorial design

RSM is a set of statistical and mathematical techniques for developing, improving, and optimising processes. Among other response surface designs (central composite, Doehlert matrix, and Box Behnken designs), the three-level full factorial design is one of the most powerful and efficient experimental designs. There are several types of RSM designs available, including factorial designs, central composite designs (CCD), Box-Behnken designs, and D-optimal designs (Sadi, 2018). A three-level full factorial design was used in this study to assess the effect of parameters (pH and adsorbent size) on the biosorption of Congo red dye using the biomass of *Serratia marcescens* strain MM06.

To estimate the influence of the different variables, the factorial experimental design was chosen, which involves changing all of the variables from one experiment to the next. Factorial designs are commonly used to investigate the effects of experimental factors as well as their interactions, that is, how the effect of one factor varies with the level of the other factors in a response. The benefits of factorial experiments include their low cost, reduced number of experiments, and increased opportunities to evaluate interactions between variables (Bingol et al., 2010; Kumar, D S Sai Ravi Kiran, 2013).

The significant parameters identified in PBD were further optimised using a three-level full factorial design. Thirteen (13) different experimental designs with five centre points were carried out, with the design and results shown in **Table 4.4.** According to Borugadda and Goud., (Borugadda & Goud, 2015), the R^2 value is always between 0 and 1, and its order of magnitude indicates the model's goodness between the predicted and model experimental values of the response variable. The highest adsorption capacity was found to be in run 13 (91.75%). Regression analysis showed a good fit of the experimental data to the third-order polynomial model. The square of the deviation between the experimental data and the calculated values is the R-squared parameter (R^2). R^2 values closer to 1 indicate a well-fitting model based on good data (Borugadda & Goud, 2015; Esfe et al., 2017). In this study, the R square was 0.9935, indicating that this model could account for more than 0.9935 of the variability in the response. The adjusted R-squared (R^2- adj) values were also high (0.9889), confirming that the models are highly significant. The model's F-value is 214.89, indicating that the proposed model

is also highly significant. Additionally, the model does not contain insignificant parameters as evidenced by the close proximity of the R-squared (R^2) and the adjusted R-squared (R^2- adj) values. The "predict R-squared" of 0.9462 and the "adjust R-squared" of 0.9889 are reasonably in agreement. The ratio of signal to noise is measured by "adeq precision." The ideal ratio is greater than 4. In this study, the adequate precision is 36.685, which denotes a good signal and prediction performance (Anderson J. Mark, 2016). The analysis of Variance (ANOVA) is shown in **Table 4.5.**

Table 4.4: Experimental layout and result for the optimization of dye using a three-level full factorial design

Run	A: pH	B: Adsorbent dosage (%)	Actual value (%)	Predicted value (%)
1	6	1	89.29	88.25
2	8	0.5	57.67	58.56
3	4	1	85.93	85.02
4	8	1.5	90.77	89.93
5	6	1	87.23	88.25
6	4	0.5	56.27	57.50
7	8	1	86.33	86.28
8	6	0.5	62.90	60.69
9	6	1	87.83	88.25
10	6	1	87.96	88.25
11	4	1.5	90.98	90.11
12	6	1	87.96	88.25
13	6	1.5	90.51	91.75

Table 4.5: Analysis of Variance (ANOVA) for a three-level full factorial model

Source	Sum of Squares	*df*	Mean Square	*F*-Value	Prob > F	
Model	2016.45	5	403.29	214.89	< 0.0001	
A	2.37	1	2.37	1.26	0.2983	
B	1447.67	1	1447.67	771.39	< 0.0001	
A2	18.67	1	18.67	9.95	0.0161	
B2	399.63	1	399.63	212.95	< 0.0001	
AB	0.093	1	0.093	0.05	0.8298	
Residual	13.14	7	1.88			
Lack of Fit	10.85	3	3.62	6.31	0.0536	Significant
Pure Error	2.29	4	0.57			
Cor Total	2029.59	12				
Std. Dev.	1.37	R-Squared	0.9935			
Mean	81.5	Adj R-Squared	0.9889			
C.V.	1.68	Pred R-Squared	0.9462			
PRESS	109.19	Adeq Precision	36.685			

A: pH, B: Adsorbent dosage (g)

The findings in this study were in accordance with the work of Esfe et al. (2017) on the Application of a three-level general factorial design approach for thermal conductivity of MgO/water nanofluids. In their findings, the model's R^2 value was 0.9994 which was close to 1, and the adjusted R-squared (R^2- adj) was also very high (0.9990). The "predict R-squared" and the "adjust R-squared" of values of 0.9978 and 0.9984 respectively were in concrete agreement with one another. Also, the value of the adequate precision was 152.669 which showed enough signal having good performance in prediction. The findings revealed that the two parameters of pH and adsorbent size, as well as their interaction, influence dye biosorption.

The similarities between the actual and predicted values obtained in the three-level full factorial design for dye adsorption are displayed in **Figure 4.7**. Once more, there was a significant correlation between the actual value and the value predicted by the model. **Equations 4.2** and **4.3** describe these in terms of actual and coded factors.

$$Y=-15.30+7.96A+126.38B-0.65A^2-48.12B^2+0.15AB \quad (4.2)$$

$$Y=88.25+0.63A+15.53B-2.6A^2-12.03B^2+0.15AB \quad (4.3)$$

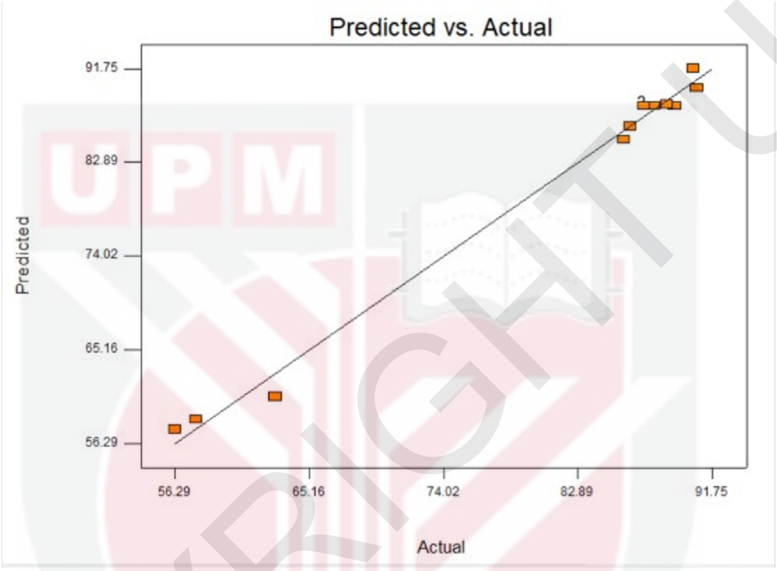

Figure 4.8: Experimental and predicted factors for optimal dye adsorption responses

4.3.3 Adsorption of Congo red dye in 3D response surface plot

The three-dimensional (3D) response surface plots of the dependent variable as a function of two independent factors can reveal information about their relationships. They can also aid in understanding both the main and interaction effects of these two independent variables (K. P. Singh et al., 2011). Using Design-Expert software, the graph, and contour for the 3D response surface model was created. The effects of the mutual interactions between the independent parameters tested are shown in each graph. Their effects on the dependent parameter, in this case, the amount of adsorption, are represented by the contour plot. Response surface analysis is used to evaluate the effectiveness of the best condition variables in achieving the maximum or desired response. When there is a significant interaction between the independent parameters, an elliptical contour is discovered (Muralidhar et al., 2001). **Figure 4.8** depicts the 3D response surfaces and contour plots of the model of the interactions between significant independent variables (A) pH and (B) biosorbent dosage in relation to the dependent variable, the percentage of Congo red dye removed from the experimental design. **Figure**

4.8 depicts the interaction between pH (A) and adsorbent dosage (B). The interaction effect between pH and adsorbent size was significant at a constant concentration of 90 PPM, contact time of 20 minutes, agitation speed of 125 rpm, and temperature of 25 ℃. Within the experimental ranges, dye adsorption increases as adsorbent size increases and decreases as pH decreases. According to Bingol et al. (2010), the 3D response surface and its associated contour plots in a two-level factorial design illustrate the interactions of three factors (temperature, pH, and ionic strength). This visualisation aids in understanding the interaction of two variables and determining the best value for each parameter. In another study by Esfe *et al*. (2017), the 3D response surface and its associated contour plots in a three-level factorial design show the interactions of three factors(volume fraction, temperature, and ionic nanoparticle size).

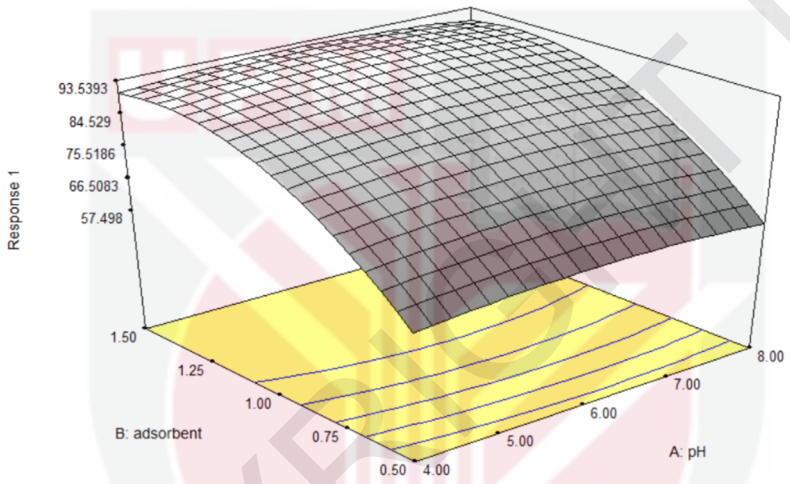

Figure 4.9: Three-dimensional response surface plots for dye adsorption showing the interactive effects between pH and, adsorbent size

4.3.4 Validation of RSM experiment

To experimentally test the predicted value of Congo red dye adsorption, the two significant variables were kept at optimum values of pH 7.18 and adsorbent dose of 1.24 g, as predicted by a three-level full factorial. All other factors (concentration, contact time, agitation, and temperature) were kept constant based on OFAT because they were not significant in the PBD analysis, and the experiment was carried out in triplicate. The experimental value obtained was 90.37% dye absorption, which was close to the model's predicted value (88.24%), thus the adsorption percentage does not differ significantly between the experimental and predicted values (t-test, $p > 0.05$). and therefore, supported the model's validity. The comparison between the predicted result from RSM and that obtained experimentally is shown in **Table 4.6.**

Table 4.6: A comparison of the predicted generated adsorption from RSM and the experimental result

Factors	Name	Predicted levels	Experimental levels
A	pH	7.18	7.18
B	Adsorbent size (g)	1.24	1.24
		Predicted	Experimental
Response (%)		88.24	90.37

4.4 Characterization of bacterial biosorbent using FTIR and SEM techniques

The Fourier Transform Infrared spectroscopy technique is a useful tool for identifying functional groups on biomass that are capable of adsorbing dye ions. The modification of the functional groups provides evidence that the biosorption process has occurred. Using this technique, the functional groups involved in biosorption can be found.

It is necessary to characterise surface chemistry and biosorbent structure in order to develop dye adsorption processes. The presence of functional groups can be determined using Fourier transform infrared spectroscopy (FTIR), which is also useful for learning more about potential interactions between adsorbent and adsorbate. The types, structures, and functional groups of the bonds in the bacterial biomass, as well as the groups responsible for the dye adsorption, were identified using FTIR spectra. Thus, the biosorption process is verified by changes in the surface functional groups. FTIR coupled with Scanning electron microscopy (SEM) and energy-dispersive X-ray spectroscopy (EDX) were used to characterised the bacterial biomass in this research.

4.4.1 FTIR analysis

The information of an unidentified material is provided and identified by FTIR analysis. It calculates the range of infrared wavelengths that the tested substance can absorb. A non-periodic function can be transformed mathematically using the Fourier transform from an amplitude against the time domain to an amplitude against the frequency domain. In each analysis, the data was converted into a spectrum plot, with the x-axis representing wavenumbers and the y-axis representing the transmittances that the compound emits. The percent transmittance of the radiation in comparison to a reference is used to measure the intensity of IR radiation. Tan et al. (2017) For example, a transmittance of 100% signifies that the sample and reference both absorbed the same quantity of radiation. A transmittance of 0% indicates that the sample completely absorbed the radiation. Bacterial biomass has a lot of potential as a dye adsorbent material due to its high carbon content and lignocellulosic component (Sharma, S. et al., 2014).

The use of FTIR is justifiable as it is instrumental in elucidating the chemical structure of dye molecules and bacterial biomass, playing a crucial role in understanding their interactions. The spectra exhibit distinct peaks linked to various chemical bonds,

enabling the identification of specific functional groups in both the dye and bacterial biomass, and facilitating the pinpointing of interaction sites. This technique proves particularly valuable in comprehending the mechanisms of interaction during biosorption, where spectral changes signify dye adsorption onto bacterial surfaces or modifications in bacterial cell components. FTIR's holistic approach enables a thorough analysis of both bacterial biomass and dye, offering a comprehensive overview of chemical changes throughout the biosorption process. Researchers can validate biosorption occurrences by using FTIR to detect spectrum changes indicative of interactions between the dye and bacterial biomass (Chilakamarry *et al*. 2022; Kurniawan et al., 2021; Pal & Maiti, 2020).

The characteristics of binding sites and the adsorption of dyes to the surface of proteins are caused by active functional groups like amino, hydroxyl, sulphonate, carboxyl, and carbonyl (Ahmad et al., 2021; Jadhav et al., 2012). By identifying the adsorption binding site through the changes of functional groups using FTIR analysis, the process of biosorption is proven.

High transmittance values indicate that there are fewer bonds in the sample that have vibrational frequencies that match the incoming light, while low transmittance values indicate that there are more bonds in the sample that absorb light. The most prevalent chemical components of bacterial biomass are polysaccharides, proteins, nucleic acids, lipids, and humic compounds. They developed several functional groups, such as carboxyl, hydroxyl, and amino, which were available on the surface site and were able to bind the sorbate ion and molecules to it (J. Gupta et al., 2019).

FTIR has been used to identify the presence of various functional groups on the surface of the bacterial biomass. The resonance features of the operational groups can be easily found on the surface of the adsorbent before and after adsorption by using FTIR spectroscopy (Pal & Maiti, 2020). The 4000-400 cm^{-1} wavenumber region contains several prominent peaks, as shown in Figure **4.9.** and **4.10.** with their respective Control (bacterial biomass without dye) in blue. The peaks in the vicinity of the current peak were split into two groups: one for molecular fingerprinting, which includes peaks below 1500 cm^{-1}, the fingerprint region is complex and challenging to reliably interpret and, another (functional region) for determining the presence of an active group (1500 cm^{-1} to 4000 cm^{-1}), it is the region where the majority of stretching frequencies manifest. The molecule is uniquely identified by its fingerprint print region (Jadhav et al., 2012). Furthermore, **Figure 4.9.** show a comparison of the FTIR spectrum of *Serratia marcescens* strain Mm06 biomass before and after treatment with 30 mg/L and 100 mg/L. With the help of this analysis, the major functional groups involved in the biosorption process that are present in the bacterial biomass were identified. Adsorption peaks in FTIR spectra suggested that the bacterial biomass was straightforward. The biosorption process was aided by the presence of several groups and substances in Congo red dye, including $-NH_2$ and $-SO_3$, C-H, C-O, and others as shown in the research by Lafi et al. (2019).

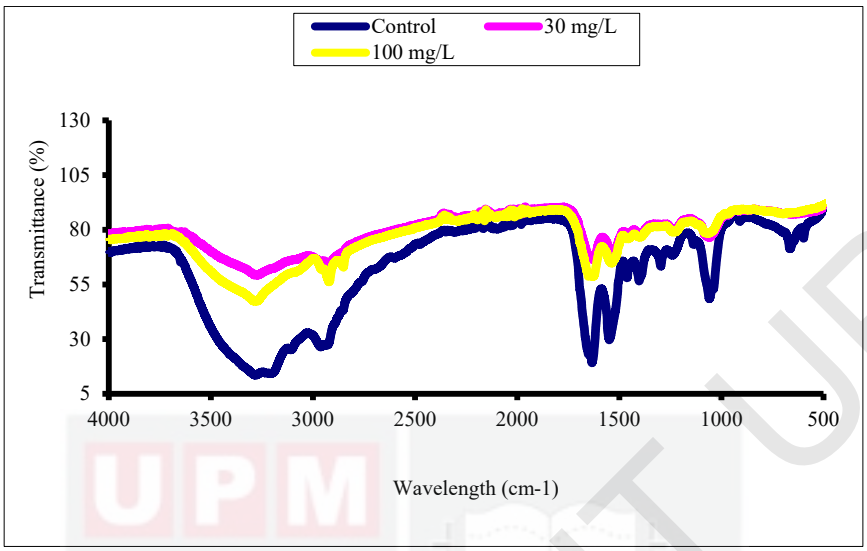

Figure 4.10: Comparison of the FTIR spectrum of *Serratia marcescens* strain Mm06 biomass before and after treatment with 30 and 100 mg/L

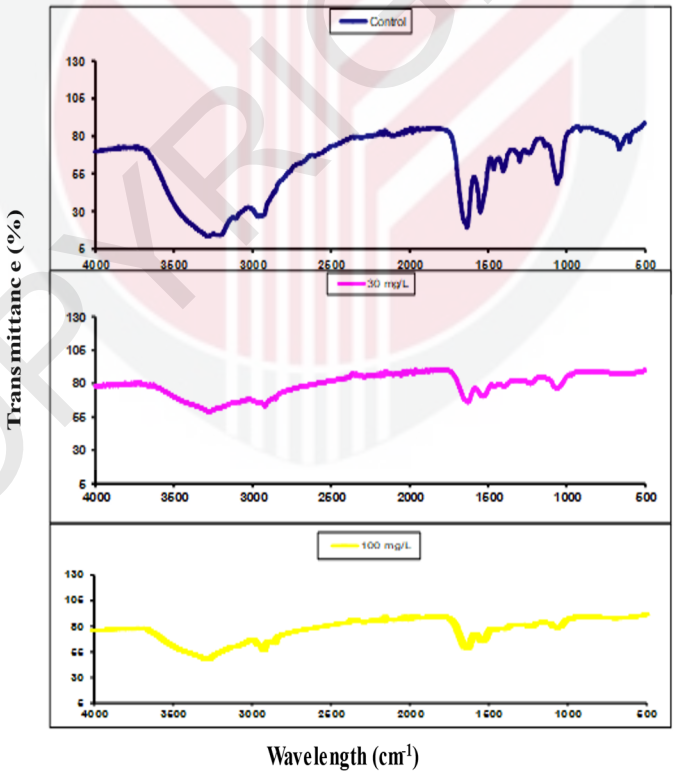

Figure 4.11: FTIR spectrum of the biomass of *Serratia marcescens* strain Mm06 before and after treatment with 30 mg/L and 100 mg/L

The results of the FTIR analysis show which functional groups are present in the biosorbate material (dye) that was used. These functional groups are involved in the dye removal mechanism. **Table 4.7** shows a comparison of peaks present before and after Congo red dye adsorption. In the wavenumber range of 4000 to 500 cm^{-1}, the FTIR analysis of the unprocessed and processed bacterial biosorbent revealed several significant bands. The band/peak at 3279.08 cm^{-1} could be caused by O-H stretching of the carboxyl group which shifted to 3271.19 cm^{-1} in 30 mg/L and 3284.47 cm^{-1} in 100 mg/L (Pal & Maiti, 2020; Fawzy et al., 2019; Kurniawan et al., 2021). The peak at 2962.10 cm^{-1} might be due to the C–H bond of aliphatic which moved to 2920.12 cm^{-1} in 30 mg/L and 2921.18 cm^{-1} in 100 mg/L (Gedam et al., 2019; Velkova et al., 2018; Ahmed & Ebrahim, 2020). The strong peak located at 1634.40 cm^{-1} is characteristic of the stretching vibration of N=N from carboxylic acid which shifted to 1628.01 cm^{-1} in 30 mg/L and 1633.60 cm^{-1} in 100 mg/L (Karthik et al., 2020; Edokpayi & Makete, 2021). The peak at 1548.99 cm^{-1} could be attributed to C–N stretching vibrations of –C–(=O)–NH– group which shifted to 1536.71 cm^{-1} in 30 mg/L and 1538.87 cm^{-1} in 100 mg/L (Velkova et al., 2018; Karthik et al., 2020). The 1462.62 cm^{-1} adsorption peak indicated C-H vibration, which shifted to 1455.02 cm^{-1} in 30 mg/L and 1456.20 cm^{-1} in 100 mg/L (Gedam et al., 2019; Lim et al., 2013). The band which shifted from 1394.56 cm^{-1} in 30 mg/L to 1397.97 cm^{-1} in 100 mg/L was assigned to C-C stretching of the aromatic ring (Regti et al., 2017). The band at 1297.24 cm^{-1} which shifted to 1231.40 cm^{-1} and 1231.97 cm^{-1} at 30 mg/L and 100 mg/L respectively suggests the presence of S=O (Yaneva & Georgieva, 2012; Mona et al., 2011). The peak at 1058.98 cm^{-1} confirms the presence of C-O stretching of ethers and was shifted to 1058.16 cm^{-1} in 30 mg/L and 1062.21 cm^{-1} in 100 mg/L (Kurniawan et al., 2021; Lafi et al., 2019; Yaneva & Georgieva, 2012). The peak at 663.95 cm^{-1} shows a C-H bend which also shifted to 666.81 cm^{-1} at 30 mg/L and 696.52 cm^{-1} at 100 mg/L(Pal & Maiti, 2020; Karthik et al., 2019).

In research by Pal & Maiti, (2020), in their finding, the FTIR bands were recorded in the range of 4000 to 400 cm^{-1}. The peak position at wavenumbers 3327 and 3200 cm^{-1} revealed that the stretching spectra of the amide (N-H) and O-H groups coincided. The C-H stretching vibrations of the methyl (-CH3) and ethyl (-CH2) groups were revealed by peaks at 2988 cm^{-1}. The presence of the -COOH group was identified by the spectra at 2691 and 2505 cm^{-1}. The carbonyl groups spanning from the R-C=OH (aldehyde) and R-C=OR (ketone) groups were represented by the peak that was identified at 1652 cm^{-1}. The detected peak at the 1351 cm^{-1} region pointed to the stretching of alkanes groups during deformation. The C-O group, which is representative of polysaccharides, was identified by distinct peaks at 1127 cm^{-1}. While the two prominent peaks at 1069 and 1028 cm^{-1} are indicative of phosphate stretching bands. The presence of the C-H group accounts for the peaks located in the region of 602 and 563 cm^{-1}.

In different research by Chilakamarry *et al*. (2022). In the FTIR study, the primary peaks for the hydroxyl group and C-H stretching had intensities between 3500 and 3000 cm^{-1} and 2900 to 2960 cm1, respectively. OH, bending was the cause of the peak at 1600–1650 cm^{-1}. Commercial glycerol and glycerol residue both have C-O-H bending at 1400–1450 cm^{-1}, CCO stretching at 1100–1150 cm^{-1}, and C-O stretching at 1000–1050 cm^{-1}. In particular, it was observed that in ethanol, the peak intensity at 3500–3000 cm^{-1} for the OH group declined drastically and that the peak at 2972 cm^{-1} increased due to the methyl group (C–H stretching) and 1044 cm^{-1} for the C–O stretching.

Table 4.7: The FTIR spectrum prediction of the biomass of *Serratia marcescens* strain Mm06 before and after treatment with Congo red dye using 30 mg/L and 100 mg/L

FTIR peaks	Biomass	30 mg/L	100 ml/L	Action
1	-	3854.21	3802.04	N-H
2	-	3808.28	-	Additional peak
3	-	3744.90	-	C-H
4	-	3714.59	3713.26	Additional peak
5	3279.08	3271.19	3284.47	O-H Stretching
6	3208.61	-	-	O-H
7	2962.10	2920.12	2921.18	C-H aliphatic vibration
8	-	2347.91	2349.10	
9	-	2283.50	2286.62	NH_3
10	-	2223.52	-	C≡C
11	-	2204.06	-	Additional peak
12	-	2187.25	2193.90	Additional peak
13	-	2173.07	2159.87	Additional peak
14	-	2159.75	2143.29	Additional peak
15	-	2103.08	2104.27	Additional peak
16	-	2088.76	-	Overtones, weak
17	-	2059.51	-	Overtones, weak
18	-	2050.37	2049.58	Overtones, weak
19	-	2036.86	2039.09	Overtones, weak
20	-	2026.82	2029.13	Overtones, weak
21	-	2007.93	2012.25	Overtones, weak
22	-	1981.02	1988.95	Overtones, weak
23	-	1973.42	1968.90	Overtones, weak
24	-	1952.19	1960.44	Overtones, weak
25	-	-	1938.19	Overtones, weak
26	1634.40	1628.01	1633.60	N=N (carboxylic and lactoic)
27	1548.99	1536.71	1538.87	C–N stretching vibrations of –C–(=O)–NH– group
28	1462.62	1455.02	1456.20	N-O
29	1403.27	-	-	Additional peak
30	-	1394.56	1397.97	C-C stretching (aromatic ring)
31	1297.24	1231.40	1231.97	S=O: C-O
32	1058.98	1058.16	1062.21	C-O stretching (ethers or lactones)
33	663.95	666.81	696.52	C-C
34	598.28	418.02	-	Additional peak

4.4.2 Scanning Electron Microscopy (SEM) and Energy Dispersive X-ray (EDX) analysis

The technique of scanning electron microscopy is employed to analyse the characteristics of surface structure. Scanning Electron Microscopy (SEM) has become increasingly useful and essential as the size of materials decreases to accommodate more applications. The SEM, as opposed to the light microscope, uses electrons for imaging. SEM images are frequently used to examine the surface properties and morphological aspects of the adsorbent material. Additionally, it displays the adsorbent's porosity and surface texture. It is crucial in establishing how much surface area is available for the dye to bind to adsorbents (Dandge et al., 2016). The EDX served as a means of examining the properties of the substances found on the adsorbent surface. An energy-dispersive X-ray spectrometer can also determine the weight percentage of the major and minor elements present in the adsorbent (biomass) materials.

The microscopic method known as scanning electron microscopy (SEM) scans the surface of a sample or material to produce images therefore it is used to validate the surface properties of bacterial biomass (Chen et al., 2015; Gopalakrishnan et al., 2020; Lim et al., 2013). Different signals that are produced when the electrons interact with the specimen's atoms reveal information on the surface composition and organisation of the specimen. These methods, along with a plethora of others, such as AFM (Atomic Force Microscopy), are used to describe dye biosorption by bacterial biomass (Nguyen et al., 2016; Kotrba et al., 2011; Nath & Ray, 2015). The biosorbent was subjected to SEM characterization before and after absorption. The samples were cleaned, dried, and ground. The samples were then examined using an SEM/EDX analyzer at a suitable resolution (x5000 magnification) and voltage, and the micrographs were recorded (Venkata et al. 2002). Before utilising a scanning electron microscope to scan the samples, the samples were first dried at 65°C to a stable weight. The surface morphology of the biomass was determined to be heterogeneous, non-porous, smooth, and tightly structured. Images showed that the surface of the dye and the bacterial biomass were adherently bound (Nguyen et al., 2016). A study using a scanning electron microscope (SEM) demonstrates the existence of macro-pores on the surface that were irregularly distributed pores and that these macro-pores enhanced the adsorption of CR dye molecules onto the surface of bacterial biomass (Dandge et al., 2016). The morphology of the surface of bacterial biomass (*Serratia marcescens* strain MM06) is shown in the SEM micrograph, indicating the availability of pores and the internal surface of the adsorbent (**Figure 4.11).** The presence of asymmetrical pores on the surface of the biosorbent, which showed that the biomass is capable of pore diffusion, was clearly visible. Due to the porosity of the material and the electrostatic interaction between the biosorbent and the Congo red dye, the results of the SEM and FTIR characterization demonstrate the dominance of the physical adsorption mechanism.

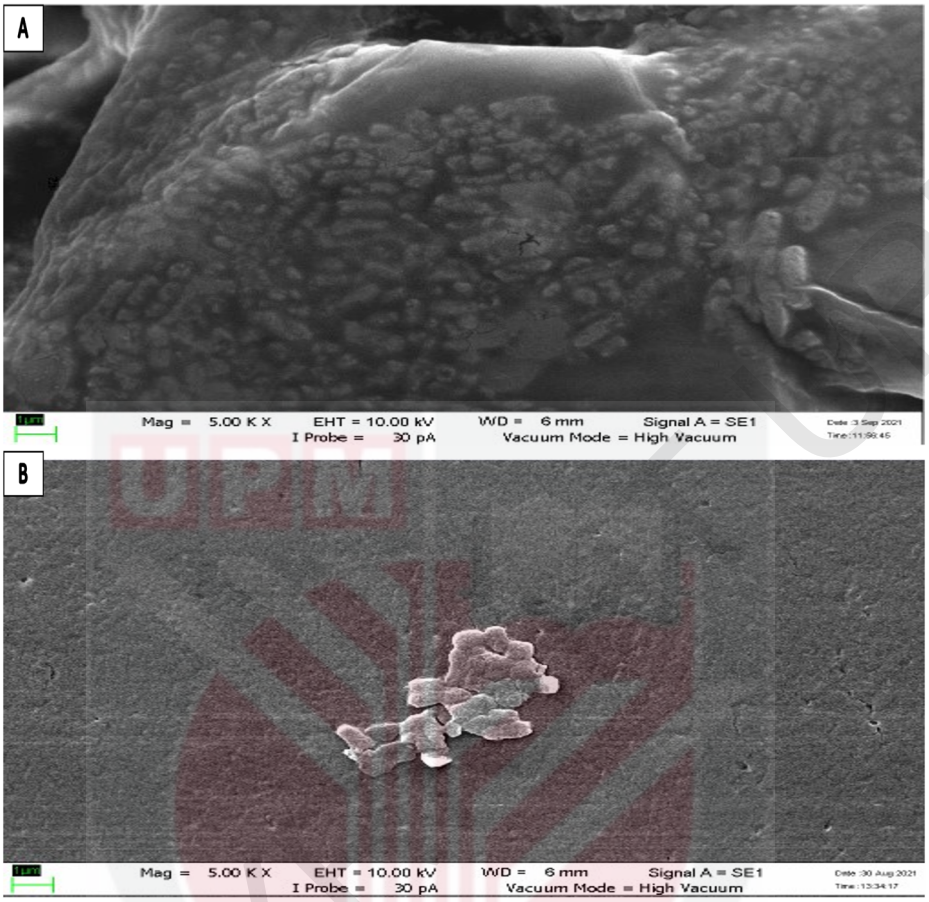

Figure 4.12: Scanning electron micrographs of *Serratia marcescens* strain MM06 (A) before dye adsorption and (B) after dye adsorption (Magnification: x5,000)

Table 4.8: *Serratia marcescens* strain MM06 biomass elemental analyses before and after dye adsorption techniques

Element	Control adsorbent (Biomass)	Biomass treated with dye
C [%]	53.44	69.63
O [%]	79.96	28.17
P [%]	10.70	2.33
S [%]	5.17	1.19
Na [%]	0.33	na
Mg [%]	na	0.24
k [%]	4.17	na

*n.d.: not detected

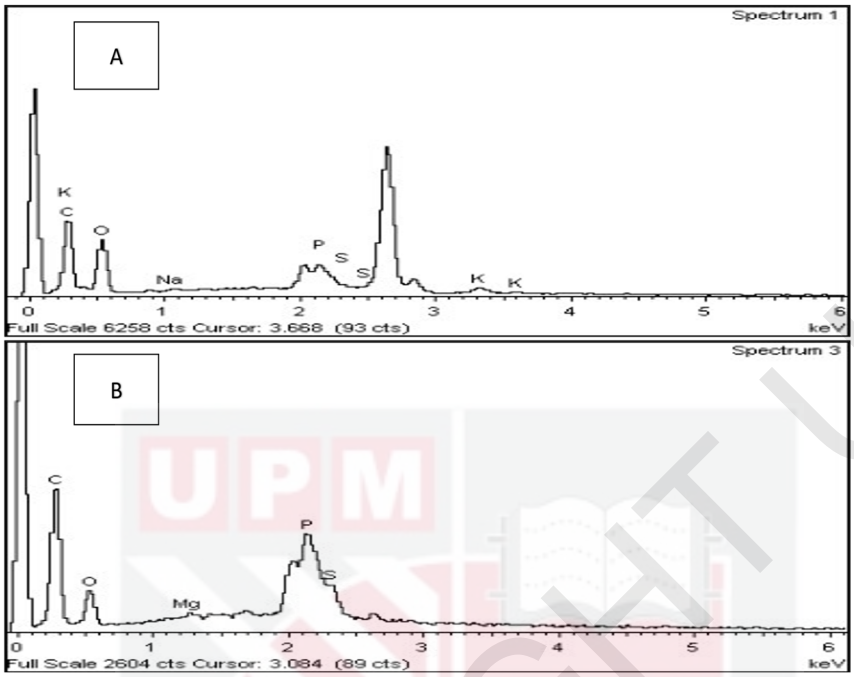

Figure 4.13: EDX design for *Serratia marcescens* strain MM06 (A) before dye adsorption, (B) after dye adsorption

The findings of an EDX elemental analysis of the bacterial biomass before and after the adsorption process are shown in **Figure 4.12.** and **Table 4.8.** These results show the percentages of C, O, P, and S elements in the bacterial biomass before and after the adsorption process. The chemical Composition of the utilised biosorbent reveals a significant quantity of C (53.44% and 69.63%) and O (79.96% and 28.17%) before and after treating the biomass with dye respectively and is in accordance with the finding of Moussa et al. (2015) These components, when converted into activated carbon, make biomass a highly efficient biosorbent for future adsorption research.

4.5 Determination of kinetic growth model for batch adsorption studies

The kinetics of an adsorption process reveal important information about the reaction rate and mechanism. It is determined by the interactions of the adsorbate and adsorbent. Given a speedy and high adsorption capacity rate as its criterion, the adsorption rate aids in determining the optimal biosorbent for use in adsorption experiments (Eris & Azizian, 2017; Viotti et al., 2019).

Kinetic data in the form of initial contact time is critical for developing accurate modeling and reliable conclusion representations. Two essential evaluation variables for an adsorption process operation unit are the mechanism and the rate of reaction. The adsorption rate is important in identifying the appropriate biosorbent for use in dye

adsorption investigations since it must match the criteria of high adsorption capacity and rapid adsorption rate. Moreover, it gives the adsorption process time to reach equilibrium. As a result, kinetic modeling is essential for research and system development for pollution removal (Tan & Hameed, 2017).

In this study, a batch kinetic experiment was performed at various dye concentrations to determine the adsorption kinetics of Congo red dye. For 30 minutes, the dye concentrations were 10, 20, 30, 40, 50, 70, and 90 mg/L. The kinetic investigation was conducted using contact time-dependent low and high dye concentrations. Based on the OFAT results, all order parameters were kept constant. The pseudo-first-order and pseudo-second-order equations were used to analyse and fit the adsorption data using nonlinear kinetic regression employing curve-fitting tools software. Since the calculations for kinetic model fitting were also performed on the same abscissa as the linear regression plot, the nonlinear regression was preferred for more precise calculations [Li et al., 2016; Gedam et al., 2019; Shukor, 2014]. These adsorption kinetic models are the most frequently suggested ones. The models fit experimental biotechnology data, were shown to be straightforward and reliable, and supported assumptions. It provides a numerical method for fitting adsorption curves that illustrate how biotechnologists visually approximate adsorption kinetics. The pseudo-first-order, pseudo-second-order, and Elovich models could describe the mechanism and the adsorption rate (Khan et al., 2018). In comparison to the 1st order models, the 2nd order kinetic model could estimate the adsorption pattern over the entire adsorption time. In many adsorption systems explored, the Pseudo- first-order and Elovich kinetic systems do not match well across the full adsorption period and are only applicable to the very early stages of the adsorption process. Furthermore, the pseudo-second-order equation confirms chemisorption as a rate control step in the adsorption process based on the sorption capacity of the solid phase.

Figure 4.13 depicts the fitting of experimental data using pseudo-second-order kinetics for Congo red dye adsorption at various concentrations using *Serratia marcescens* strain MM06 biomass, while **Table 4.9** shows the adsorption kinetic parameters. Because the lowest AICc value, -46.76, and adjR^2 that is 1.0 **(Table 4.9)** and more relative equilibrium adsorption capacity for dye, the pseudo-second-order kinetic model, as opposed to the pseudo-first-order models, provides a better description of the adsorption process. The fitting of pseudo-first- and pseudo-second-order kinetics for Congo red dye is shown in **Figures 4.14 A** and **B**, respectively.

The kinetics occurred within shorter time intervals (0,1.5,3,4,5,10,15,20,25 and 30 min), especially in the early stages of adsorption. the choice of time points and time range align with the result obtained, the characteristics of the adsorbate, and the properties of the adsorbent.

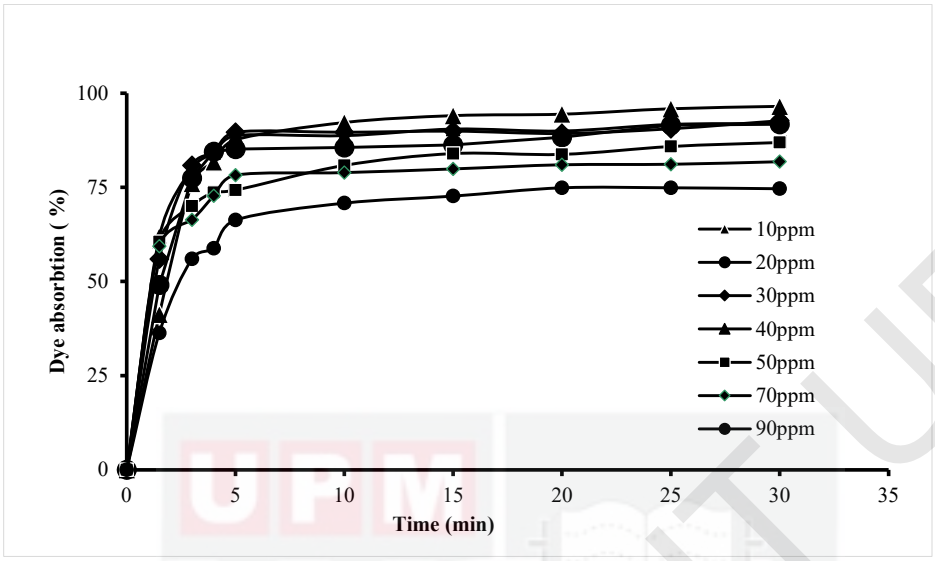

Figure 4.14: Adsorption curve of *Serratia marcescens* strain MM06 biomass fitted to a pseudo-second-order kinetic model at varied Congo red dye concentrations

Table 4.9: Statistical analyses of Congo red dye adsorption using kinetics models

Model	Parameter	SSE	MSE	RMSE	R^2	adR^2	AICc	BIC	HQC	AF	BF
Pseudo-1st order	2.00	0.03	0.00	0.07	1.00	1.00	-36.53	-46.93	-48.18	1.0219	1.01
Pseudo-2nd order	2.00	0.01	0.00	0.04	1.00	1.00	-46.76	-57.16	-58.41	1.0983	0.92

Note:

RMSE	Root mean Square Error
p	no of parameters
adR^2	Adjusted Coefficient of determination
BF	Bias factor
AF	Accuracy factor
AICc	Adjusted Akaike Information Criterion
BIC	Bayesian Information Criterion
HQC	Hannan–Quinn information criterion

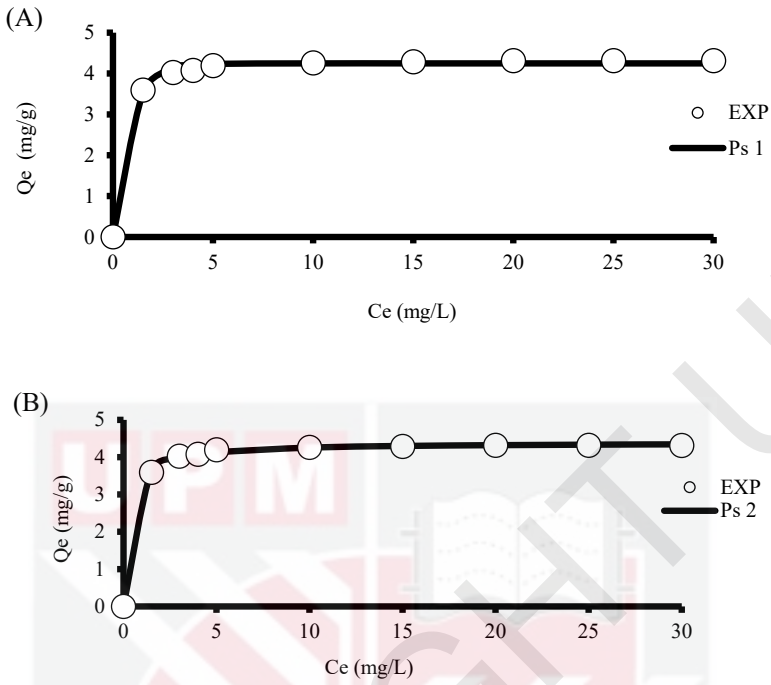

Figure 4.15: Adsorption profile of *Serratia marcescens* strain MM06 biomass and Congo red dye fitted to (A) 1st pseudo-order kinetic model and (B) pseudo-second-order kinetic model

The amount of time required for the adsorption process to reach equilibrium is determined by the rate of adsorption, which is controlled by adsorption kinetics. On adsorption paths and potential mechanisms, kinetic models can offer information. Additionally, this information is also useful for process development and adsorption system design. The process is concluded to be pseudo-second order rather than pseudo-first order. Adsorption may also occur in nature as chemisorption, including valence forces via electron sharing or exchange, as suggested by the best match to pseudo-second-order kinetics, however, kinetics investigations alone are insufficient to uncover the mechanistic insights of adsorption (K. V. Kumar et al., 2007; Tran et al., 2017).

This is in accordance with multiple published papers that have identified pseudo-first and Pseudo- second-order kinetics as the best models for adsorption studies (Edokpayi & Makete, 2021; Cai et al., 2020; Tran et al., 2017). Velkova et al. (2018) in their studies used PFO and PSO to predict the best kinetic model. It was demonstrated that the experimental and theoretical data were in excellent agreement with the second-order model in another study by Wu et al. (2020). Mansour et al. (2020) also used PFO and PSO to predict Brilliant Green Dye Biosorption Using Activated Carbon Derived from Guava Tree Wood and it was found that the pseudo-second-order model was suitable for the behavior of the BG dye adsorption.

The rate-controlling step in the pseudo-second-order reaction is linked to a chemical reaction known as chemisorption in this context. In this scenario, the rate of adsorption controls the adsorption mechanism chemically. When the sorbate/sorbent ratio is low (first order at very low ratios), a reversible second-order process frequently controls the sorption kinetics. When the sorbate/sorbent ratio is higher, two reversible second-order reactions that are competitive with one another control the sorption kinetics (Venkata et al. 2002). Therefore, the kinetic result shows that the PSO model was used to fit data for all concentrations of Congo red dye. The data exhibited good agreement with the pseudo-second-order equation, with adjR^2 values of 1.0 for all regressed lines.

4.6 Determination of the best isotherm model

The adsorption isotherm is the most often utilised depiction of the adsorbate concentration and quantity of pollutant adsorbed. The equilibrium adsorption isotherm is significant for the design of an adsorption system equilibrium of dye adsorption because it describes the interacting behaviour between the solute and the adsorbent (Mansour et al., 2020). The isotherm research gives significant physicochemical data for future evaluation of the adsorption process in the laboratory as a single operation. As a result, isothermal investigations and isothermal modeling are critical in optimising the design for any adsorption parameter (Vijayaraghavan & Yun, 2008).

To select a suitable model for the process design, it is required to obtain precise equilibrium data that fits suitably into a number of isotherm models. Important details on the mechanism of the adsorption process, the surface properties, and the affinities of the adsorbent that are not available from other sources, such as laboratory experiments, are provided by the variable obtained from various models. This information is crucial for developing an adsorption system for usage on an industrial scale. It is preferred if the kinetic isotherm can shed light on intrinsic kinetics, which is chemical kinetics that occurs on the adsorbent surface when there are no transport restrictions, in order to be most informative about it (Vijayaraghavan & Yun, 2008; Neag et al., 2019). Isotherm curves can be examined by altering the initial solute concentrations while maintaining environmental parameters like pH and temperature constant. In general, absorption increases with increasing concentration and reaches saturation at higher concentrations. In most biosorption investigations, pH appears to be a significant parameter for evaluating an isotherm. However, there is some ambiguity in reporting isotherms based on the pH. Isotherms have been documented in the biosorption literature based on the initial, final, or controlled pH circumstances. Because of the chemical interaction that occurs between the biomass and the sorbent during biosorption, the pH of the reaction mixture tends to fluctuate. Any pH shift seems to be mostly caused by the chemical components of a biosorbent and the type of the biosorption mechanism (Vijayaraghavan & Yun, 2008). The numerous kinds of adsorption isotherms including Henry, Langmuir, Freundlich, BET, Toth, Sips, Fritz-Schlunder IV, and Fritz-Schlunder V were explored and described using a variety of theoretical and empirical models. **Figure 4.15** and **Table 4.10.** show the different isotherms models and the error function analysis for the fitting of the isotherms of dye adsorption.

Table 4.10: Error function analysis for the dye adsorption model fitting of the 8 selected isotherms

Model	***p***	**RMSE**	***adR2***	**AICc**	**BIC**	**HQC**	**BF**	AF
Henry	1	2.44	-0.33	24.47	19.06	18.42	0.47	2.44
Langmuir	2	0.02	1.00	-67.74	-77.13	-78.40	0.80	1.25
Freundlich	2	0.11	0.99	-31.75	-41.14	-42.41	1.29	1.31
BET	3	0.04	1.00	-47.31	-62.40	-64.30	1.28	1.29
Toth	3	1.73	-0.92	29.39	14.30	12.40	0.54	1.86
Sips	3	0.02	1.00	-60.85	-75.94	-77.85	0.79	1.26
F4	4	0.02	1.00	-49.86	-73.65	-76.19	0.80	1.25
F5	5	0.02	1.00	-31.74	-70.22	-73.39	0.79	1.26

Note:

RMSE	Root mean Square Error
p	no of parameters
adR^2	Adjusted Coefficient of determination
BF	Bias factor
AF	Accuracy factor
AICc	Adjusted Akaike Information Criterion
BIC	Bayesian Information Criterion
HQC	Hannan–Quinn information criterion

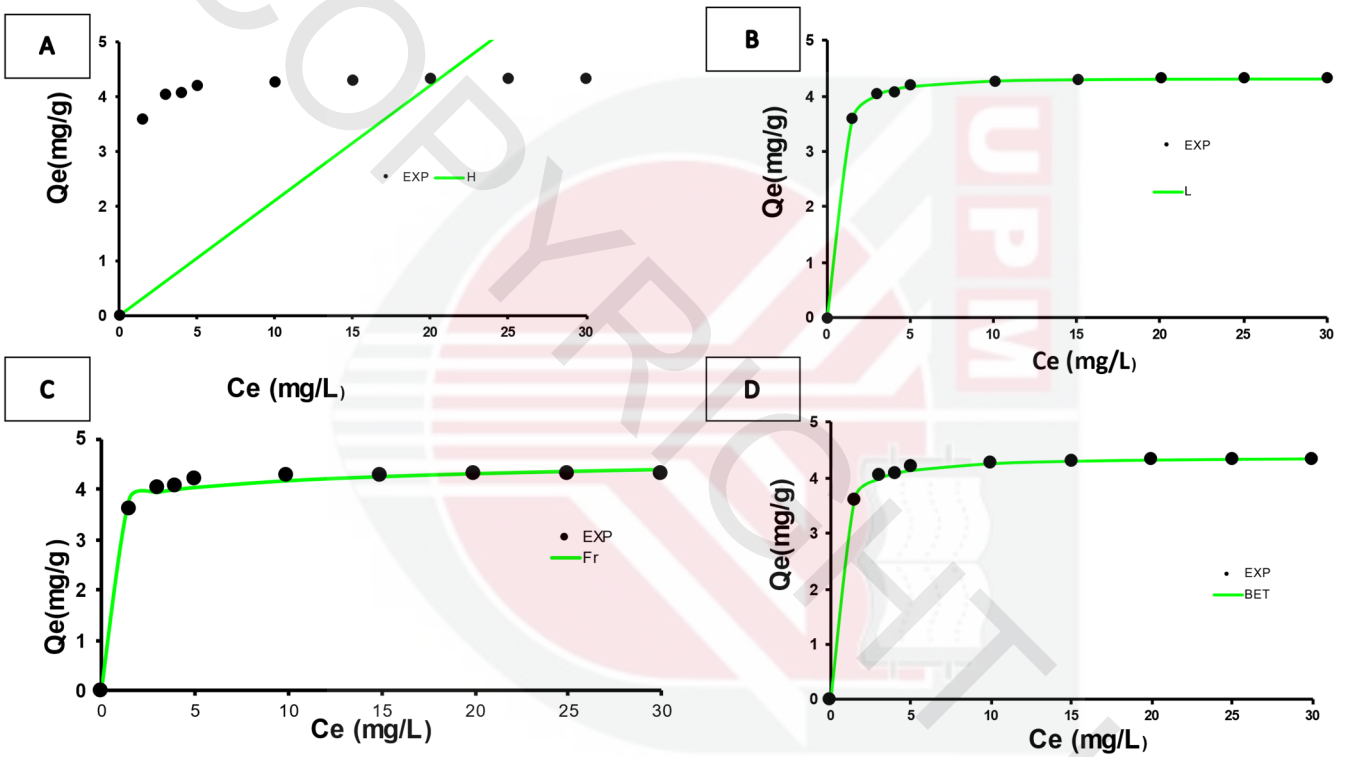

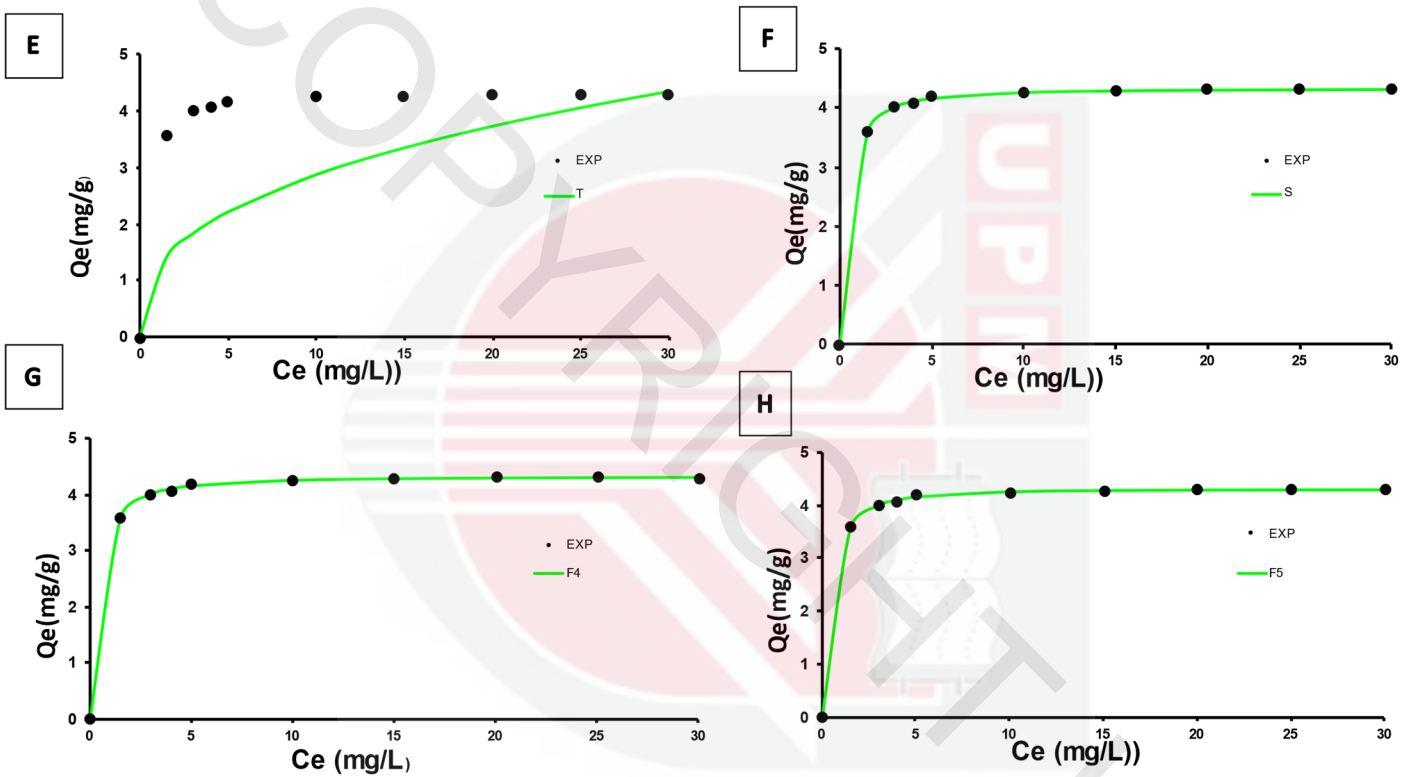

Figure 4.16: Isotherms model of the biosorption of congo red dye by the biomass of *Serratia marcescens* strain MM06 using (A) Henry, (B) Langmuir, (C) Freundlich, (D) BET, (E) Toth, (F) Sips, (G) Fritz-Schlunder IV and (H) Fritz-Schlunder V respectively

A batch operation is a desirable method to employ in the study of the kinetics isotherm. As a result, a batch experiment was carried out to collect the isotherm data while ensuring uniform experimental conditions throughout the investigation. Using eight (8) different isotherm models, including Henry, Langmuir, Freundlich, BET, Toth, Sips, Fritz-Schlunder IV, and Fritz-Schlunder V, the equilibrium data from the batch adsorption studies were analysed and fitted using nonlinear regression figure 4.15. All eight of the isotherm models that were tested on the dye produced a good fitting result, with the exception of the Henry and Toth model. The Langmuir model was found to be the best isotherm model for dye adsorption following statistical analysis using the corrected Akaike Information Criterion (AICc), root-mean-square error (RMSE), adjusted coefficient of determination ($adjR^2$), accuracy factor (AF), and bias factor (BF) (**Table 4.10)**. Thus, the Langmuir fitting as the best isotherm model suggests that the adsorption was a monolayer process**.**

Chen & Zhao, (2009) used the Langmuir and Freundlich isotherms models to analyse equilibrium data for the adsorption study for the removal of congo red anionic dye using organo-attapulgite, and the distinguishing parameters for each isotherm were identified. The results showed that the Langmuir adsorption isotherm matched the experimental data fairly well. In another research by Dandge et al., (2016), Langmuir and Freundlich models are used to study the equilibrium isotherm. The plot produces a straight line for all of the organics investigated, indicating that the sorption data closely follows the Langmuir sorption model. In a study also by Viotti et al. (2019), adsorption isotherms were used to present equilibrium data. For data fitting, the Langmuir and Freundlich models were used, and their parameters provide details on the adsorbent surface characteristics and the adsorbent/adsorbate affinity, which help in understanding the mechanisms of adsorption. For both adsorbents, the Freundlich model best fits the experimental data, showing the t R^2 value closest to 1 and the lowest SSE value. The Freundlich model is used to describe adsorption in heterogeneous systems. The result shows that the sorption did not reach a limit value or adsorbent saturation, indicating that the process was multilayer.

4.7 Thermodynamic studies

In the adsorption investigation, whether it is chemical or physical adsorption, it is crucial to establish the adsorption mechanisms. Van der Waals forces and other relatively weak interactions lead to physical adsorption, whereas stronger chemical bonds and subsequent electron transfer between the adsorbent and adsorbate lead to chemical adsorption (Tran et al., 2016). The thermodynamic characteristics of an adsorption process determine its viability and spontaneity. An important criterion for spontaneity is Gibb's free energy change, or ΔG°, which indicates the spontaneity of a chemical reaction The equilibrium KC constant is essential for accurately calculating these thermodynamic properties. Calculations of Gibbs free energy and other thermodynamic properties are performed using partition constants, distribution coefficients, and constants derived from various isothermal models. According to IUPAC, a regular balancing constant called KC is used to calculate the Gibbs free energy change (ΔG°) (Nguyen et al., 2020; Tran et al., 2017). The thermodynamic parameters in this study were calculated using nonlinear regression of the van't Hoff plot and the Langmuir constant, KC, as shown in the previous research (Nguyen et al., 2020; Tran et al., 2016; Dotto et al., 2013; Mahmoud et al.,

2012; Gedam et al., 2019). Despite the fact that the linearized variant is frequently used, the nonlinear van't Hoff plot was used in this study. In linearized kinetics, isotherms, and thermodynamics models, the peculiar error distribution described by Lima et al. (2019) may result in significant error deviations. Nonlinear regression typically yields a lower 95% confidence interval (Moussout et al., 2018). The thermodynamics study was carried out using five temperature data points (25, 30, 35, 40, and 45°C), which allowed for more degree of freedom to be used, which improved the non-linear plot's ability to fit the data and maximise the benefits of nonlinear regression. When there are more data points, it is preferable to use the non-linear equation. The dye's kinetic and Langmuir equilibrium isotherms were investigated at various concentrations (10, 20,30,40, 50, 70, and 90 mg/L) and temperatures (25, 30, 35, 40, and 45°C). Based on the kinetic results, the order of the kinetic reaction used was pseudo-second-order (PSO). Thus, the qe constants from the PSO model were used to calculate the Langmuir constant, KL, by plotting the Langmuir isotherm model. The Langmuir constant, KL, is a thermodynamic equilibrium constant that has dimension and must be transformed into a dimensionless form (KC) in order to be used in standard thermodynamic calculations. Based on the above statement the region containing the actual data about adsorption equilibrium may be the Langmuir isotherms zone, which is characterised by saturation at high concentrations. Consequently, when estimating thermodynamic parameters, the Langmuir constant (KL) is used as a replacement for the thermodynamic equilibrium constant (KC).

The values of the thermodynamics parameters for the whole adsorption process are summarized and presented in **Table 4.11.** Based on the van't Hoff plot in **Figure 4.16**., the values of $\Delta H°$ and $\Delta S°$ are computed, The slope of the van't Hoff plot, also, determines whether the system is exothermic (negative slope) or endothermic (positive slope) (Tran et al., 2016).

Table 4.11: shows the thermodynamic parameters (Δ*G*, *ΔH*, and *ΔS)* calculated from the van't Hoff plot and the dimensionless Langmuir constant for dye adsorption

Temp (*K*)	K_C	*ΔG° (kJ/mol)*	95% CI Lower	95% CI Upper	*ΔH°* (KJ/mol)	*ΔS°* (kJ/(mol.K)
298.15	1,442,274	-34.15	-39.52	-28.79		
303.15	1,914,009	-36.24	-37.55	-34.92		
308.15	2,838,147	-37.68	-40.00	-35.35	65.46	336.1
313.15	4,075,486	-39.47	-40.37	-38.57		
318.15	6,554,031	-41.25	-42.82	-39.69		

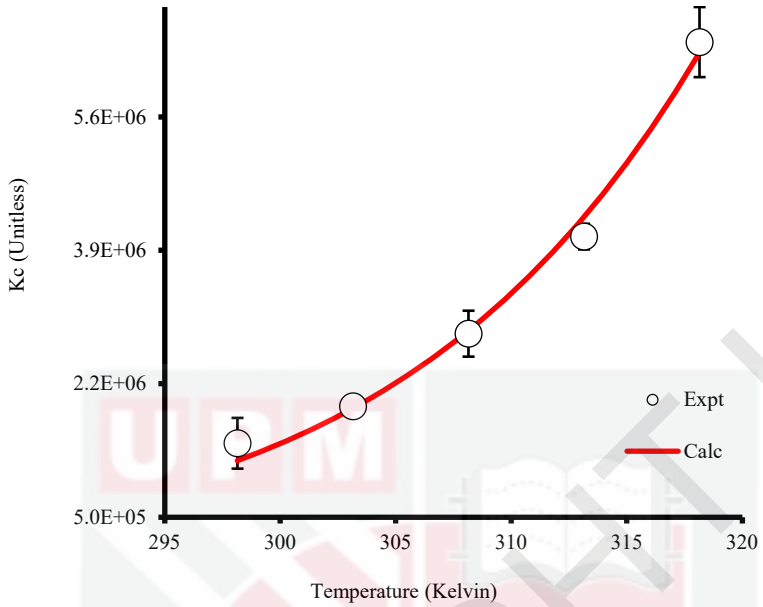

Figure 4.17: A non-linear van't Hoff plot of the dimensionless constant, *Kc* against temperature, K of the dye adsorption process. Error bars are mean +/- standard error (n=3)

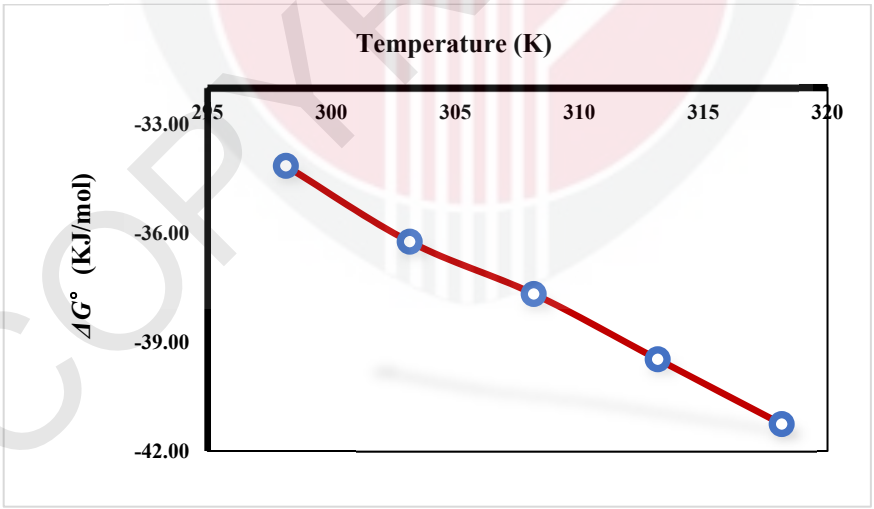

Figure 4.18: Plot of Gibb's free energy change (*ΔG*°) versus temperature of dye adsorption process indicating the spontaneous reaction process

Gibbs' free energy ($\Delta G°$) parameters were computed directly from the equations provided in section 3.9.6, as discussed in Chapter 3. The other parameters (entropy change, $\Delta S°$, and enthalpy change, $\Delta H°$) were calculated from a non-linear plot of dimensionless KC versus temperature. The results of the current study showed that the adsorption occurred through chemisorption because adsorption with $-\Delta G°$ values between -400 and -80 kJ/mol corresponds to chemisorption. Chemosorption encompasses chemical interactions between the dye (adsorbate) and the bacterial biomass (adsorbent). This specificity facilitates selective binding, relying on the chemical characteristics of the dye and the functional groups present on the surface of the adsorbent. In contrast to physisorption, chemosorption usually entails more robust and targeted binding forces. Chemical interactions, including covalent bonds or ion exchange, frequently lead to increased affinity and stability of the dye on the adsorbent surface (Mudhoo & Pittman, 2023). The preference for chemosorption in the study results is justified by the specific chemical interactions between the adsorbate and adsorbent, leading to stronger and more selective binding. These factors enhance the effectiveness, stability, and real-world relevance of the adsorption process (Mudhoo & Pittman, 2023; Tran et al., 2016). The positive values of standard enthalpy ($\Delta H°$) suggest that the process of Congo red dye adsorption onto the biomass of *Serratia marcescens* strain MM06 was feasible, spontaneous, and endothermic, indicating that heat is absorbed from the environment into the system (Tran et al., 2016; Velkova et al., 2018; Sivasamy et al., 2012). Studying thermodynamics is justified despite **Figures 4.5 and 4.2** indicating insignificance in temperature and time effects respectively. The thermodynamic analysis contributes valuable insights into the energetics which reveal whether adsorption is driven by enthalpy changes, entropy changes, or a combination of both, driving forces, and optimization of the adsorption process, enriching the overall understanding of thermodynamic parameters, such as Gibbs free energy ($\Delta G°$), enthalpy ($\Delta H°$), and entropy ($\Delta S°$), of the system (Mudhoo & Pittman, 2023).

Many studies have shown that increasing the temperature causes the biosorption process to slow down, and this is referred to as an exothermic ($-\Delta H$) reaction since the heat in the form of energy is released into the environment throughout the process (Wang et al., 2006; Tran et al., 2016; Moussa et al., 2015). Endothermic reactions, on the other hand, are defined as those in which energy is taken from the environment in the form of heat ($+\Delta H$) produced (Velkova et al., 2018; Sivasamy et al., 2012). In a solid-liquid system, the adsorption process consists of two steps: the adsorption of adsorbate molecules and the desorption of previously adsorbed solvent molecules. Exothermic adsorption happens when the amount of energy released during the formation of bonds between the molecules of the adsorbent and the adsorbate is greater than the amount of energy that is adsorbed during bond breaking. This results in the release of additional energy in the form of heat and a negative H° value. The presence of heat or energy caused an increase in the mobility of dye molecules as well as an increase in the number of active adsorption sites as temperature increased (Foo & Hameed, 2010; Tran et al., 2016). The increased disorder and randomness at the solid solution interface of the adsorbate with the adsorbent are indicated by the positive values of ΔS. Additionally, a high value of ΔS indicates that the adsorbent has a high affinity for the adsorbate species (Suyamboo, 2012; Foo & Hameed, 2010; Tran et al., 2016).

The finding in this study was in agreement with the work by Ghatbandhe et al. (2013) The outcome demonstrated that the adsorption process occurred endothermally (+ΔH), spontaneously (-$\Delta G°$), and with increased randomness (+$\Delta S°$). Other related thermodynamics studies by Gedam et al. (2019). The results also revealed that the adsorption process was spontaneous, endothermal, and with increased randomness. In another study by Abbas & Trari (2015). The thermodynamic parameters show that the adsorption process is endothermic and spontaneous. The increase in randomness at the solid-solution interface during the CR adsorption is demonstrated by the positive entropy (+$\Delta S°$), which suggests that some structural exchange occurs between the active sites of the adsorbent and CR molecules.

CHAPTER 5

CONCLUSION AND RECOMMENDATIONS

This study serves as a critical step toward addressing the broader challenges of sustainable water management, environmental conservation, and safeguarding public health. By elucidating effective and selective dye removal processes, we contribute to the advancement of responsible industrial practices and the protection of our ecosystems and communities. As we move forward, the lessons learned from this study offer actionable insights for policymakers, environmentalists, and industries alike, promoting a harmonious balance between industrial progress and environmental preservation. To safeguard living creatures, it is essential to remove dyes from wastewater before releasing them into the environment since industrial effluents typically contain dyes that contaminate aquatic environments. Some dyes have poisonous, long-lasting, non-biodegradable, and bioaccumulative properties. Their biodegradable byproducts are known to be highly toxic, mutagenic, and even carcinogenic, and when they reach the food web, they are known to pose several health risks to the ecosystem.

Serratia marcescens strain MM06 biomass exhibited superior dye removal (81.9%) among twelve bacterial isolates tested against Congo red dye. Adsorption, influenced by factors like initial dye concentration, contact time, pH, temperature, and adsorbent dosage, was optimized using One-Factor-at-a-Time (OFAT) and Response Surface Methodology (RSM). OFAT and RSM optimization increased dye removal from 85.08% to 91.75%. Nevertheless, OFAT is influenced more by adsorbent dosage, rpm, contact time, and pH, while RSM is primarily affected by adsorbent dosage and pH. It was discovered that the RSM optimization provides the most ideal conditions for dye removal.

FT-IR analysis established the involvement of various surface functional groups in dye sorption, providing evidence of the biosorption process. The approach thoroughly investigated the functional groups engaged in the biosorption of Congo red dye. SEM examination of biomass surface morphology before and after adsorption revealed the presence of macro-pores that were unevenly distributed, enhancing the adsorption of dye molecules onto the Serratia marcescens strain MM06 surface. SEM and FTIR characterization reveals the dominance of physical adsorption due to material porosity and electrostatic interactions with Congo red dye. The EDX study detected elements (C, O, P, S) in biomass before and after biosorption, with C and O having the highest percentages before (C: 53.44%, O: 79.96%) and after dye treatment (C: 69.63%, O: 28.17%).

Kinetics was analysed at various concentrations (10, 20, 50, 70, and 90 mg/L) and times (0, 1.5, 3, 4, 5, 10, 15, 20, 25, and 30 mins). For simple kinetics models, 10 data points are sufficient to obtain reasonable results. However, in more complex systems or when using sophisticated kinetics models, a larger number of data points could be beneficial for capturing the nuances of the adsorption process. The adsorption kinetics and Isotherms of the bacterial biomass on dye were examined, and the kinetics were

discovered to obey a pseudo-second-order kinetic. Moreover, in the isotherms investigations, all eight of the isotherm models tested on the dye (Henry, Langmuir, Freundlich, BET, Toth, Sips, Fritz-Schlunder IV, and Fritz-Schlunder V), with the exception of the Henry and Toth model, yielded a satisfactory fitting result. Following statistical research utilising the corrected Akaike Information Criterion (AICc), root-mean-square error (RMSE), adjusted coefficient of determination (adjR^2), accuracy factor (AF), and bias factor (BF), it was discovered that the Langmuir model was the best and applicable isotherm model for dye adsorption. The choice of the pseudo-second-order kinetic model is significant due to its ability to describe chemisorption, suggesting that the adsorption process involves chemical interactions between the dye molecules and the adsorbent surface. This aligns with the earlier emphasis on chemosorption in the study. The good fit of the pseudo-second-order model implies that the rate-limiting step is likely influenced by chemical reactions, providing valuable insights into the nature of the adsorption mechanism. The utilization of the Langmuir isotherm model holds significance as it suggests monolayer adsorption with a finite number of adsorption sites. The model's fit to the experimental data implies that the adsorption process reaches a point of saturation, indicating the formation of a complete monolayer of dye molecules on the adsorbent surface. This understanding is crucial for practical applications, as it helps estimate the maximum adsorption capacity of the adsorbent under the studied conditions. Additionally, the Langmuir model provides insights into the homogeneity of the adsorption sites, shedding light on the uniformity of the adsorbent surface in terms of its affinity for dye molecules.

The thermodynamics study included five temperature data points (25, 30, 35, 40, and 45°C), which allowed for a greater degree of freedom to be used, which increased the non-linear plot's capacity to match the data and maximise the benefits of nonlinear regression. The dye's kinetic and Langmuir equilibrium isotherms were examined at various concentrations (10, 20, 30, 40, 50, 70, and 90 mg/L) at temperatures (25, 30, 35, 40, and 45°C). The order of the kinetic reaction employed was pseudo-second-order based on the kinetic data (PSO). Thus, by visualising the Langmuir isotherm model, the qe constants from the PSO model were used to determine the Langmuir constant, KL. A thermodynamic equilibrium constant with dimension, the Langmuir constant (KL), must be converted into a dimensionless version (KC) in order to be employed in typical thermodynamic computations.

The computed thermodynamic parameters **(**$\Delta G°$**,** $\Delta H°$**,** and $\Delta S°$**)** using van't Hoff equation, play a crucial role in assessing the feasibility and spontaneity of the Congo red dye adsorption process. The negative value of ΔG° suggests that the adsorption happened by chemisorption because adsorption with -$\Delta G°$ values between -400 and -80 kJ/mol corresponded to chemisorption, a positive value of $\Delta H°$ (65.46) suggests endothermic adsorption and a positive $\Delta S°$ (336.1) indicates an increase in disorder, contributing to the spontaneity of the process. Understanding the entropy change is critical for determining how adsorption affects the overall system entropy. These parameters contribute to a clearer and more compelling message from the study by providing vital insights into the energetics and driving forces of adsorption. By emphasising these key findings, the study goes beyond being "just a normal study" by offering a thorough knowledge of the thermodynamics that drive the dye adsorption process. The calculated

parameters not only prove the feasibility of the investigated process but also provide practical insights for optimising conditions in real-world wastewater treatment systems. Biosorption is cheaper compared to conventional treatments such as reverse osmosis (RO) or coagulation-flocculation as it includes the use of bacterial biomass like *Serratia marcescens* strain MM06, and has potential advantages in terms of lower initial costs, as they rely on biological materials that could be locally sourced. The study indicates that (bacterial biomass*) Serratia marcescens* strain MM06 effectively removes Congo red dye, exhibiting improved sorption under diverse operational parameters. Langmuir and pseudo-second-order kinetic models were applied for adsorption isotherm and kinetic analysis, respectively.

The main findings emphasize enhanced dye removal efficacy through optimization and the critical roles of specific parameters in shaping the adsorption process, enhancing practical applicability, and deepening our understanding of more effective wastewater treatment solutions.

With the following recommendations for further research, there should be a turning point in the speedy elimination of dye pollution from our environments.

1. Given the laboratory nature of this study, its practical effectiveness remains uncertain. To assess the strain's performance in real-world scenarios, a field study in naturally dyed or dye-polluted locations is essential

2. Before commercialization, a pilot study is crucial to evaluate bacterial biomass adsorption capabilities beyond laboratory-scale studies. Conducting column studies will provide essential information on biosorbent performance, potential scale-up constraints, and insights into biosorbent recycling through column desorption investigations

3. To enhance statistical optimization, artificial neural networks (ANN) should replace response surface techniques due to their high prediction accuracy and versatile capabilities.

4. Research on bacterial biomass consortiums, utilizing *Serratia marcescens* strain MM06 biomass with other bacterial strains or activated carbon, is essential to improve dye pollution removal from the ecosystem

5. Future studies should explore dye multisorption as real-world dye effluent often contains diverse pollutants, including different dyes, minerals, and heavy metals.

6. Immobilization boosts bacteria's adsorptive capacity, and an even more promising future enhancement is converting high-potential bacterial biomass into activated carbon through conventional and hydrothermal methods.

REFERENCES

Abbas, M., & Trari, M. (2015). Kinetic, equilibrium and thermodynamic study on the removal of Congo Red from aqueous solutions by adsorption onto apricot stone. *Process Safety and Environmental Protection*, *98*, 424–436. https://doi.org/10.1016/j.psep.2015.09.015

Abdi, O., & Kazemi, M. (2015). A review study of biosorption of heavy metals and comparison between different biosorbents. *Journal of Materials and Environmental Science*, *6*(5), 1386–1399.

Abdullah, M. I., Öztürk, A., & Bayol, E. (2021). Biosorption of astrazon red dye by the bacterium Rhodopseudomonas sp. strain 51ATA. *Environmental Earth Sciences*, *80*(2), 1–8. https://doi.org/10.1007/s12665-020-09314-7

Adamson, A. W. (1993). *Physical Chemistry of Surfaces* (6 edition). John Wiley & Sons, Inc.

Ahmad, A. A., Hameed, B. H., & Ahmad, A. L. (2008). Equilibrium and Kinetics of Disperse Dye Adsorption on Activated Carbon Prepared From. *International Conference on Environment 2008 (ICENV 2008)*, *2008*(Icenv), 1–8.

Ahmad et al. (2015). Recent Advances in New Generation Dye Removal Technologies: Novel Search of Approaches to Reprocess Waste Water. *RSC Advances*, *5*, 30801–30818.

Ahmad, Hassan, M. A., Roslan, A. M., Ariffin, H., Norrrahim, M. N. F., Othman, M. R., & Yoshihito, S. (2021). Improving the decolorization of glycerol by adsorption using activated carbon derived from oil palm biomass. *Environmental Science and Pollution Research*, *28*(22), 27976–27987. https://doi.org/10.1007/s11356-021-12585-7

Ahmed, H. A. B., & Ebrahim, S. E. (2020). Removal of methylene blue and congo red dyes by pretreated fungus biomass-equilibrium and kinetic studies. *Journal of Advanced Research in Fluid Mechanics and Thermal Sciences*, *66*(2), 84–100.

Akaike, H. (1974). A New Look at the Statistical Model Identification. *IEEE Transactions on Automatic Control*, *19*(6), 716–723.

Aksu, Z. (2005). Application of biosorption for the removal of organic pollutants: A review. *Process Biochemistry*, *40*(3–4), 997–1026. https://doi.org/10.1016/j.procbio.2004.04.008

Aljeboree, A. M., Alshirifi, A. N., & Alkaim, A. F. (2017). Kinetics and equilibrium study for the adsorption of textile dyes on coconut shell activated carbon. *Arabian Journal of Chemistry*, *10*, S3381–S3393. https://doi.org/10.1016/j.arabjc.2014.01.020

Alnajrani, M. N., & Alsager, O. A. (2020). Removal of Antibiotics from Water by Polymer of Intrinsic Microporosity: Isotherms, Kinetics, Thermodynamics, and Adsorption Mechanism. *Scientific Reports*, *10*(1), 1–14. https://doi.org/10.1038/s41598-020-57616-4

Aly-Eldeen, M. A., El-Sayed, A. A. M., Salem, D. M. S. A., & El Zokm, G. M. (2018). The uptake of Eriochrome Black T dye from aqueous solutions utilizing waste activated sludge: Adsorption process optimization using factorial design. *Egyptian Journal of Aquatic Research*, *44*(3), 179–186. https://doi.org/10.1016/j.ejar.2018.09.001

Anderson J. Mark, P. J. W. (2016). *Optimizing Processes Using Response Surface Methods For Design of Experiments* (Second Edi). Taylor & Francis.

Aryal, M. (2020). A comprehensive study on the bacterial biosorption of heavy metals: Materials, performances, mechanisms, and mathematical modellings. *Reviews in Chemical Engineering*. https://doi.org/10.1515/revce-2019-0016

Asgher, M. (2012). Biosorption of reactive dyes: A review. *Water, Air, and Soil Pollution*, *223*(5), 2417–2435. https://doi.org/10.1007/s11270-011-1034-z

Atar, N., Olgun, A., & Çolak, F. (2008). Thermodynamic, equilibrium and kinetic study of the biosorption of basic blue 41 using Bacillus macerans. *Engineering in Life Sciences*, *8*(5), 499–506. https://doi.org/10.1002/elsc.200800036

Bag, S., Hasan, M. I., Halder, D., & Ghosh, A. (2021). Biosorption of organic dye Acridine orange from aqueous solution using dry biomass of Bacillus cereus M116. *Archives of Microbiology*, *203*(7), 3811–3823. https://doi.org/10.1007/s00203-021-02355-x

Baranyi, J., Pin, C. and R. (1999). Validating and comparing predictive models ′. *International Journal of Food Microbiology*, *48*, 159–166.

Baudu, M. (1990). Etude des interactions solute–fibres de charbon actif. Application et regeneration. In *Universite de Rennes I.*

Benkhaya, S., Harfi, S. El, & Harfi, A. El. (2018). Classifications , properties and applications of textile dyes : A review. *Applied Journal of Environmental Engineering Science*, *3*(January 2017), 311–320.

Benkhaya, S., M' rabet, S., & El Harfi, A. (2020). A review on classifications, recent synthesis and applications of textile dyes. *Inorganic Chemistry Communications*, *115*(March), 1–69. https://doi.org/10.1016/j.inoche.2020.107891

Bharathi, K. S., & Ramesh, S. T. (2013). Removal of dyes using agricultural waste as low-cost adsorbents: a review. *Applied Water Science*, *3*(4), 773–790. https://doi.org/10.1007/s13201-013-0117-y

Bingol, D., Tekin, N., & Alkan, M. (2010). Brilliant Yellow dye adsorption onto sepiolite using a full factorial design. *Applied Clay Science*, *50*(3), 315–321.

Biswas, S and Basak, P. (2021). Biosorption of the Industrial Dye Remazol Brilliant Blue R by Bacillus rigiliprofundi. *Microbiology*, *90*(November 2021), 816–828.

Borugadda, V. B., & Goud, V. V. (2015). Response surface methodology for optimization of bio-lubricant basestock synthesis from high free fatty acids castor oil. *Energy Science & Engineering*, *3*(4), 371–383. https://doi.org/10.1002/ese3.77

Bouras, H. D., Yeddou, A. R., Bouras, N., Hellel, D., Holtz, M. D., Sabaou, N., Chergui, A., & Nadjemi, B. (2017). Biosorption of Congo red dye by Aspergillus carbonarius M333 and Penicillium glabrum Pg1: Kinetics, equilibrium and thermodynamic studies. *Journal of the Taiwan Institute of Chemical Engineers*, *80*, 915–923. https://doi.org/10.1016/j.jtice.2017.08.002

Brunauer S, Emmett PH, T. E. (1938). Adsorption of gases in multimolecular layers. *Journal of the American Chemical Society 60*, *60*(1), 309–319. https://doi.org/10.1016/j.fuel.2016.10.086

Burnham, and Anderson, D. . (2002). *Model Selection and Multimodel Inference: A Practical Information-Theoretic Approach* (K. P. B. D. R. Anderson & Model (eds.); second edi). Springer Science & Business Media.

Buthelezi, S. P., Olaniran, A. O., & Pillay, B. (2012). Textile dye removal from wastewater effluents using bioflocculants produced by indigenous bacterial isolates. *Molecules*, *17*(12), 14260–14274. https://doi.org/10.3390/molecules171214260

Cai Y, Li, X., Liu, D., Xu, C., Ai, Y., Sun, X., Zhang, M., Gao, Y., Zhang, Y., Yang, T., Wang, J., Wang, L., Li, X., & Yu, H. (2018). A novel Pb-resistant Bacillus subtilis bacterium isolate for co-biosorption of hazardous Sb(III) and Pb(II): Thermodynamics and application strategy. *International Journal of Environmental Research and Public Health*, *15*(4), 1–18. https://doi.org/10.3390/ijerph15040702

Cai, Z., Deng, X., Wang, Q., Lai, J., Xie, H., Chen, Y., Huang, B., & Lin, G. (2020). Core-shell granular activated carbon and its adsorption of trypan blue. *Journal of Cleaner Production*, *242*. https://doi.org/10.1016/j.jclepro.2019.118496

Caner, N., Kiran, I., Ilhan, S., & Iscen, C. F. (2009). Isotherm and kinetic studies of Burazol Blue ED dye biosorption by dried anaerobic sludge. *Journal of Hazardous Materials*, *165*(1–3), 279–284. https://doi.org/10.1016/j.jhazmat.2008.09.108

Caner, N., Kiran, I., Ilhan, S., Pinarbasi, A., & Iscen, C. F. (2011). Biosorption of reactive yellow 145 dye by dried Penicillum restrictum: Isotherm, kinetic, and thermodynamic studies. *Separation Science and Technology*, *46*(14), 2283–2290. https://doi.org/10.1080/01496395.2011.585211

Canizo, B. V., Agostini, E., Wevar Oller, A. L., Dotto, G. L., Vega, I. A., & Escudero, L. B. (2019). Removal of Crystal Violet from Natural Water and Effluents Through Biosorption on Bacterial Biomass Isolated from Rhizospheric Soil. *Water, Air, and Soil Pollution*, *230*(8), 1–14. https://doi.org/10.1007/s11270-019-4235-5

Chairat, M., & Bremner, J. B. (2016). Biosorption of lac dye by the red marine alga Gracilaria tenuistipitata: biosorption kinetics, isotherms, and thermodynamic parameters. *Coloration Technology*, *132*(6), 472–480. https://doi.org/10.1111/cote.12241

Chatterjee, S., Lee, M. W., & Wooa, S. H. (2010). Adsorption of congo red by chitosan hydrogel beads impregnated with carbon nanotubes. *Bioresource Technology*, *101*(6), 1800–1806. https://doi.org/10.1016/j.biortech.2009.10.051

Chemaly, R. F., Rathod, D. B., Sikka, M. K., Hayden, M. K., Hutchins, M., Horn, T., Tarrand, J., Adachi, J., Nguyen, K., Trenholme, G., & Raad, I. (2011). Serratia marcescens bacteremia because of contaminated prefilled heparin and saline syringes: A multi-state report. *American Journal of Infection Control*, *39*(6), 521–524. https://doi.org/10.1016/j.ajic.2010.08.020

Chen, H., & Zhao, J. (2009). Adsorption study for removal of Congo red anionic dye using organo-attapulgite. *Adsorption*, *15*(4), 381–389. https://doi.org/10.1007/s10450-009-9155-z

Chen, Z., Chen, H., Pan, X., Lin, Z., & Guan, X. (2015). Investigation of Methylene Blue Biosorption and Biodegradation by Bacillus thuringiensis 016. *Water, Air, and Soil Pollution*, *226*(5). https://doi.org/10.1007/s11270-015-2417-3

Cheng, Z., Feng, K., Su, Y., Ye, J., Chen, D., Zhang, S., Zhang, X., & Dionysiou, D. D. (2020). Novel biosorbents synthesized from fungal and bacterial biomass and their applications in the adsorption of volatile organic compounds. *Bioresource Technology*, *300*, 122705. https://doi.org/10.1016/j.biortech.2019.122705

Chikri, R., Elhadiri, N., Benchanaa, M., & El maguana, Y. (2020). Efficiency of sawdust as low-cost adsorbent for dyes removal. *Journal of Chemistry*, *2020*. https://doi.org/10.1155/2020/8813420

Chilakamarry, C. R., Mimi Sakinah, A. M., Zularism, A. W., Khilji, I. A., & Kumarasamy, S. (2022). Glycerol Waste to Bio-Ethanol: Optimization of Fermentation Parameters by the Taguchi Method. *Journal of Chemistry*, *2022*(October). https://doi.org/10.1155/2022/4892992

Chojniak, J., Jałowiecki, Ł., Dorgeloh, E., Hegedusova, B., Ejhed, H., Magnér, J., & Płaza, G. (2015). Application of the BIOLOG system for characterization of Serratia marcescens ss marcescens isolated from onsite wastewater technology (OSWT). *Acta Biochimica Polonica*, *62*(4), 799–805. https://doi.org/10.18388/abp.2015_1138

Choudhary, P., Singh, J., & Subramanian, S. (2015). Bio sorption of acidic dye from an aqueous solution by a marine bacterium, Planococcussp. VITP21. *International Journal of ChemTech Research*, *8*(4), 1763–1768.

Cid, H., Ortiz, C., Pizarro, J., Barros, D., Castillo, X., Giraldo, L., & Moreno-Piraján, J. C. (2015). Characterization of copper (II) biosorption by brown algae Durvillaea antarctica dead biomass. *Adsorption*, *21*(8), 645–658. https://doi.org/10.1007/s10450-015-9715-3

Çolak, F., Atar, N., & Olgun, A. (2009). Biosorption of acidic dyes from aqueous solution by Paenibacillus macerans: Kinetic, thermodynamic and equilibrium studies. *Chemical Engineering Journal*, *150*(1), 122–130. https://doi.org/10.1016/j.cej.2008.12.010

Crini, G. (2006). Non-conventional low-cost adsorbents for dye removal : A review. *Bioresource Technology*, *97*, 1061–1085. https://doi.org/10.1016/j.biortech.2005.05.001

Crini, Grégorio, & Badot, P. M. (2008). Application of chitosan, a natural aminopolysaccharide, for dye removal from aqueous solutions by adsorption processes using batch studies: A review of recent literature. *Progress in Polymer Science (Oxford)*, *33*(4), 399–447. https://doi.org/10.1016/j.progpolymsci.2007.11.001

Cristani, M., Naccari, C., Nostro, A., Pizzimenti, A., Trombetta, D., & Pizzimenti, F. (2012). Possible use of Serratia marcescens in toxic metal biosorption (removal). *Environ Sci Pollut Res*, *19*, 161–168. https://doi.org/10.1007/s11356-011-0539-8

Dandge, R., Ubale, M., Farooqui, M., & Rathod, S. (2016). Adsorption study for the Removal of Hazardous Dye Congo Red by Biowaste Materials as Adsorbents. *International Journal of Application or Innovation in Engineering & Management*, *5*(11), 9–16.

Das, A., & Mishra, S. (2017). Removal of textile dye reactive green-19 using bacterial consortium: Process optimization using response surface methodology and kinetics study. *Journal of Environmental Chemical Engineering*, *5*(1), 612–627. https://doi.org/10.1016/j.jece.2016.10.005

Das, S. K., Shome, I., & Guha, A. K. (2012). Biotechnological Potential of Soil Isolate, Flavobacterium mizutaii for Removal of Azo Dyes: Kinetics, Isotherm, and Microscopic Study. *Separation Science and Technology (Philadelphia)*, *47*(13), 1913–1925. https://doi.org/10.1080/01496395.2012.663446

Dawood, S., & Sen, T. K. (2014). Review on Dye Removal from Its Aqueous Solution into Alternative Cost Ef-fective and Non-Conventional Adsorbents Citation: Tushar K Sen, et al. (2014) Review on Dye Removal from Its Aqueous Solution into Alternative Cost Effective and Non-Conventional Ads. *J Chem Proc Eng*, *1*, 104.

Demirbas, A. (2009). Agricultural based activated carbons for the removal of dyes from aqueous solutions: A review. *Journal of Hazardous Materials*, *167*(1–3), 1–9. https://doi.org/10.1016/j.jhazmat.2008.12.114

Dey, S., & Islam, A. (2015). A Review on Textile Wastewater Characterization in Bangladesh. *Resources and Environment*, *5*(1), 15–44. https://doi.org/10.5923/j.re.20150501.03

Dotto, G. L., Vieira, M. L. G., Esquerdo, V. M., & Pinto, L. A. A. (2013). Equilibrium and thermodynamics of azo dyes biosorption onto Spirulina platensis. *Brazilian Journal of Chemical Engineering*, *30*(1), 13–21. https://doi.org/10.1590/S0104-66322013000100003

Du, L. N., Wang, B., Li, G., Wang, S., Crowley, D. E., & Zhao, Y. H. (2012). Biosorption of the metal-complex dye Acid Black 172 by live and heat-treated biomass of Pseudomonas sp. strain DY1: Kinetics and sorption mechanisms. *Journal of Hazardous Materials*, *205–206*, 47–54. https://doi.org/10.1016/j.jhazmat.2011.12.001

Dubinin, M. (1965). Modern state of the theory of volume filling of micropore adsorbents during adsorption of gases and steams on carbon adsorbents. *Zh Fiz Khim*, *39*, 1305–1317.

Edokpayi, J. N., & Makete, E. (2021). Removal of Congo red dye from aqueous media using Litchi seeds powder: Equilibrium, kinetics and thermodynamics. *Physics and Chemistry of the Earth*, *123*(April 2020), 103007. https://doi.org/10.1016/j.pce.2021.103007

El messaoudi, N., Elkhomri, M., Dbik, A., Bentahar, S., Lacherai, A., & Bakiz, B. (2016). Biosorption of Congo red in a fixed-bed column from aqueous solution using jujube shell: Experimental and mathematical modeling. *Journal of Environmental Chemical Engineering*, *4*(4), 3848–3855. https://doi.org/10.1016/j.jece.2016.08.027

Eris, S., & Azizian, S. (2017). Analysis of adsorption kinetics at solid/solution interface using a hyperbolic tangent model. *Journal of Molecular Liquids*, *231*, 523–527. https://doi.org/10.1016/j.molliq.2017.02.052

Esfe, M. H., Rostamian, H., & Shabani-samghabadi, A. (2017). Application of three-level general factorial design approach for thermal conductivity of MgO / water nanofluids. *Applied Thermal Engineering*. https://doi.org/10.1016/j.applthermaleng.2017.07.211

Essawy, A. A., Ali, A. E. H., & Abdel-Mottaleb, M. S. A. (2008). Application of novel copolymer-TiO2 membranes for some textile dyes adsorptive removal from aqueous solution and photocatalytic decolorization. *Journal of Hazardous Materials*, *157*(2–3), 547–552. https://doi.org/10.1016/j.jhazmat.2008.01.072

Farooq, S., Saeed, A., Sharif, M., Hussain, J., Mabood, F., & Iftekhar, M. (2017). Process optimization studies of crystal violet dye adsorption onto novel, mixed metal Ni0.5Co0.5Fe2O4 ferrospinel nanoparticles using factorial design. *Journal of Water Process Engineering*, *16*, 132–141. https://doi.org/10.1016/j.jwpe.2017.01.001

Fathollahi, A., Khasteganan, N., Coupe, S. J., & Newman, A. P. (2021). A meta-analysis of metal biosorption by suspended bacteria from three phyla. *Chemosphere*, *268*, 129290. https://doi.org/10.1016/j.chemosphere.2020.129290

Fawzy, M., Nasr, M., Abdel-Rahman, A. M., Hosny, G., & Odhafa, B. R. (2019). Techno-economic and environmental approaches of Cd2+ adsorption by olive leaves (Olea europaea L.) waste. *International Journal of Phytoremediation*, *21*(12), 1205–1214. https://doi.org/10.1080/15226514.2019.1612848

Fomina, M., & Gadd, G. M. (2014). Biosorption: Current perspectives on concept, definition and application. *Bioresource Technology*, *160*(January 2014), 3–14. https://doi.org/10.1016/j.biortech.2013.12.102

Foo, K. Y., & Hameed, B. H. (2010). Insights into the modeling of adsorption isotherm systems. *Chemical Engineering Journal*, *156*, 2–10. https://doi.org/10.1016/j.cej.2009.09.013

Fritz, W., & Schluender, E. U. (1974). Simultaneous adsorption equilibria of organic solutes in dilute aqueous solutions on activated carbon. *Chemical Engineering Science*, *29*(5), 1279–1282. https://doi.org/10.1016/0009-2509(74)80128-4

Gadd, G. M. (2009). Biosorption: Critical review of scientific rationale, environmental importance and significance for pollution treatment. *Journal of Chemical Technology and Biotechnology*, *84*(1), 13–28. https://doi.org/10.1002/jctb.1999

Garg, V. K., Amita, M., Kumar, R., & Gupta, R. (2004). Basic dye (methylene blue) removal from simulated wastewater by adsorption using Indian Rosewood sawdust: A timber industry waste. *Dyes and Pigments*, *63*(3), 243–250. https://doi.org/10.1016/j.dyepig.2004.03.005

Gb, O. (2016). Advance Research in Textile Engineering Textile Dye Removal using Dried Sun Flower Seed Hull a New Low Cost Biosorbent : Equilibrium , Kinetics and Thermodynamic Studies. *Advance Research in Textile Engineering*, *1*(1), 1–7.

Gedam, V. V., Raut, P., Chahande, A., & Pathak, P. (2019). Kinetic, thermodynamics and equilibrium studies on the removal of Congo red dye using activated teak leaf powder. *Applied Water Science*, *9*(3), 1–13. https://doi.org/10.1007/s13201-019-0933-9

Ghatbandhe, A. S., Jahagirdar, H. G., Yenkie, M. K. N., & Deosarkar, S. D. (2013). Evaluation of thermodynamic parameters of 2, 4-dichlorophenoxyacetic acid (2, 4-D) adsorption. *Journal of Chemistry*, *2013*, 1–6. https://doi.org/10.1155/2013/519304

Gopalakrishnan, Y., Al-Gheethi, A., Malek, M. A., Azlan, M. M., Al-Sahari, M., Radin Mohamed, R. M. S., Alkhadher, S., & Noman, E. (2020). Removal of basic brown 16 from aqueous solution using durian shell adsorbent, optimisation and techno-economic analysis. *Sustainability (Switzerland)*, *12*(21), 1–22. https://doi.org/10.3390/su12218928

Gorman, R., & Adley, C. C. (2004). Characterization of Salmonella enterica Serotype Typhimurium Isolates from Human, Food, and Animal Sources in the Republic of Ireland. *Journal of Clinical Microbiology*, *42*(5), 2314–2316. https://doi.org/10.1128/JCM.42.5.2314-2316.2004

Gulnaz, O., Kaya, A., & Dincer, S. (2006). The reuse of dried activated sludge for adsorption of reactive dye. *Journal of Hazardous Materials*, *134*(1–3), 190–196. https://doi.org/10.1016/j.jhazmat.2005.10.050

Gupta, V.K., & S. (2009). Application of low-cost adsorbents for dye removal – A review. *Journal of Environmental Management*, *90*(8), 2313–2342. https://doi.org/10.1016/j.jenvman.2008.11.017

Gupta, A., & Balomajumder, C. (2015). Biosorptive performance of Escherichia coli supported on Waste tea biomass (WTB) for removal of Cr(VI) to avoid the contamination of ground water: A comparative study between biosorption and SBB system. *Groundwater for Sustainable Development*, *1*(1–2), 12–22. https://doi.org/10.1016/j.gsd.2016.01.001

Gupta, J., Rathour, R., Medhi, K., Tyagi, B., & Thakur, I. S. (2019). Microbial-derived natural bioproducts for a sustainable environment: A bioprospective for waste to wealth. In *Refining Biomass Residues for Sustainable Energy and Bioproducts: Technology, Advances, Life Cycle Assessment, and Economics*. Elsevier Inc. https://doi.org/10.1016/B978-0-12-818996-2.00003-X

Gupta, V. K., Agarwal, S., Ahmad, R., Mirza, A., & Mittal, J. (2020). Sequestration of toxic congo red dye from aqueous solution using ecofriendly guar gum/ activated carbon nanocomposite. *International Journal of Biological Macromolecules*, *158*, 1310–1318. https://doi.org/10.1016/j.ijbiomac.2020.05.025

Hamzeh, Y., Ashori, A., Azadeh, E., & Abdulkhani, A. (2012). Removal of Acid Orange 7 and Remazol Black 5 reactive dyes from aqueous solutions using a novel biosorbent. *Materials Science and Engineering C*, *32*(6), 1394–1400. https://doi.org/10.1016/j.msec.2012.04.015

Hassan, M. M., & Carr, C. M. (2018). Graphical abstract SC. *ECSN*. https://doi.org/10.1016/j.chemosphere.2018.06.043

Hastuti, B., Nur Afifah, S., Mulyani, B., & Susilowati, E. (2020). Adsorption of Methylene Blue Dyes Using Pectin Membrane. *Journal of Physics: Conference Series*, *1503*(1). https://doi.org/10.1088/1742-6596/1503/1/012031

Haul, R. (1969). Adsorption, Surface Area and Porosity. In *Zeitschrift für Physikalische Chemie* (Vol. 63, Issue 1_4, pp. 220–221).

Hill, A. (1910). The possible effects of the aggregation of the molecules of haemoglobin on its dissociation curves. *J Physiol*, *40*, iv–vii.

Ho YS and McKay, G. (1999). Pseudo-second order model for sorption processes. *Process Biochemistry*, *34*, 451–465.

Hu, M. Z. C., & Reeves, M. (1997). Biosorption of uranium by Pseudomonas aeruginosa strain CSU immobilized in a novel matrix. *Biotechnology Progress*, *13*(1), 60–70. https://doi.org/10.1021/bp9600849

Hubbe, M. A., Beck, K. R., O'Neal, W. G., & Sharma, Y. C. (2012). Cellulosic substrates for removal of pollutants from aqueous systems: A review. 2. Dyes. *BioResources*, *7*(2), 2592–2687. https://doi.org/10.15376/biores.7.2.2592-2687

Hunger, K. (2002). Industrial Dyes. In *Industrial Dyes*. https://doi.org/10.1002/3527602011

Iddou, A., Hadj Youcef, M., Aziz, A., & Ouali, M. S. (2011). Biosorptive removal of lead (II) ions from aqueous solutions using Cystoseira stricta biomass: Study of the surface modification effect. *Journal of Saudi Chemical Society*, *15*(1), 83–88. https://doi.org/10.1016/j.jscs.2010.10.007

Iftekhar, S., Ramasamy, D. L., Srivastava, V., Asif, M. B., & Sillanpää, M. (2018). Understanding the factors affecting the adsorption of Lanthanum using different adsorbents: A critical review. *Chemosphere*, *204*, 413–430. https://doi.org/10.1016/j.chemosphere.2018.04.053

Ihsanullah, I., Jamal, A., Ilyas, M., Zubair, M., Khan, G., & Atieh, M. A. (2020). Bioremediation of dyes: Current status and prospects. *Journal of Water Process Engineering*, *38*(October), 101680. https://doi.org/10.1016/j.jwpe.2020.101680

Ismail, M., Akhtar, K., Khan, M. I., Kamal, T., Khan, M. A., M. Asiri, A., Seo, J., & Khan, S. B. (2019). Pollution, Toxicity and Carcinogenicity of Organic Dyes and their Catalytic Bio-Remediation. *Current Pharmaceutical Design*, *25*(34), 3645–3663. https://doi.org/10.2174/1381612825666191021142026

Jadhav, S. B., Yedurkar, S. M., Phugare, S. S., & Jadhav, J. P. (2012). Biodegradation Studies on Acid Violet 19, a Triphenylmethane Dye, by Pseudomonas aeruginosa BCH. *Clean - Soil, Air, Water*, *40*(5), 551–558. https://doi.org/10.1002/clen.201100236

Jayan, N. and Bhatlu, M. L. D. (2021). removal of lead using isolated microorganisms from contaminated soil. *Advances in Materials Processing and Manufacturing Applications*, 335–344.

Jayasri, Y., Naidu, M. D., & Mallikarjuna, M. (2014). Review article microbial degradation of chlorpyrifos. *Int J Recent Sci Res*, *5*(11), 2043–2047.

Jeyavishnu, K., & Alagesan, V. (2020). Cereus sp. as potential biosorbent for removal of Congo red from aqueous solution: isotherm and kinetic investigations. *Environmental Monitoring and Assessment*, *192*(4). https://doi.org/10.1007/s10661-020-8197-2

Jinwon K, Hee-Jong Y, Gwangsu H, Su-Ji J, Hee-Gun Y, Ho-Jin J, Se-Won P, D.-Y. J. (2021). Biosorption of CR Dye in Aqueous Solution by Bacillus licheniformis SRCM 120569 Isolated from Korean Turbid Rice Wine (Makgeolli). *Food Engineering Progress*, *25*(2), 95–101.

Jovanović, D. S. (1969). Physical adsorption of gases - I: Isotherms for monolayer and multilayer adsorption. *Kolloid-Zeitschrift & Zeitschrift Für Polymere*, *235*(1), 1203–1213. https://doi.org/10.1007/BF01542530

Kamath Miyar, H., Pai, A., & Goveas, L. C. (2021). Adsorption of Malachite Green by extracellular polymeric substance of Lysinibacillus sp. SS1: kinetics and isotherms. *Heliyon*, *7*(6). https://doi.org/10.1016/j.heliyon.2021.e07169

Kant, R. (2012). Textile dyeing industry an environmental hazard. *Natural Science*, *04*(01), 22–26. https://doi.org/10.4236/ns.2012.41004

Karakagh, R. M., Chorom, M., Motamedi, H., Kalkhajeh, Y. K., & Oustan, S. (2012). Biosorption of Cd and Ni by inactivated bacteria isolated from agricultural soil treated with sewage sludge. *Ecohydrology & Hydrobiology*, *12*(3), 191–198. https://doi.org/10.1016/s1642-3593(12)70203-3

Karthik, V., Arunkumar, M., & Dhanakumar, S. (2020). Biosorption of Anionic Reactive Dye From Aqueous Solution Using Red Seaweed : Kappaphycus Alvarezii. *Asian Jr. of Microbiol. Biotech. Env. Sc.*, *22*(1), 111–119.

Karthik, V., Saravanan, K., Sivarajasekar, N., & Suriyanarayanan, N. (2016). Bioremediation of dye bearing effluents using microbial biomass. *Eco. Env. & Cons. 22*, 22.

Karthik, V., Sivarajasekar, N., Padmanaban, V. C., Nakkeeran, E., & Selvaraju, N. (2019). Biosorption of xenobiotic Reactive Black B onto metabolically inactive T. harzianum biomass: optimization and equilibrium studies. *International Journal of Environmental Science and Technology*, *16*(7), 3625–3636. https://doi.org/10.1007/s13762-018-1841-5

Katheresan, V., Kansedo, J., & Lau, S. Y. (2018). Efficiency of Various Recent Wastewater Dye Removal Methods: A Review. *Biochemical Pharmacology*. https://doi.org/10.1016/j.jece.2018.06.060

Khan, A. R., Ataullah, R., & Al-Haddad, A. (1997). Equilibrium adsorption studies of some aromatic pollutants from dilute aqueous solutions on activated carbon at different temperatures. *Journal of Colloid and Interface Science*, *194*(1), 154–165. https://doi.org/10.1006/jcis.1997.5041

Khan, M. I., Ansari, T. M., Zafar, S., Buzdar, A. R., Khan, M. A., Mumtaz, F., Prapamonthon, P., & Akhtar, M. (2018). Acid green-25 removal from wastewater by anion exchange membrane: Adsorption kinetic and thermodynamic studies. *Membrane Water Treatment*, *9*(2), 79–85. https://doi.org/10.12989/mwt.2018.9.2.079

Kim, S. Y., Jin, M. R., Chung, C. H., Yun, Y. S., Jahng, K. Y., & Yu, K. Y. (2015). Biosorption of cationic basic dye and cadmium by the novel biosorbent Bacillus catenulatus JB-022 strain. *Journal of Bioscience and Bioengineering*, *119*(4), 433–439. https://doi.org/10.1016/j.jbiosc.2014.09.022

Kiran, I., Akar, T., Ozcan, A. S., Ozcan, A., & Tunali, S. (2006). Biosorption kinetics and isotherm studies of Acid Red 57 by dried Cephalosporium aphidicola cells from aqueous solutions. *Biochemical Engineering Journal*, *31*(3), 197–203. https://doi.org/10.1016/j.bej.2006.07.008

Kotrba, P., Mackova, M., & Macek, T. (2011). Microbial biosorption of metals. In *Microbial Biosorption of Metals*. https://doi.org/10.1007/978-94-007-0443-5

Kousha, M., Tavakoli, S., Daneshvar, E., Vazirzadeh, A., & Bhatnagar, A. (2015). Central composite design optimization of Acid Blue 25 dye biosorption using shrimp shell biomass. *Journal of Molecular Liquids*, *207*, 266–273. https://doi.org/10.1016/j.molliq.2015.03.046

Kucuker, M. A., Wieczorek, N., Kuchta, K., & Copty, N. K. (2017). Biosorption of neodymium on Chlorella vulgaris in aqueous solution obtained from hard disk drive magnets. *PLoS ONE*, *12*(4), 1–13. https://doi.org/10.1371/journal.pone.0175255

Kumar, D S Sai Ravi Kiran, S. P. (2013). Multi objective optimization of tool life and total cost using 3-level full factorial method in CNC end milling process. *International Journal of Mechanical Engineering and Robotics Research*, *2*(3), 255–270.

Kumar, K. V., Porkodi, K., & Rocha, F. (2007). Comments on "Removal of lead from aqueous solution using Syzygium cumini L.: Equilibrium and kinetic studies." *Journal of Hazardous Materials*, *147*(1–2), 677–678. https://doi.org/10.1016/j.jhazmat.2007.01.074

Kumar, P., Bhati, H., Rani, A., & Singh, R. (2015). Role of Biosorption of Dyes and Microorganisms in Environment. *Life Sciences*, *4*(2), 38–41. https://doi.org/10.13140/RG.2.2.15083.44326

Kurniawan, S. B., Abdullah, S. R. S., Othman, A. R., Purwanti, I. F., Imron, M. F., Ismail, N. I., Ahmad, A., & Hasan, H. A. (2021). Isolation and characterisation of bioflocculant-producing bacteria from aquaculture effluent and its performance in treating high turbid water. *Journal of Water Process Engineering*, *42*(July). https://doi.org/10.1016/j.jwpe.2021.102194

Lafi, R., Montasser, I., & Hafiane, A. (2019). Adsorption of congo red dye from aqueous solutions by prepared activated carbon with oxygen-containing functional groups and its regeneration. *Adsorption Science and Technology*, *37*(1–2), 160–181. https://doi.org/10.1177/0263617418819227

Lagergren, S. (1898). Zur theorie der sogenannten adsorption gelöster stoffe (About the theory of so-called adsorption of soluble substances). *Kungliga Svenska Vetenskapsakademiens Handlingar*, *24*, 1–39.

Langmuir I. (1918). The adsorption of gases on plane surfaces of. *Journal of the American Chemical Society 40*, *345*(1914), 1361–1403.

Li, C., Zhang, L., Xia, H., Peng, J., Zhang, S., Cheng, S., & Shu, J. (2016). Kinetics and isotherms studies for congo red adsorption on mesoporous Eupatorium adenophorum-based activated carbon via microwave-induced H3PO4 activation. *Journal of Molecular Liquids*, *224*, 737–744. https://doi.org/10.1016/j.molliq.2016.10.048

Lim, C. K., Bay, H. H., Aris, A., Abdul Majid, Z., & Ibrahim, Z. (2013). Biosorption and biodegradation of Acid Orange 7 by Enterococcus faecalis strain ZL: Optimization by response surface methodological approach. *Environmental Science and Pollution Research*, *20*(7), 5056–5066. https://doi.org/10.1007/s11356-013-1476-5

Lima, E. C., Hosseini-bandegharaei, A., & Carlos, J. (2019). A critical review of the estimation of the thermodynamic parameters on adsorption equilibria. Wrong use of equilibrium constant in the Van't Hoof equation for calculation of thermodynamic parameters of adsorption Eder. *Journal of Molecular Liquids*, #pagerange#. https://doi.org/10.1016/j.molliq.2018.10.048

Litefti, K., Freire, M. S., Stitou, M., & González-Álvarez, J. (2019). Adsorption of an anionic dye (Congo red) from aqueous solutions by pine bark. *Scientific Reports*, *9*(1), 1–11. https://doi.org/10.1038/s41598-019-53046-z

Liu Chen, Yuan, H., Yang, J., & Li, B. (2011). Effective biosorption of reactive blue 5 by pH-independent lyophilized biomass of Bacillus megaterium. *African Journal of Biotechnology*, *10*(73), 16626–16636. https://doi.org/10.5897/ajb11.1824

Liu, L. E., Liu, J., Li, H., Zhang, H., Liu, J., & Zhang, H. (2012). Equilibrium, kinetic, and thermodynamic studies of lead (II) biosorption on sesame leaf. *BioResources*, *7*(3), 3555–3572. https://doi.org/10.15376/biores.7.3.3555-3572

Mahmood, S., Khalid, A., Arshad, M., Mahmood, T., & Crowley, D. E. (2016). Detoxification of azo dyes by bacterial oxidoreductase enzymes. *Critical Reviews in Biotechnology*, *36*(4), 639–651.

Mahmoud, D. K., Salleh, M. A. M., Karim, W. A. W. A., Idris, A., & Abidin, Z. Z. (2012). Batch adsorption of basic dye using acid treated kenaf fibre char: Equilibrium, kinetic and thermodynamic studies. *Chemical Engineering Journal*, *181–182*, 449–457.

Mall, I. D., Srivastava, V. C., Agarwal, N. K., & Mishra, I. M. (2005). Removal of congo red from aqueous solution by bagasse fly ash and activated carbon: Kinetic study and equilibrium isotherm analyses. *Chemosphere*, *61*(4), 492–501. https://doi.org/10.1016/j.chemosphere.2005.03.065

Mane, U. ., Gurav, P. N., Deshmukh, A. M., & Govindwar, S. P. (2008). Degradation of textile dye reactive navy-blue Rx (Reactive blue?9) by an isolated Actinomycete Streptomyces krainskii SUK-5. *Malaysian Journal of Microbiology*, *4*(2), 1–5. https://doi.org/10.21161/mjm.10408

Manogaran, M., Yasid, N. A., Othman, A. R., Gunasekaran, B., Izuan, M., Halmi, E., Yunus, M., & Shukor, A. (2021). Biodecolourisation of Reactive Red 120 as a Sole Carbon Source by a Bacterial Consortium — Toxicity Assessment and Statistical Optimisation. *International Journal of Environmental Research and Public Health*, *18*(2424).

Mansour, R. A., El Shahawy, A., Attia, A., & Beheary, M. S. (2020). Brilliant Green Dye Biosorption Using Activated Carbon Derived from Guava Tree Wood. *International Journal of Chemical Engineering*, *2020*(July), 1–12. https://doi.org/10.1155/2020/8053828

Maurya, R., Ghosh, T., Paliwal, C., Shrivastav, A., Chokshi, K., Pancha, I., Ghosh, A., & Mishra, S. (2014). Biosorption of methylene blue by de-oiled algal biomass: Equilibrium, kinetics and artificial neural network modelling. *PLoS ONE*, *9*(10), 1–13. https://doi.org/10.1371/journal.pone.0109545

Mawad, A., Yousef, N., & Shoreit, A. (2014). Bioremediation of Acid blue 25 dye by anthracene degrading Pseudomonas pseudoalcaligenes ASU-016. *Catrina: The International Journal of Environmental Sciences*, *10*(1), 27–34. https://doi.org/10.12816/0010695

McKay, G., Ho, Y. S., & Ng, J. C. Y. (1999). Biosorption of copper from waste waters: A review. *Separation and Purification Methods*, *28*(1), 87–125. https://doi.org/10.1080/03602549909351645

Mishra, H. P., & Jalan, A. (2021). Analysis of faults in rotor-bearing system using three-level full factorial design and response surface methodology. *Noise &Vibration Worldwide*, *0(0)*, 1–12. https://doi.org/10.1177/09574565211030711

Mohammadi, N., Khani, H., Gupta, V. K., Amereh, E., & Agarwal, S. (2011). Adsorption process of methyl orange dye onto mesoporous carbon material-kinetic and thermodynamic studies. *Journal of Colloid and Interface Science*, *362*(2), 457–462. https://doi.org/10.1016/j.jcis.2011.06.067

Mohan, S. V., Bhaskar, Y. V., & Karthikeyan, J. (2004). Biological decolourisation of simulated azo dye in aqueous phase by algae Spirogyra species. *International Journal of Environment and Pollution*, *21*(3), 211–222. https://doi.org/10.1504/IJEP.2004.004190

Mona, S., Kaushik, A., & Kaushik, C. P. (2011). Biosorption of reactive dye by waste biomass of Nostoc linckia. *Ecological Engineering*, *37*(10), 1589–1594. https://doi.org/10.1016/j.ecoleng.2011.04.005

Moradihamedani, P. (2022). Recent advances in dye removal from wastewater by membrane technology: a review. *Polymer Bulletin*, *79*(4), 2603–2631. https://doi.org/10.1007/s00289-021-03603-2

Motulsky, H. J., & Ransnas, L. a. (1987). Fitting curves nonlinear regression : review a practical. *FASEB Journal*, *1*(5), 365–374.

Moussa, A., Abdelhamid, C., Samia, K., Tounsia, A., & Mohamed, T. (2015). Kinetic and Equilibrium Studies of Coomassie Blue G-250 Adsorption on Apricot Stone Activated Carbon. *J Environ Anal Toxicol*, *5*(2), 2–8. https://doi.org/10.4172/2161-0525.1000264

Moussout, H., Ahlafi, H., Aazza, M., & Maghat, H. (2018). Critical of linear and nonlinear equations of pseudo-first order and pseudo-second order kinetic models. *Karbala International Journal of Modern Science*, 1–11. https://doi.org/10.1016/j.kijoms.2018.04.001

Mudhoo, A., & Pittman, C. U. (2023). Adsorption data modeling and analysis under scrutiny: A clarion call to redress recently found troubling flaws. *Chemical Engineering Research and Design*, *192*, 371–388. https://doi.org/10.1016/j.cherd.2023.02.033

Muralidhar, R. V, Chirumamila, R. R., Marchant, R., & Nigam, P. (2001). A response surface approach for the comparison of lipase production by Candida cylindracea using two different carbon sources. *Biochemical Engineering Journal*, *9*, 17–23.

Nacèra, Y., & Aicha, B. (2006). Equilibrium and kinetic modelling of methylene blue biosorption by pretreated dead streptomyces rimosus: Effect of temperature. *Chemical Engineering Journal*, *119*(2–3), 121–125. https://doi.org/10.1016/j.cej.2006.01.018

Nagendrappa, G. (2010). Sir William Henry Perkin: The man and his "Mauve." *Resonance*, *15*(9), 779–793. https://doi.org/10.1007/s12045-010-0088-3

Nath, J., Das, A., & Ray, L. (2015). Biosorption of Malachite Green from Aqueous Solution Using Resting and Immobilised Biomass of Bacillus cereus M116 (MTCC 5521). *Indian Chemical Engineer*, *57*(1), 82–100. https://doi.org/10.1080/00194506.2014.997813

Nath, J., & Ray, L. (2015). Biosorption of Malachite green from aqueous solution by dry cells of Bacillus cereus M116 (MTCC 5521). *Journal of Environmental Chemical Engineering*, *3*(1), 386–394. https://doi.org/10.1016/j.jece.2014.12.022

Nayak, A. K., & Pal, A. (2020). Utilization of Lignocellulosic Waste for Acridine Orange Uptake: Insights into Multiparameter Isotherms Modeling with ANN-Aimed Formulation. *Journal of Environmental Engineering*, *146*(9), 04020096.

Neag, E., Moldovan, A., Băbălău-Fuss, V., Török, A., Cadar, O., & Roman, C. (2019). Kinetic, equilibrium and phytotoxicity studies for dyes removal by low cost natural activated plant-based carbon. *Acta Chimica Slovenica*, *66*(4), 850–858. https://doi.org/10.17344/acsi.2018.4924

Netzahuatl-Muñoz, A. R., Del Carmen Cristiani-Urbina, M., & Cristiani-Urbina, E. (2015). Chromium biosorption from Cr(VI) aqueous solutions by Cupressus lusitanica bark: Kinetics, equilibrium and thermodynamic studies. *PLoS ONE*, *10*(9), 1–23. https://doi.org/10.1371/journal.pone.0137086

Nguyen, D., Tran, H. N., Juang, R. S., Dat, N. D., Tomul, F., Ivanets, A., Woo, S. H., Hosseini-Bandegharaei, A., Nguyen, V. P., & Chao, H. P. (2020). Adsorption process and mechanism of acetaminophen onto commercial activated carbon. *Journal of Environmental Chemical Engineering*, *8*(6), 104408. https://doi.org/10.1016/j.jece.2020.104408

Nguyen, T. A., Fu, C. C., & Juang, R. S. (2016). Biosorption and biodegradation of a sulfur dye in high-strength dyeing wastewater by Acidithiobacillus thiooxidans. *Journal of Environmental Management*, *182*, 265–271. https://doi.org/10.1016/j.jenvman.2016.07.083

Ning, X. A., Yang, C., Wang, Y., Yang, Z., Wang, J., & Li, R. (2014). Decolorization and biodegradation of the azo dye Congo red by an isolated Acinetobacter baumannii YNWH 226. *Biotechnology and Bioprocess Engineering*, *19*(4), 687–695. https://doi.org/10.1007/s12257-013-0729-y

Nordin, N., Zakaria, M., Halmi, M., Ariff, A., Zawawi, R., & Wasoh, H. (2013). Isolation and screening of high efficiency biosurfactant-producing Pseudomonas sp. In *Journal of Biochemistry, Microbiology and Biotechnology* (Vol. 1, Issue 1, pp. 25–31).

O'Mahony, T., Guibal, E., & Tobin, J. M. (2002). Reactive dye biosorption by Rhizopus arrhizus biomass. *Enzyme and Microbial Technology*, *31*(4), 456–463. https://doi.org/10.1016/S0141-0229(02)00110-2

Olayinka, J. A., Tope, B. I., Olubunmi, O. O., & Omoniyi, M. S. (2020). Evaluation of kinetics and equilibrium studies of biosorption potentials of bamboo stem biomass for removal of Lead (II) and Cadmium (II) ions from aqueous solution. *African Journal of Pure and Applied Chemistry*, *14*(2), 24–41. https://doi.org/10.5897/ajpac2019.0812

Öztürk, A., Bayol, E., & Abdullah, M. I. (2020). Characterization of the biosorption of fast black azo dye K salt by the bacterium Rhodopseudomonas palustris 51ATA strain. *Electronic Journal of Biotechnology*, *46*(xxxx), 22–29. https://doi.org/10.1016/j.ejbt.2020.05.002

Pal, D., & Maiti, S. K. (2020). An approach to counter sediment toxicity by immobilization of heavy metals using waste fish scale derived biosorbent. *Ecotoxicology and Environmental Safety*, *187*(October 2019), 109833. https://doi.org/10.1016/j.ecoenv.2019.109833

Parker, G. R. (1995). Optimum isotherm equation and thermodynamic interpretation for aqueous 1,1,2-trichloroethene adsorption isotherms on three adsorbents. *Adsorption*, *1*(2), 113–132. https://doi.org/10.1007/BF00705000

Pereira, L., & Alves, M. (2012). Dyes-environmental impact and remediation. *Environmental Protection Strategies for Sustainable Development*, 111–162. https://doi.org/10.1007/978-94-007-1591-2_4

Pillai, H. P. J. S. (2017). Optimization of process conditions for effective degradation of azo blue dye by streptomyces DJP15. *Journal of Pure and Applied Microbiology*, *11*(4), 1757–1765. https://doi.org/10.22207/JPAM.11.4.14

Radhakrishnan, S. (2014). *Roadmap to Sustainable Textiles and Clothing*. https://doi.org/10.1007/978-981-287-065-0

Radushkevich, L. (1949). Potential theory of sorption and structure of carbons. *Zhurnal Fizicheskoi Khimii*, *23*, 1410–1420.

Rai, H. S., Bhattacharyya, M. S., Singh, J., Bansal, T. K., Vats, P., & Banerjee, U. C. (2005). Removal of dyes from the effluent of textile and dyestuff manufacturing industry: A review of emerging techniques with reference to biological treatment. *Critical Reviews in Environmental Science and Technology*, *35*(3), 219–238. https://doi.org/10.1080/10643380590917932

Ramachandra, T. V. (2014). *Biosorption : Techniques and Mechanisms*. *May*.

Ramakreshnan, L., Rajandra, A., & Aghamohammadi, N. (2019). A preliminary insight into the environmental awareness of community in the vicinity of batik manufacturing units in Kelantan , Malaysia. *GeoJournal*, *0123456789*. https://doi.org/10.1007/s10708-019-10046-w

Rascoe, J., Berg, M., Melcher, U., Mitchell, F. L., Bruton, B. D., Pair, S. D., & Fletcher, J. (2003). Identification, Phylogenetic Analysis, and Biological Characterization of Serratia marcescens Strains Causing Cucurbit Yellow Vine Disease. *Phytopathology*, *93*(10), 1233–1239. https://doi.org/10.1094/PHYTO.2003.93.10.1233

Redlich, & Peterson. (1958). hydrochloric acid was then filtered through the fritted glass. Following this a 9.3. *Notes*, *63*(1955), 1958.

Regti, A., Laamari, M. R., Stiriba, S. E., & EI Haddad, M. E. (2017). Removal of Basic Blue 41 dyes using Persea americana-activated carbon prepared by phosphoric acid action. *International Journal of Industrial Chemistry*, *8*(2), 187–195. https://doi.org/10.1007/s40090-016-0090-z

Ribas, M. C., de Franco, M. A. E., Adebayo, M. A., Lima, E. C., Parkes, G. M. B., & Feris, L. A. (2020). Adsorption of Procion Red MX-5B dye from aqueous solution using homemade peach and commercial activated carbons. *Applied Water Science*, *10*(6), 1–13. https://doi.org/10.1007/s13201-020-01237-9

Ridha, F. N., & Webley, P. A. (2009). Anomalous Henry ' s law behavior of nitrogen and carbon dioxide adsorption on alkali-exchanged chabazite zeolites. *Separation and Purification Technology*, *67*, 336–343.

Rizzi, V., Longo, A., Fini, P., Semeraro, P., Cosma, P., Franco, E., García, R., Ferrándiz, M., Núñez, E., Gabaldón, J. A., Fortea, I., Pérez, E., & Ferrándiz, M. (2014). Applicative Study (Part I): The Excellent Conditions to Remove in Batch Direct Textile Dyes (Direct Red, Direct Blue and Direct Yellow) from Aqueous Solutions by Adsorption Processes on Low-Cost Chitosan Films under Different Conditions. *Advances in Chemical Engineering and Science*, *04*(04), 454–469. https://doi.org/10.4236/aces.2014.44048

Rosca, M., Hlihor, R. M., Cozma, P., Dragoi, E. N., Diaconu, M., Silva, B., Tavares, T., & Gavrilescu, M. (2018). Comparison of Rhodotorula sp. and Bacillus megaterium in the removal of cadmium ions from liquid effluents. *Green Processing and Synthesis*, *7*(1), 74–88. https://doi.org/10.1515/gps-2016-0218

Roy, U., Manna, S., Sengupta, S., Das, P., Datta, S., Mukhopadhyay, A., & Bhowal, A. (2018). *Dye Removal Using Microbial Biosorbents*. https://doi.org/10.1007/978-3-319-92162-4_8

Sadi, J. Al. (2018). Designing Experiments : 3 Level Full Factorial Design and Variation of Processing Parameters Methods for Polymer Colors. *Advances in Science, Technology and Engineering Systems Journal*, *3*(5), 109–115.

Saha, P., & Chowdhury, S. (2011). Insight Into Adsorption Thermodynamics. *Thermodynamics*, 349–364. https://doi.org/10.5772/13474

Saratale, R. G., Saratale, G. D., Chang, J. S., & Govindwar, S. P. (2011). Bacterial decolorization and degradation of azo dyes: A review. *Journal of the Taiwan Institute of Chemical Engineers*, *42*(1), 138–157. https://doi.org/10.1016/j.jtice.2010.06.006

Sarim, K. M., Kukreja, K., Shah, I., & Choudhary, C. K. (2019). Biosorption of direct textile dye Congo red by Bacillus subtilis HAU-KK01. *Bioremediation Journal*, *23*(3), 185–195. https://doi.org/10.1080/10889868.2019.1641466

Sarkar, S., Echeverr, A., & Banerjee, A. (2021). *Decolourisation and Biodegradation of Textile Di-azo Dye Congo Red by Chryseobacterium geocarposphaerae DD3*.

Sassi Mohamed, Bestani Benaouda, and G. E. (2014). Biosorption of an Industrial Dye (A-BG) by a Dairy Sludge. *American Journal of Environmental Protection*, *3*(5), 292. https://doi.org/10.11648/j.ajep.20140305.23

Serap Ç, Savaş K, Aysun A, Halil İÇ, Nida SJ, Sultan E, R. M. (2023). Equilibrium and DFT modeling studies for the biosorption of Safranin O dye from water samples using Bacillus subtilis biosorbent. *Journal of Molecular Structure*, *1276*, 134761.

Sharma, S., Saxena, R., & Gaur, G. (2014). Study of Removal Techniques for Azo Dyes by Biosorption: A Review. *IOSR Journal of Applied Chemistry*, *7*(10), 06–21.

Sharma, Sangeeta, & Kaur, A. (2018). Various methods for removal of dyes from industrial effluents - a review. *Indian Journal of Science and Technology*, *11*(12), 1–21. https://doi.org/10.17485/ijst/2018/v11i12/120847

Sharma, Swati, Hasan, A., Kumar, N., & Pandey, L. M. (2018). Removal of methylene blue dye from aqueous solution using immobilized Agrobacterium fabrum biomass along with iron oxide nanoparticles as biosorbent. *Environmental Science and Pollution Research*, *25*(22), 21605–21615. https://doi.org/10.1007/s11356-018-2280-z

Shukor, M. S., & Shukor, M. . (2014). Statistical Evaluation of the Mathematical Modelling on the Molybdenum Reduction Kinetics of a Molybdenum-reducing Bacterium. *Journal of Environmental Bioremediation and Toxicology*, *2*(2), 62–66. https://doi.org/10.54987/jebat.v2i2.220

Silva, F., Nascimento, L., Brito, M., da Silva, K., Paschoal, W., & Fujiyama, R. (2019). Biosorption of methylene blue dye using natural biosorbents made from weeds. *Materials*, *12*(15). https://doi.org/10.3390/ma12152486

Singh, K. P., Gupta, S., Singh, A. K., & Sinha, S. (2011). Optimizing adsorption of crystal violet dye from water by magnetic nanocomposite using response surface modeling approach. *Journal of Hazardous Materials*, *186*(2–3), 1462–1473. https://doi.org/10.1016/j.jhazmat.2010.12.032

Singh, P. K., & Singh, R. L. (2017). Bio-removal of Azo Dyes: A Review. *International Journal of Applied Sciences and Biotechnology*, *5*(2), 108–126. https://doi.org/10.3126/ijasbt.v5i2.16881

Sips, R. (1948). On the structure of a catalyst surface. *The Journal of Chemical Physics*, *16*(5), 490–495. https://doi.org/10.1063/1.1746922

Sivarajasekar, N., & Baskar, R. (2019). Adsorption of Basic Magenta II onto H2SO4 activated immature Gossypium hirsutum seeds: Kinetics, isotherms, mass transfer, thermodynamics and process design. *Arabian Journal of Chemistry*, *12*(7), 1322–1337. https://doi.org/10.1016/j.arabjc.2014.10.040

Sivasamy, A., Nethaji, S., & Nisha, L. L. J. L. (2012). Equilibrium, kinetic and thermodynamic studies on the biosorption of reactive acid dye on Enteromorpha flexuosa and Gracilaria corticata. *Environmental Science and Pollution Research*, *19*(5), 1687–1695. https://doi.org/10.1007/s11356-011-0666-2

Slama, H. Ben, Bouket, A. C., Pourhassan, Z., Alenezi, F. N., Silini, A., Cherif-Silini, H., Oszako, T., Luptakova, L., Golińska, P., & Belbahri, L. (2021). Diversity of synthetic dyes from textile industries, discharge impacts and treatment methods. *Applied Sciences (Switzerland)*, *11*(14), 1–21. https://doi.org/10.3390/app11146255

Smith, E., & Smith, E. (1944). *E. smith*. *69*(240).

Sung, W. W., Sun, B. C., & Yun, Y. S. (2005). Interaction between protonated waste biomass of Corynebacterium glutamicum and anionic dye Reactive Red 4. *Colloids and Surfaces A: Physicochemical and Engineering Aspects*, *262*(1–3), 175–180. https://doi.org/10.1016/j.colsurfa.2005.04.028

Suteu, D., Blaga, A. C., Diaconu, M., & Malutan, T. (2013). Biosorption of reactive dye from aqueous media using Saccharomyces cerevisiae biomass. Equilibrium and kinetic study. *Central European Journal of Chemistry*, *11*(12), 2048–2057. https://doi.org/10.2478/s11532-013-0338-9

Suyamboo, B. K. (2012). Equilibrium, Thermodynamic and Kinetic Studies on Adsorption of a Basic Dye by Citrullus Lanatus Rind. *Iranica Journal of Energy & Environment*, *3*(1), 23–34. https://doi.org/10.5829/idosi.ijee.2012.03.01.0130

Tafakori, V., Zadmard, R., Tabandeh, F., Amoozegar, M. A., & Ahmadian, G. (2017). Equilibrium isotherm, kinetic modeling, optimization, and characterization studies of cadmium adsorption by surface-engineered Escherichia coli. *Iranian Biomedical Journal*, *21*(6), 380–391. https://doi.org/10.18869/acadpub.ibj.21.6.380

Tan, Ahmad, A. L., & Hameed, B. H. (2008). Adsorption of basic dye on high-surface-area activated carbon prepared from coconut husk: Equilibrium, kinetic and thermodynamic studies. *Journal of Hazardous Materials*, *154*(1–3), 337–346. https://doi.org/10.1016/j.jhazmat.2007.10.031

Tan, K. L., & Hameed, B. H. (2017). Insight into the adsorption kinetics models for the removal of contaminants from aqueous solutions. *Journal of the Taiwan Institute of Chemical Engineers*, *74*, 25–48. https://doi.org/10.1016/j.jtice.2017.01.024

Temkin MI and Pyzhev, V. (1940). Kinetics of ammonia synthesis on promoted iron catalysts. *Acta Physicochim USSR*, *12*, 327–356.

Tonghao, L., Li, Y., Du, Q., Sun, J., Jiao, Y., Yang, G., Wang, Z., Xia, Y., Zhang, W., Wang, K., Zhu, H., & Wu, D. (2012). Adsorption of methylene blue from aqueous solution by graphene. *Colloids and Surfaces B: Biointerfaces*, *90*(1), 197–203. https://doi.org/10.1016/j.colsurfb.2011.10.019

Torres, E. (2020). Biosorption : A Review of the Latest Advances. *Processes*, *8*, 1–23.

Toth, J. (1971). State equations of the solid-gas interface layers. *Acta Chim Acad Sci Hung*, *69*, 311–328.

Tran, H. N., You, S. J., & Chao, H. P. (2016). Thermodynamic parameters of cadmium adsorption onto orange peel calculated from various methods: A comparison study. *Journal of Environmental Chemical Engineering*, *4*(3), 2671–2682. https://doi.org/10.1016/j.jece.2016.05.009

Tran, H. N., You, S. J., Hosseini-Bandegharaei, A., & Chao, H. P. (2017). Mistakes and inconsistencies regarding adsorption of contaminants from aqueous solutions: A critical review. *Water Research*, *120*, 88–116.

Tripathi, A. (2012). Biodegradation of orange G by a novel isolated bacterial strain Bacillus megaterium ITBHU01 using response surface methodology. *African Journal of Biotechnology*, *11*(7), 1768–1781. https://doi.org/10.5897/ajb11.2560

Tural, B., Ertaş, E., Enez, B., Fincan, S. A., & Tural, S. (2017). Preparation and characterization of a novel magnetic biosorbent functionalized with biomass of Bacillus Subtilis: Kinetic and isotherm studies of biosorption processes in the removal of Methylene Blue. *Journal of Environmental Chemical Engineering*, *5*(5), 4795–4802. https://doi.org/10.1016/j.jece.2017.09.019

Valenzuela DP, M. AL. (1989). *Adsorption equilibrium data handbook.' (Prentice Hall: Englewood Cliffs, N.J)*.

van Vliet, B. M., Weber, W. J., & Hozumi, H. (1980). Modeling and prediction of specific compound adsorption by activated carbon and synthetic adsorbents. *Water Research*, *14*(12), 1719–1728. https://doi.org/10.1016/0043-1354(80)90107-4

Velkova, Z. Y., Kirova, G. K., Stoytcheva, M. S., & Gochev, V. K. (2018). Biosorption of Congo Red and methylene blue by pretreated waste streptomyces fradiae biomass - Equilibrium, kinetic and thermodynamic studies. *Journal of the Serbian Chemical Society*, *83*(1), 107–120. https://doi.org/10.2298/JSC170519093V

Venkata Mohan, S., Chandrasekhar Rao, N., & Karthikeyan, J. (2002). Adsorptive removal of direct azo dye from aqueous phase onto coal based sorbents: A kinetic and mechanistic study. *Journal of Hazardous Materials*, *90*(2), 189–204. https://doi.org/10.1016/S0304-3894(01)00348-X

Verma, P., & Madamwar, D. (2003). Decolourization of synthetic dyes by a newly isolated strain of Serratia marcescens. *World Journal of Microbiology & Biotechnology*, *19*, 615–618.

Vieth, W. R., & Sladek, K. J. (1965). A model for diffusion in a glassy polymer. *Journal of Colloid Science*, *20*(9), 1014–1033. https://doi.org/10.1016/0095-8522(65)90071-1

Vijayalaks, G., Ramkumar, B., & Mohan, S. C. (2019). Isotherm and Kinetic Studies of Methylene Blue Adsorption Using Activated Carbon Prepared from Teak Wood Waste Biomass. *Journal of Applied Sciences*, *19*(9), 827–836. https://doi.org/10.3923/jas.2019.827.836

Vijayaraghavan, K., Han, M. H., Choi, S. B., & Yun, Y. S. (2007). Biosorption of Reactive black 5 by Corynebacterium glutamicum biomass immobilized in alginate and polysulfone matrices. *Chemosphere*, *68*(10), 1838–1845. https://doi.org/10.1016/j.chemosphere.2007.03.030

Vijayaraghavan, K., & Yun, Y. (2008). Bacterial biosorbents and biosorption. *Biotechnology Advances*, *26*(26), 266–291. https://doi.org/10.1016/j.biotechadv.2008.02.002

Vijayaraghavan, K., & Yun, Y. S. (2007). Utilization of fermentation waste (Corynebacterium glutamicum) for biosorption of Reactive Black 5 from aqueous solution. *Journal of Hazardous Materials*, *141*(1), 45–52. https://doi.org/10.1016/j.jhazmat.2006.06.081

Vikrant, K., Giri, B. S., Raza, N., Roy, K., Kim, K. H., Rai, B. N., & Singh, R. S. (2018). Recent advancements in bioremediation of dye: Current status and challenges. *Bioresource Technology*, *253*, 355–367. https://doi.org/10.1016/j.biortech.2018.01.029

Viotti, P. V., Moreira, W. M., Santos, O. A. A. dos, Bergamasco, R., Vieira, A. M. S., & Vieira, M. F. (2019). Diclofenac removal from water by adsorption on Moringa oleifera pods and activated carbon: Mechanism, kinetic and equilibrium study. *Journal of Cleaner Production*, *219*, 809–817. https://doi.org/10.1016/j.jclepro.2019.02.129

Volesky, B., & Naja, G. (2007). Biosorption technology: starting up an enterprise. *International Journal of Technology Transfer and Commercialisation*, *6*(2/3/4), 196. https://doi.org/10.1504/ijttc.2007.017806

Wang, H., Zheng, X. W., Su, J. Q., Tian, Y., Xiong, X. J., & Zheng, T. L. (2009). Biological decolorization of the reactive dyes Reactive Black 5 by a novel isolated bacterial strain Enterobacter sp. EC3. *Journal of Hazardous Materials*, *171*(1–3), 654–659. https://doi.org/10.1016/j.jhazmat.2009.06.050

Wang, Y., Mu, Y., Zhao, Q. B., & Yu, H. Q. (2006). Isotherms, kinetics and thermodynamics of dye biosorption by anaerobic sludge. *Separation and Purification Technology*, *50*(1), 1–7. https://doi.org/10.1016/j.seppur.2005.10.012

Wanyonyi, W. C., Onyari, J. M., & Shiundu, P. M. (2014). Adsorption of congo red dye from aqueous solutions using roots of eichhornia crassipes: Kinetic and equilibrium studies. *Energy Procedia*, *50*, 862–869. https://doi.org/10.1016/j.egypro.2014.06.105

Witek-Krowiak, A. (2013). Application of beech sawdust for removal of heavy metals from water: Biosorption and desorption studies. *European Journal of Wood and Wood Products*, *71*(2), 227–236. https://doi.org/10.1007/s00107-013-0673-8

Won, S. W., Han, M. H., & Yun, Y. S. (2008). Different binding mechanisms in biosorption of reactive dyes according to their reactivity. *Water Research*, *42*(19), 4847–4855. https://doi.org/10.1016/j.watres.2008.09.003

Wu, K., Pan, X., Zhang, J., Zhang, X., Salah Zene, A., & Tian, Y. (2020). Biosorption of Congo Red from Aqueous Solutions Based on Self-Immobilized Mycelial Pellets: Kinetics, Isotherms, and Thermodynamic Studies. *ACS Omega*, *5*(38), 24601–24612. https://doi.org/10.1021/acsomega.0c03114

Yaashikaa, P. R., Kumar, P. S., Saravanan, A., & Vo, D. V. N. (2021). Advances in biosorbents for removal of environmental pollutants: A review on pretreatment, removal mechanism and future outlook. *Journal of Hazardous Materials*, *420*(May), 126596. https://doi.org/10.1016/j.jhazmat.2021.126596

Yagub, M. T., Sen, T. K., Afroze, S., & Ang, H. M. (2014). Dye and its removal from aqueous solution by adsorption: A review. *Advances in Colloid and Interface Science*, *209*(2014), 172–184. https://doi.org/10.1016/j.cis.2014.04.002

Yahuza, S., Sabo, I. A., Abubakar, A., Yunus, M., & Shukor, A. (2020). Thermodynamic Study on the Biosorptive Removal of Lead (II) Ions from Aqueous Solutions using Acid-treated Cystoseira tricta Biomass. *Journal of Environmental Microbiology and Toxicology*, *8*(2), 1–5.

Yaneva, Z. L., & Georgieva, N. V. (2012). Insights into Congo Red Adsorption on Agro-Industrial Materials - Spectral , Equilibrium , Kinetic , Thermodynamic , Dynamic and Desorption Studies . A Review. *International Review of Chemical Engineering (I.RE.CH.E.)*, *4*(September 2003), 127–146.

Yasid, N. A., Halmi, M. I. E., & ... (2020). Kinetic Studies on the Biosorption of the Brominated Flame Retardant 4-Dibromodiphenyl ether (BDE-3) using Coconut Palm Leaf Powders. *Bioremediation ...*, *8*(2), 2–7. https://journal.hibiscuspublisher.com/index.php/BSTR/article/view/550

Yenikaya, C., Atar, E., Olgun, A., Atar, N., Ilhan, S., & Çolak, F. (2010). Biosorption study of anionic dyes from aqueous solutions using Bacillus amyloliquefaciens. *Engineering in Life Sciences*, *10*(3), 233–241. https://doi.org/10.1002/elsc.200900108

Zeldovich, J. (1934). Über den mechanismus der katalytischen oxydation von CO an MnO2. *Acta Physicochimica URSS*, *1*, 364–499.

Zhou, Y., Lu, J., Zhou, Y., & Liu, Y. (2019). Recent advances for dyes removal using novel adsorbents: A review. *Environmental Pollution*, *252*, 352–365. https://doi.org/10.1016/j.envpol.2019.05.072

BIODATA OF STUDENT

Ibrahim Alhaji Sabo was born and brought up in Kano State, North-western Nigeria works with the microbiology department at federal university wukari, Taraba state. held a bachelor's degree in microbiology from Bayero University Kano and a master's degree in biotechnology from Sharda University in India. Currently, a Ph.D. research Student at the Universiti Putra Malaysia. Ibrahim Alhaji Sabo is happily married with two male children.

LIST OF PUBLICATIONS

Ibrahim Alhaji Sabo, Salihu Yahuza, and Mohd Yunus Shukor (2021). Mathematical Modeling of the growth of Acinetobacter baumanniiYNWH 226 on Azo dye Congo red. Journal of Environmental Bioremediation and Toxicology (JEBAT), Vol 4, No 1, 7-10

Ibrahim Alhaji Sabo, Salihu Yahuza, Abdussamad Abubakar and Bilal Ibrahim Dan-Iya (2022). Kinetic Study of Malathion Biosorption Using Dry Cells of an Isolated Bacillus sp. S14. Journal of Biochemistry, Microbiology, and Biotechnology (JOBIMB). Vol 10, No 1, 1-4.